FOREWORD

This is the Final Report on IIT Research Institute Project No. D6089, "Evaluation of Hybrid Composite Materials in Cylindrical Specimen Geometries," prepared by IITRI for NASA-Langley Research Center under Contract No. NAS1-12645. The work described herein was performed in the period August 23, 1973 to March 31, 1976. It was financially supported by the U.S. Army Mobility Research and Development Laboratory-Langley Directorate. Mr. Carl E. Swindlehurst, Jr. was the Technical Representative of the Contracting Officer. IITRI personnel who made primary contributions to the program are Dr. I.M. Daniel, Dr. T. Liber, and Mr. Tahei Niiro. Additional contributions to the program were made by Messrs. K.E. Hofer, Jr., L.C. Bennett, M. Senninger and B. Nowak.

Respectfully submitted,
IIT RESEARCH INSTITUTE

T. Liber

T. Liber
Senior Research Engineer

I.M. Daniel
Science Advisor
Mechanics of Materials Division

APPROVED:

S.A. Bortz
Assistant Director
Mechanics of Materials Division

EVALUATION OF HYBRID COMPOSITE MATERIALS IN CYLINDRICAL SPECIMEN GEOMETRIES*

ABSTRACT

The objective of this program was to determine static and fatigue properties of three composite materials and hybrids thereof with edgeless cylindrical specimens. The materials investigated were graphite/epoxy, S-glass/epoxy, PRD-49 (Kevlar 49)/epoxy and hybrids in angle-ply configurations, mainly $[\pm 45/0_2]_s$. A new type of edgeless cylindrical specimen was developed. It is a flattened tube with two flat sides connected by curved sections and it is handled much like the standard flat coupon. Special specimen fabrication, tabbing and tab region reinforcing techniques were developed. Axial modulus, Poisson's ratio, strength and ultimate strain were obtained under static loading from flattened tube specimens of nine laminate configurations. In a few cases these results were compared with those of corresponding flat coupon specimens. In the case of graphite/epoxy the tubular specimens appeared to yield somewhat higher strength and ultimate strain values than flat specimens. Tensile fatigue tests were conducted with all nine types of specimens and S-N curves obtained. Although no direct comparison was made with the flat coupons indications are that in some cases results from tubular specimens are better than might be expected from flat coupons. Specimens surviving 10^7 cycles of tensile loading were subsequently tested statically to failure to determine residual properties. No stiffness or strength degradation was indicated.

*The contract research effort which has led to the results in this report was financially supported by USAAMRDL (Langley Directorate)

TABLE OF CONTENTS

LIST OF FIGURES

LIST OF FIGURES (Cont'd)

LIST OF FIGURES

LIST OF FIGURES (Cont'd)

LIST OF TABLES

IITRI Final Report No. D6089

EVALUATION OF HYBRID COMPOSITE MATERIALS IN CYLINDRICAL SPECIMEN GEOMETRIES

1.0 INTRODUCTION

It has been observed that fatigue failures in composite materials are preceded by material degradation corresponding to a reduction in residual stiffness.[1] Stiffness variations in dynamically tuned structures can produce resonance resulting in catastrophic failures. It is not certain that the indicated stiffness degradation is a true material response or attributable to specimen geometry.

Static and fatigue tensile properties of composite laminates are normally evaluated by testing flat coupons. It has been shown analytically[2,3] and verified experimentally[4,5] that significant interlaminar stress components exist near free edges in uniaxially loaded laminates. These stresses are restricted to a region near the edge approximately equal to the laminate thickness. The state of stress in the interior regions of the laminate was found to be accurately predicted by the plane stress relations of laminated plate theory. It is hypothesized that damage is initiated at the edges of these flat specimens and propagates toward the interior. This damage propagation mechanism may be more pronounced under cyclic than under static loading.

To eliminate the influence of these edge effects in the determination of tensile properties of composites one must eliminate the edges by making an edgeless specimen. The most common edgeless specimen is the circular cylindrical specimen. It has been demonstrated that laminated tubular specimens can be manufactured with properties identical to those of flat laminates. Atttempts to conduct valid uniaxial tests with round tubular

specimens have been unsuccessful because of the differential Poisson effect between the test section and the grips. This problem has been particularly more difficult under cyclic loading which is more sensitive to stress discontinuities.

A new type of edgeless cylindrical specimen was developed at IITRI under the present contract with NASA-Langley Research Center. It is a flattened tube with two flat sides connected by curved sections and it can be handled much like the standard flat coupon. The present report describes the initial development, fabrication, testing and evaluation of this type of specimen. The specimens were composite angle-ply laminates of graphite/epoxy, S-glass/epoxy, PRD-49 (Kevlar 49/epoxy) and hybrids thereof.

2.0 THE FLATTENED TUBULAR SPECIMEN

2.1 Specimen Configuration

The geometric configuration and nominal dimensions of the flattened tubular specimen are shown in Fig. 1. The specimen is 22.9 cm (9 in.) long, 2.3 cm (0.90 in.) wide, with 3.80 cm (1.5 in.) long and 2.54 cm (1 in.) wide fiberglass tabs and inserts at each end. These are essentially the same dimensions as used for flat composite specimens. The thickness of the flattened tube shown in Fig. 1, (0.58 cm; 0.23 in.) is only a typical one. It varies with the number of plies in the laminate and the ply thickness of the material used.

The cross sectional area A of the specimen is determined by the formula

$$A = (G-\pi t)t \qquad (1)$$

where G = the specimen girth (outer circumference)
t = laminate thickness

The girth is readily measured with satisfactory accuracy by wrapping a single strip of paper around the specimen and marking the length of a single wrap.

2.2 Fabrication Technique for Flattened Composite Tubes

The development of a successful fabrication technique for flattened tubular specimens required substantial effort. Many promising approaches were pursued but most failed to produce specimens of consistent and satisfactory quality. The approach which was finally selected is described below.

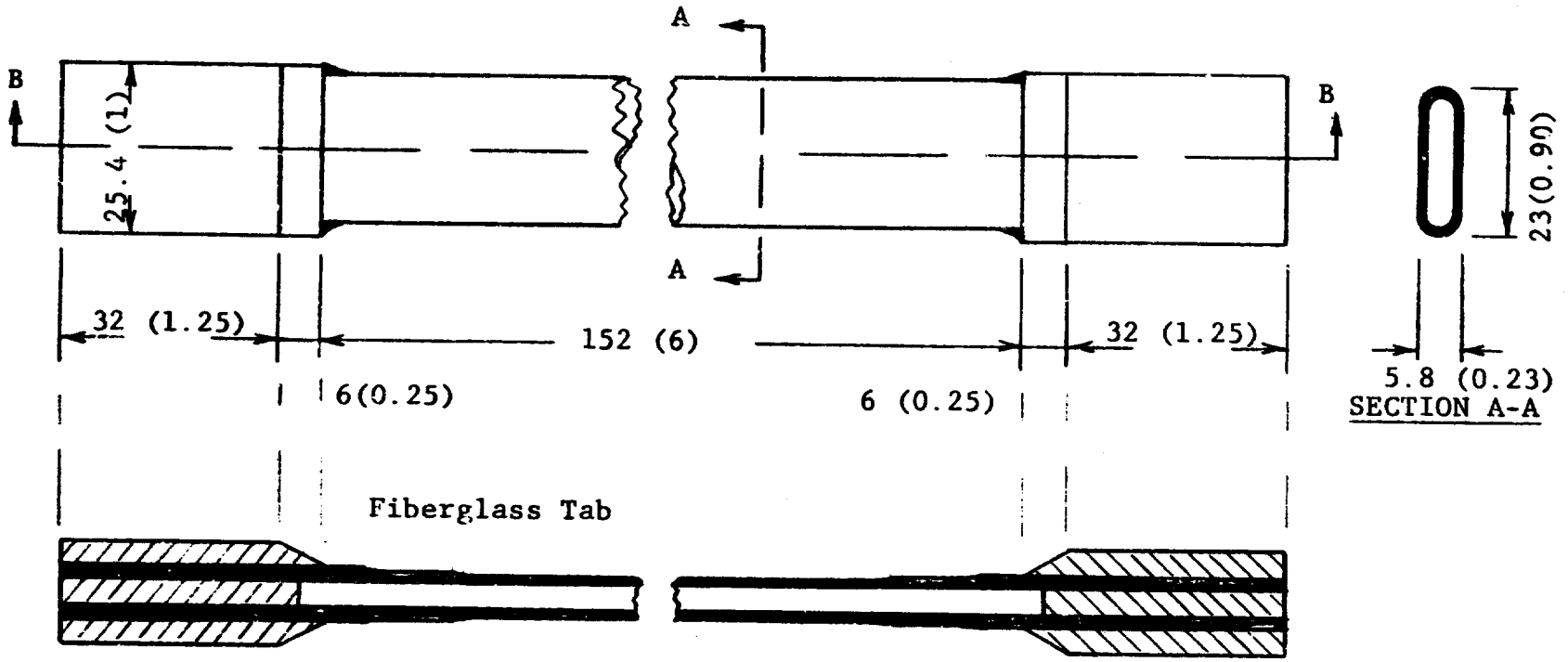

SECTION B-B

Fig. 1 DIMENSIONS OF FLATTENED COMPOSITE TUBULAR SPECIMEN
(Dimensions are in mm and inches)

The fabrication starts by rolling the prepreg plies around a rod mandrel and subsequently shaping the circular tube into the flattened shape by use of a special molding tool and process. The material for the tube is cut from prepreg tape into single-ply strips somewhat longer than the final tube length. The fiber orientation of these strips is parallel to the strip length.

The tube layup is done on a 1.27 cm (0.5 in.) diameter aluminum mandrel which is sprayed with mold release to prevent the first ply from sticking to it. The first ply is rolled directly onto the mandrel. Subsequent plies are each rolled on top of the preceeding one. Strips where fiber orientation is to be parallel to the tube axis are rolled on with their edges butting against each other and parallel to the mandrel axis. Strips whose fiber orientation is to be 45 degrees to the tube axis are rolled in a spiral fashion at a 45-degree angle to the mandrel axis. The edges are butted against each other during this operation. During the layup phase short lengths of reinforcing plies may be inserted at both ends of the tube between the tube plies. They serve subsequently to reinforce the transition area between the specimen gripping tabs and test section. After the prepreg laminate tube is layed up the aluminum mandrel is withdrawn and replaced with a silicone rubber tube of 0.95 cm (3/8 in.) inside diameter and 0.08 cm (0.030 in.) wall thickness, used for internal pressurization of the specimen during the curing process.

To prepare for the curing process the specimen is overwrapped with one layer of separator cloth (Emfab TX1040 Teflon treated 104 fiberglass cloth). The separator cloth is spirally overwrapped with strips of paper bleeder (Mochburg CW1850 glass fiber paper); one layer of bleeder for each 2 plies of specimen. The specimen is then partially flattened between two plates and

transferred into the cavity of an aluminum molding tool, whose surfaces have been sprayed with mold release.

The molding tool is shown in exploded view in Fig. 2 and assembled in Fig. 3. It consists of a lower and upper platen, two side restraint bars, two end caps and two specimen edge mold bars. Of the latter, the edges to be in contact with the specimen (see Fig. 2) were machined into a concave semicylindrical surface. These edge bars are made in various thicknesses, to accomodate specimens of various numbers of plies. The two end caps contain central pressure pipes, one capped blind and the other used to pressurize the silicone rubber tube inside the specimen. All parts of the molding tool are assembled and fastened tight by means of screws.

To prepare the mold assembly for specimen curing one end of the silicone rubber tube passing through the specimen is secured by means of a tightly fitting plug inside the pipe of the blind end cap. The other end of the rubber tube is similarly secured to the pipe of the pressurizing end cap by means of a tightly fitting tubular plug. With the specimen inside the mold cavity the two end caps are fastened into place to the lower platen. Next, the upper platen is fastened into place forcing the specimen into initial conformity to the flattened tube shape of the mold cavity. The end caps are next secured to the upper platen. The molding tool, now fully assembled, Fig. 3, is then bagged for vacuum application to the specimen during cure.

Prior to curing air pressure at 1380 kPa (200 psi) is applied through the rubber tube to force the specimen against the mold cavity. The specimen is heated to 399 degK (150°F) and held at this temperature at the above pressure for approximately 6 hours prior to the application of the full curing cycle. This long-time pressurization at a moderate temperature allows the specimen to creep into its final shape against the tool cavity

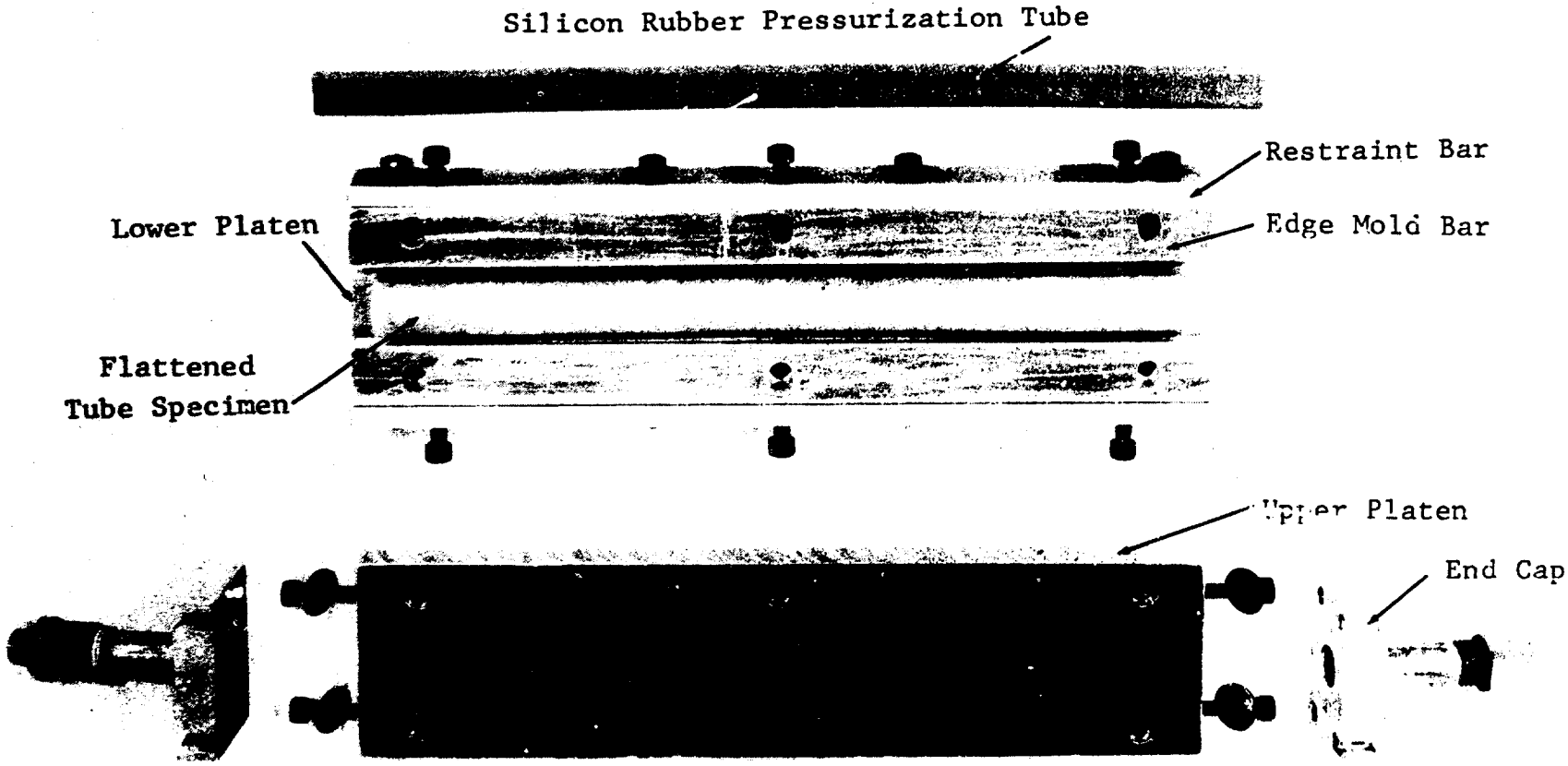

Fig. 2 FLATTENED TUBE SPECIMEN MOLDING TOOL (EXPLODED VIEW)

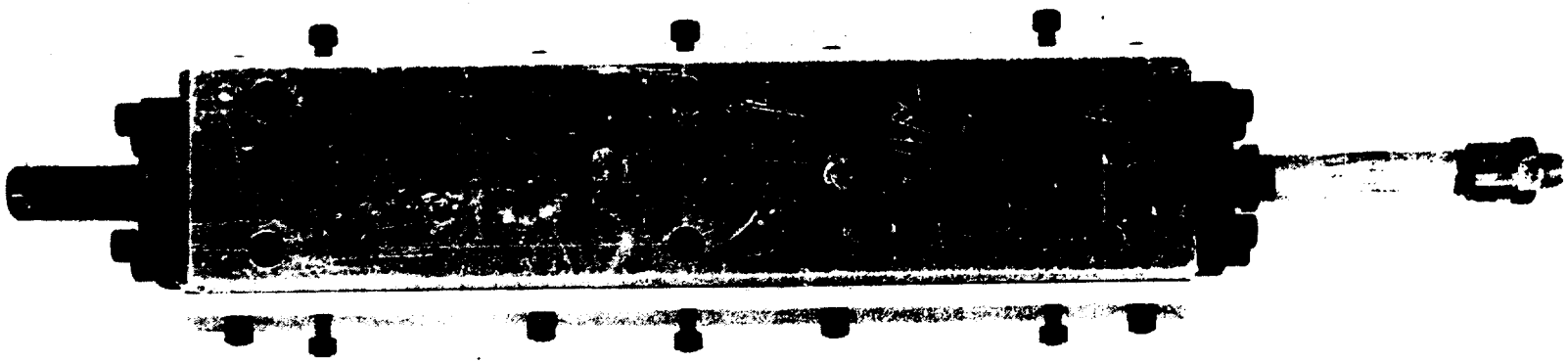

Fig. 3 FLATTENED TUBE SPECIMEN MOLDING TOOL (ASSEMBLY)

wall before final curing. Curing is done by raising the temperature at a gradual rate of approximately 2.8 degK (5°F) per minute to the recommended cure temperature of 450 degK (350°F) for the present epoxy matrix (PR 286 resin, made by the 3M Company) while maintaining the specimen internal pressurization and applying vacuum to the bag enclosing the specimen. The cure temperature, pressure and vacuum are maintained for one hour for full cure. After cure the pressure and vacuum are released, the tool allowed to cool to room temperature and the specimen removed from the tool at the end of the cooldown period. After the rubber tube is extracted and the specimen is visually inspected for quality and accepted, its ends are trimmed and end tabs provided to make it into a tensile test specimen.

2.3 Specimen Loading Tabs

All specimens were provided for tensile loading with flat glass/epoxy gripping tabs of 7-ply crossply construction bonded to the specimen ends on the flat outside surfaces. Cross-plied glass/epoxy inserts, extending into the specimens a distance equal to that of the outside tabs, were bonded inside the specimen ends. These inserts were installed to prevent specimen crushing during tightening of the gripping jaws of the test machine. The adhesive used for the tabbing process was Scotch-Weld 1838 structural adhesive made by the 3M Company.

Figure 4 shows the six tab sections comprising the tabbing system and the specimen before the tab bonding operation. The outer tabs have a 20- to 30-degree taper at the transition end from tab to test section. The end inserts are both rounded and tapered at the transition end from insert to specimen test section. These inserts are slightly undersized to accomodate an adhesive layer for bonding. Tab and insert bonding is done by putting a layer of adhesive on all mating surfaces, sliding

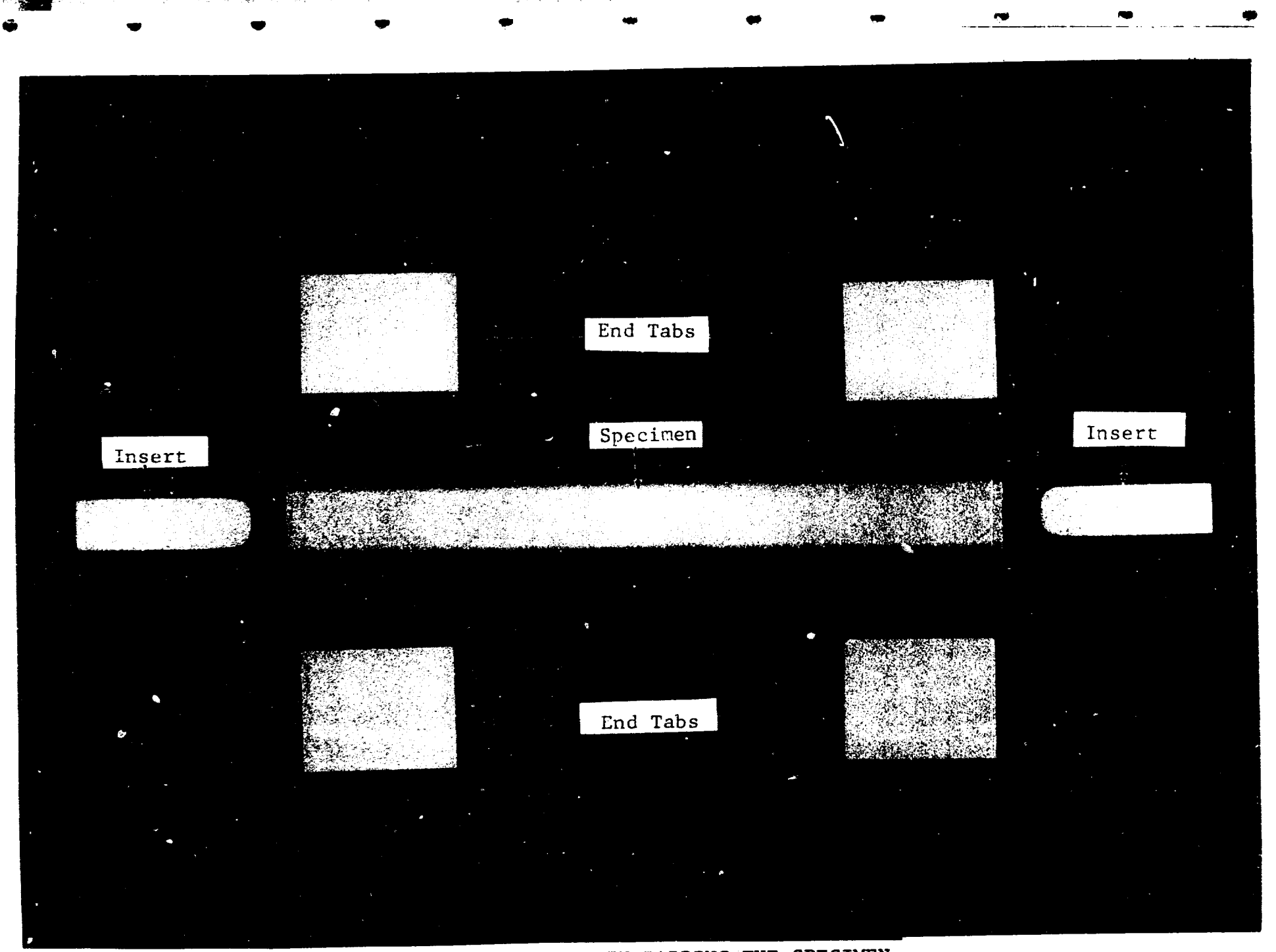

Fig. 4 END TABS AND INSERTS USED IN TABBING THE SPECIMEN

the inserts in place into the tube ends, placing the flat tabs on the specimen ends and clamping them in place by a set of spring clamps until the adhesive cures. Figure 5 shows the tab sections assembled in place without adhesive. During the bonding operation the space around the rounded edges of the specimen between the flat tabs is intentionally filled with adhesive to promote load transfer through the edges during tensile testing. After the tab bonds are cured the tab sides are sanded to the desired width, usually 2.54 cm (1 in.).

2.4 Reinforcing Techniques

An initial batch of tensile test specimens was fabricated and tested according to program requirements, some statically and some under cyclic loading. A number of these specimens failed near the tabs, especially in fatigue testing. It was concluded that this type of failure could be avoided by proper reinforcement of the transition region between the tabs and specimen test section.

Several reinforcing techniques were tried during the progress of the project. Some were better than others and one very promising technique did emerge. However, since it did not always produce test section failures, it needs further refinement, possibly in combination with improvements in the tabbing method. The various reinforcement techniques which were tried are described below.

For those tensile specimens which were already fabricated tab draping was used. In this technique the tabs were generally overdraped with two layers of PRD-49, graphite or glass/epoxy; the layer in contact with the tab extending 1.26 cm (0.5 in.) into the test section beyond the tab and the next layer on top extending an additional 1.26 cm (0.5 in.) beyond that. Straight [0°] axial

Fig. 5 ASSEMBLED SPECIMEN AND TAB SECTIONS

OF THE
ORIGINAL PAGE IS POOR

draping and angle-ply [±30°] and [±45°] draping was tried. No special advantage was found in the angle-ply draping. The overdrape was applied in prepreg form to the tab area, mechanically pressed in place by winding a wide silicon rubber band around it and cured for 1 hour at 450 degK (350°F). Figure 6a shows an overdraped tab. The visible transverse marks are impressions due to the rubber band.

In a second reinforcing technique, two plies of prepreg extending beyond the tab length are applied directly to the outside surface of the specimen at the two ends and cured in place. The flat tabs are then bonded onto them. Figure 6b shows such an underdraped reinforced tab region.

A third reinforcing technique consisted of inserting two extra 0-degree plies, 5.08 cm (2 in.) and 6.35 cm (2.5 in.) long, between the outer continuous plies at both ends of the specimen, during specimen fabrication. Specimen and reinforcement were then cured together. The difference in insert length produces a tapered transition. This mode of reinforcement is illustrated in Fig. 1. Its advantage resides in the fact that the ends of the reinforcing plies are locked in making their delamination and delamination propagation during loading more difficult than is the case of external draping. The tabs are bonded to the specimen in the usual way, and no overdraping is used.

A fourth reinforcement technique utilized the internal reinforcement plus tab overdraping. This did not improve performance and in case of fatigue it worsened it.

Of all the reinforcing techniques tried the best results were obtained with the use of internal reinforcement only. This can possibly be further optimized by inserting one of the reinforcing plies between the outer specimen plies and the second reinforcing ply between next pair of specimen plies.

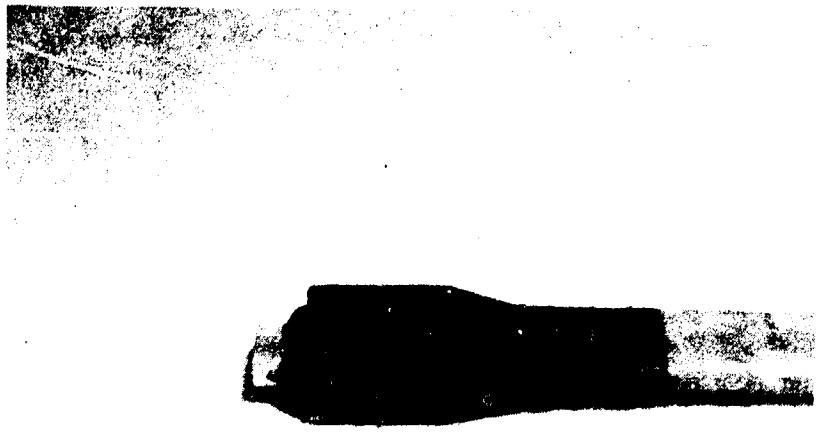

(6a) Overdraped Reinforced Tab

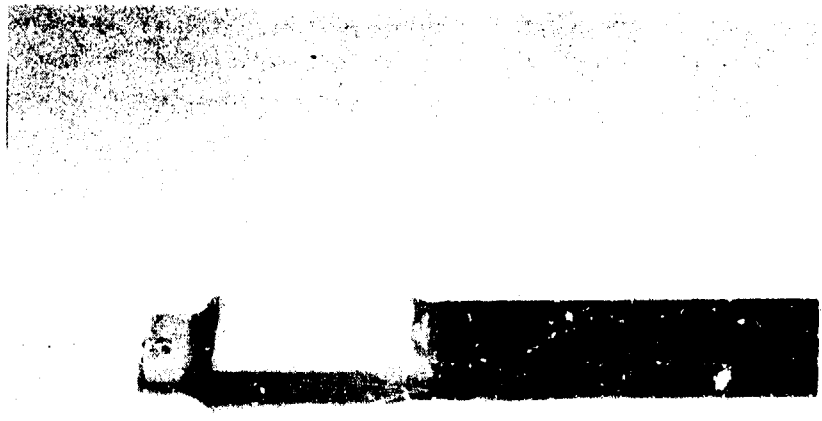

(6b) Underdraped Reinforced Tab Regicn

Fig. 6 TWO TAB REINFORCING TECHNIQUES

3.0 TEST PROGRAM

3.1 Materials and Specimens

Three materials were used for the specimens of the program; S-glass/epoxy, PRD-49-III (Kevlar 49)/epoxy and HT grpahite/epoxy. A single resin system, PR 286 made by the 3M Company, was employed as the resin system for all three materials. The materials were procured in continuous prepreg tape form.

Flattened tubular angle-ply specimens of nine different layups were fabricated from the three basic materials as described in Table 1. They consist of both single-material and two-material hybrid specimens. All layups were symmetric about the middle surface with $\pm$45-degree outer plies and 0-degree center plies. There are two six-ply layups, six eight-ply layups and one twelve-ply layup. Of these nine layups three are single-material and six are hybrids.

In addition to the above layups, HT graphite/epoxy flattened tubular specimens and flat coupons of $[\pm 45/0]_s$ construction were fabricated. They were used for preliminary static testing and strength comparison. Flat coupons of S-glass/epoxy, PRD-49-III/epoxy and HT graphite/epoxy of $[\pm 45/0_2]_s$ construction were also fabricated for static testing and comparison of results with the corresponding tubular specimens listed in Table 1. All flat coupons were nominally 2.54 cm (1 in.) wide and 22.9 cm (9 in.) long with a 15.2 cm (6 in.) test section. They were instrumented with two two-gage strain gage rosettes, one on each side of the specimen along the centerline.

For all specimens used in the program, wall thickness used in stress calculations were based on nominal ply thicknesses as obtained from cured flat laminates fo the three basic materials. These thicknesses are:

Table 1

TEST PROGRAM

Laminate Identification	Layup Description*	Materials	No. Specimens	
			Static	Fatigue
1. SG	$[\pm 45/0_2]_s$	S-glass/epoxy	3	4
2. PRD	$[\pm 45/0_2]_s$	PRD-49-III/epoxy	3	4
3. HTGR	$[\pm 45/0_2]_s$	HT graphite/epoxy	3	4
4. GRSG-1	$[\pm 45^C/0^G]_s$	±45° HT graphite/epoxy 0° S-glass/epoxy	3	4
5. GRSG-2	$[\pm 45^C/0^G{}_2]_s$	±45° HT graphite/epoxy 0° S-glass/epoxy	3	4
6. PRDSG-1	$[\pm 45^P/0^G{}_2]_s$	±45° PRD-49-III/epoxy 0° S-glass/epoxy	3	4
7. PRDSG-2	$[\pm 45^P/0^G{}_4]_s$	±45° PRD-49-III/epoxy 0° S-glass/epoxy	3	4
8. GRPRD-1	$[\pm 45^C/0^P]_s$	±45° HT graphite/epoxy 0° PRD-49-III/epoxy	3	4
9. GRPRD-2	$[\pm 45^C/0^P{}_2]_s$	±45° HT graphite/epoxy 0° PRD-49-III/epoxy	3	4

*C = Graphite
G = Glass
P = PRD-49

S-glass/epoxy - 0.013 cm (0.005 in.) per ply
PRD-49-III/epoxy - 0.017 cm (0.0065 in.) per ply
HT graphite/epoxy - 0.013 cm (0.005 in.) per ply

3.2 Instrumentation and Testing

The test program required that static tensile tests and tensile fatigue tests be conducted at room temperature on the specimens outlined in Table 1. For each laminate configuration three specimens were to be tested statically and four specimens in fatigue.

To satisfy static test requirements, to determine stress-strain curves and to detect extraneous bending, each static specimen was instrumented with two two-gage strain gage rosettes located centrally, one rosette on each flat side of the specimen.

Each static specimen was tested to failure in an Instron or Riehle testing machine. Strains were monitored and recorded throughout the test at each load increment. Abnormal behavior and failure modes, when noticeable, were recorded by appropriate remarks. Stress-strain curves were plotted from the recorded data and the following properties determined from them:

Initial axial modulus, E_{xx}

Poisson's ratio, ν_{xy}

Axial tensile strength, S_{xxT}

Axial ultimate strain, ϵ^{u}_{xx}

Nonlinearities in the stress-strain curves which could be associated with material degradation during testing were looked for and identified.

Fatigue testing was done on a Sonntag Universal Fatigue Test Machine. In accordance with test requirements each fatigue specimen was subjected to tensile load cycling at the standard rate of 30 cycles per second, at a stress ratio R = 0.1 and a constant maximum load amplitude. The maximum load amplitude for each test was selected in accordance with the requirement that the specimen fail within the range of 5×10^5 to 10^7 cycles. These load selections were made based on past experience with fatigue testing of S-glass/epoxy, PRD-49/epoxy and graphite/epoxy flat coupon specimens. The load range for S-glass/epoxy was selected below 25 percent of static strength. For PRD-49/epoxy the range selected was below 55 percent and for graphite/epoxy above 60 percent of static strength. For hybrids with S-glass/epoxy, the load region selected was that for S-glass/epoxy and for hybrids with PRD-49/epoxy it was selected to be the same as for PRD-49/epoxy.

Each test was run continuously to failure or 10^7 cycles, whichever occurred first. The continuous running avoided possible extranous damage from stop-restart transient loads. Maximum stress amplitudes and cycles to failure were recorded, tabulated and S-N curves drawn. Those specimens which survived 10^7 cycles were tested statically to failure to determine residual properties. Instrumentation, testing and data analysis for these tests were the same as for the static specimens.

4.0 RESULTS AND EVALUATION

4.1 Static Tests

Preliminary static testing of flattened tubular specimens was done on HT graphite specimens of $[+45/0]_s$ construction. Failure modes of these specimens are shown in Fig. 7. Stress-strain curves for two of these tests are shown in Figs. 8 and 9. Average properties obtained from these data are:

$$E_{xx} = 54 \text{ GPa } (7.9 \times 10^6 \text{ psi})$$

$$\nu_{xy} = 0.64$$

$$S_{xxT} = 450 \text{ MPa } (65 \text{ ksi})$$

$$\varepsilon^u_{xx} = 8.4 \times 10^{-3}$$

For comparison purposes flat coupons of the same material and layup were prepared and tested in uniaxial tension. Stress-strain curves for these coupons are shown in Figs. 10 and 11. Average properties obtained from these data are:

$$E_{xx} = 58 \text{ GPa } (8.5 \times 10^6 \text{ psi})$$

$$\nu_{xy} = 0.74$$

$$S_{xxT} = 418 \text{ MPa } (61 \text{ ksi})$$

$$\varepsilon^u_{xx} = 7.2 \times 10^{-3}$$

Both the strength and ultimate strain in the flattened tubular specimens are somewhat higher than those in the flat coupons of the same layup.

Static test results for the flattened tubular specimens of the nine different layups of Table 1 are presented in Table 2. Various tab reinforcing schemes were used on these specimens as described before. The most successful one, that of inserting

Fig. 7 FLATTENED TUBE SPECIMENS OF $[\pm 45/0]_s$ HT GRAPHITE/EPOXY AFTER FAILURE UNDER UNIAXIAL TENSION.

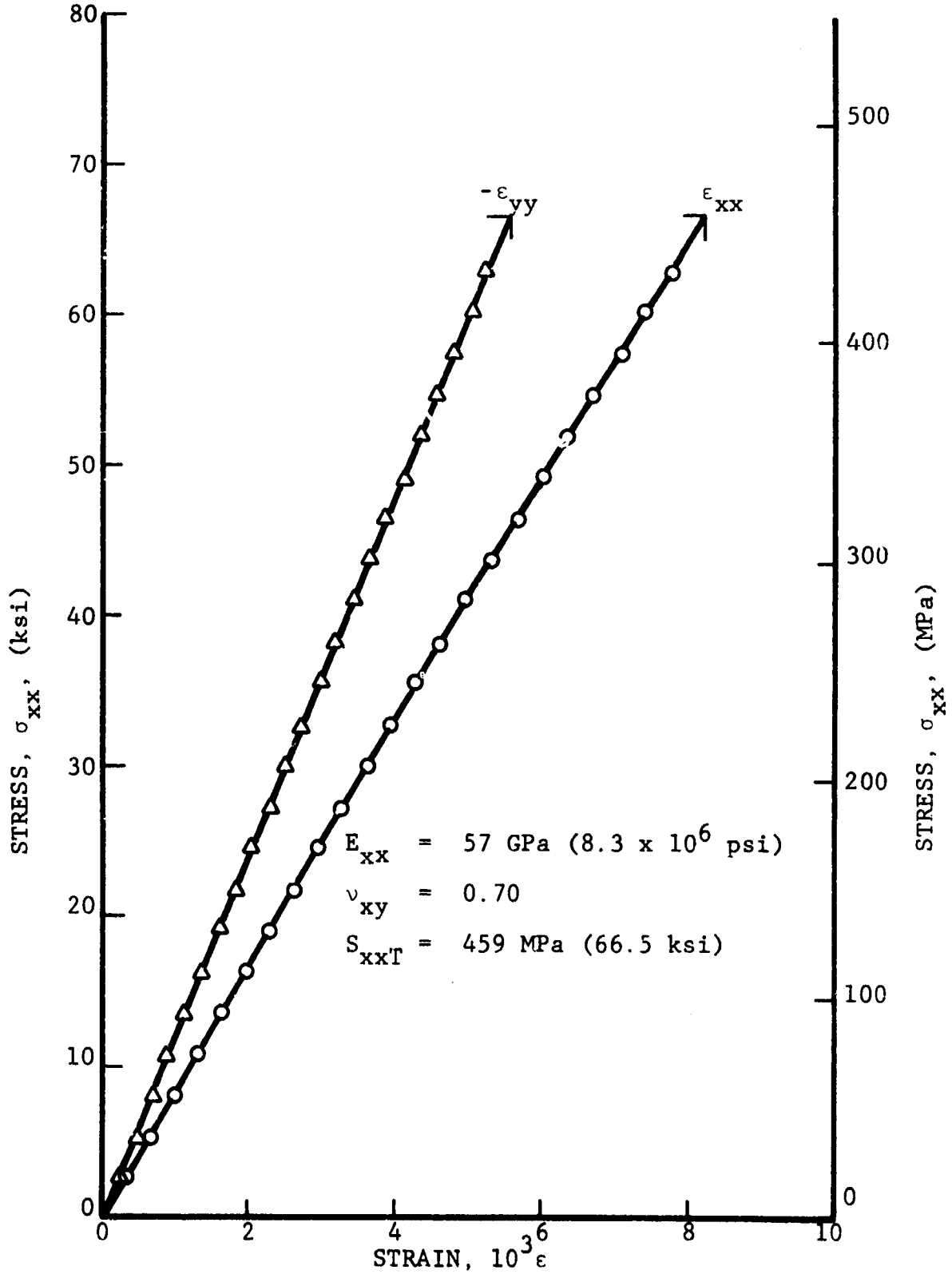

Fig. 8 STRAINS IN UNIAXIALLY LOADED FLATTENED TUBE OF $[\pm 45/0]_s$ HT GRAPHITE/EPOXY

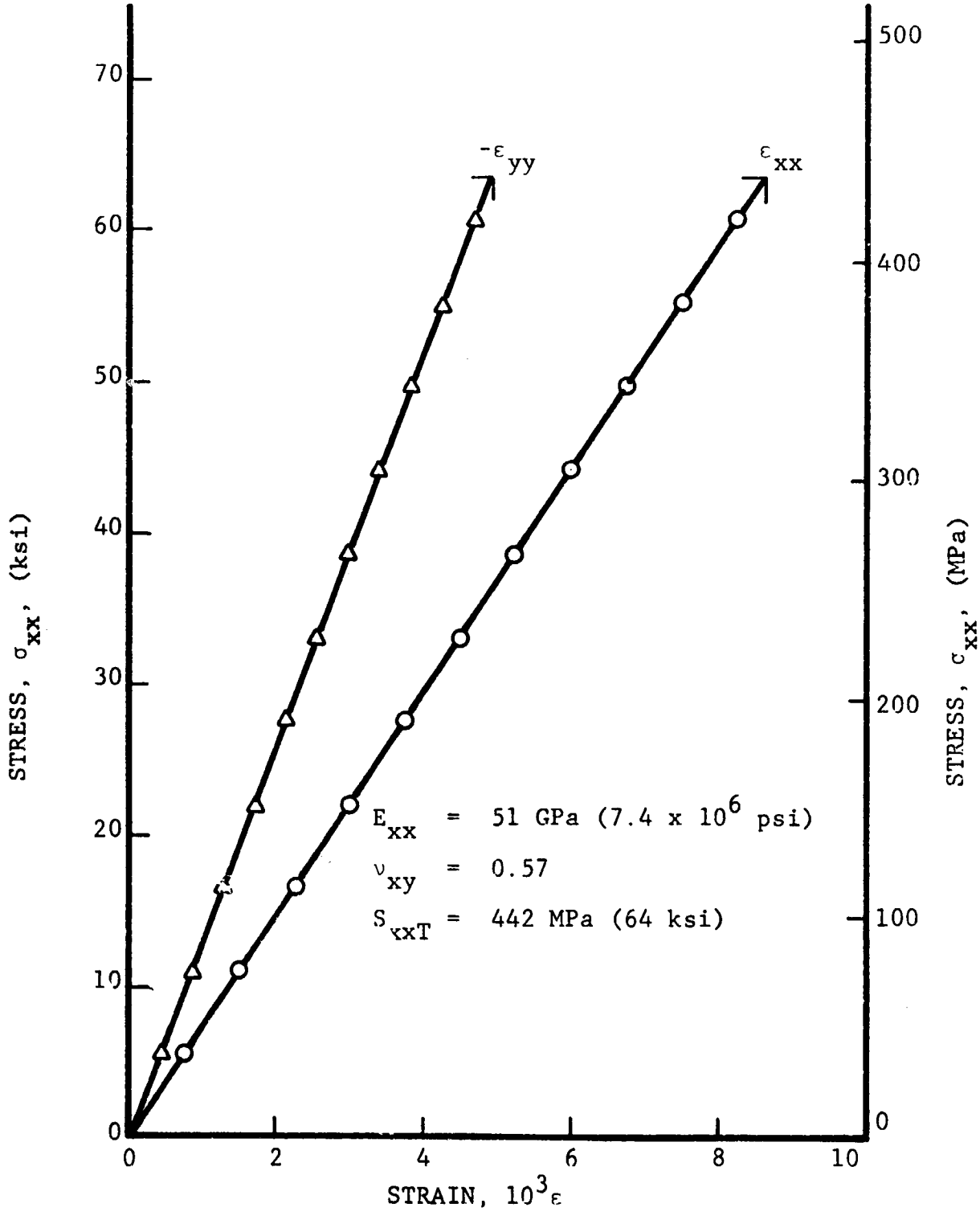

Fig. 9 STRAINS IN UNIAXIALLY LOADED FLATTENED TUBE OF $[\pm 45/0]_s$ HT-GRAPHITE/EPOXY

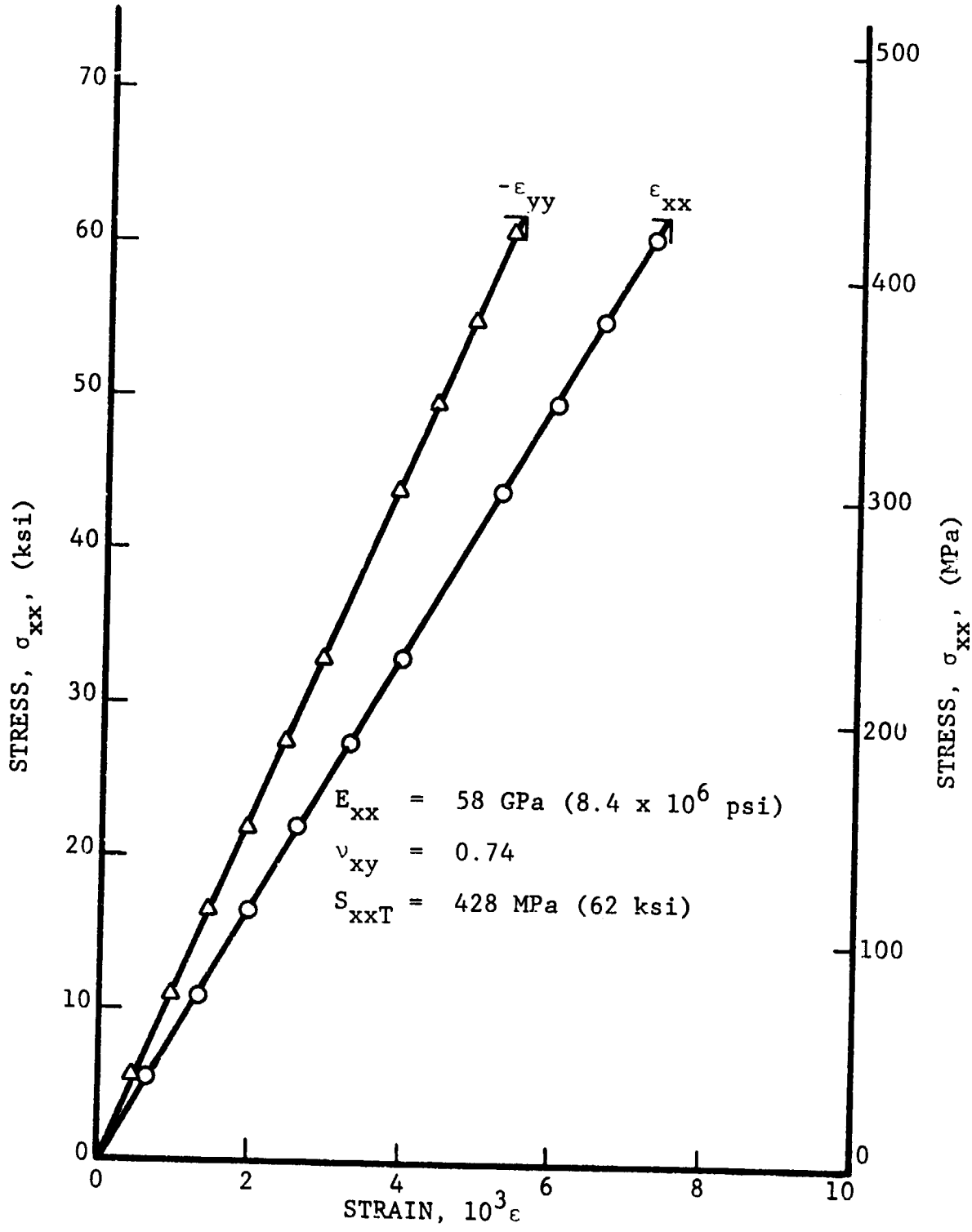

Fig. 10 STRAINS IN UNIAXIALLY LOADED FLAT COUPON OF $[\pm 45/0]_s$ HT-GRAPHITE/EPOXY

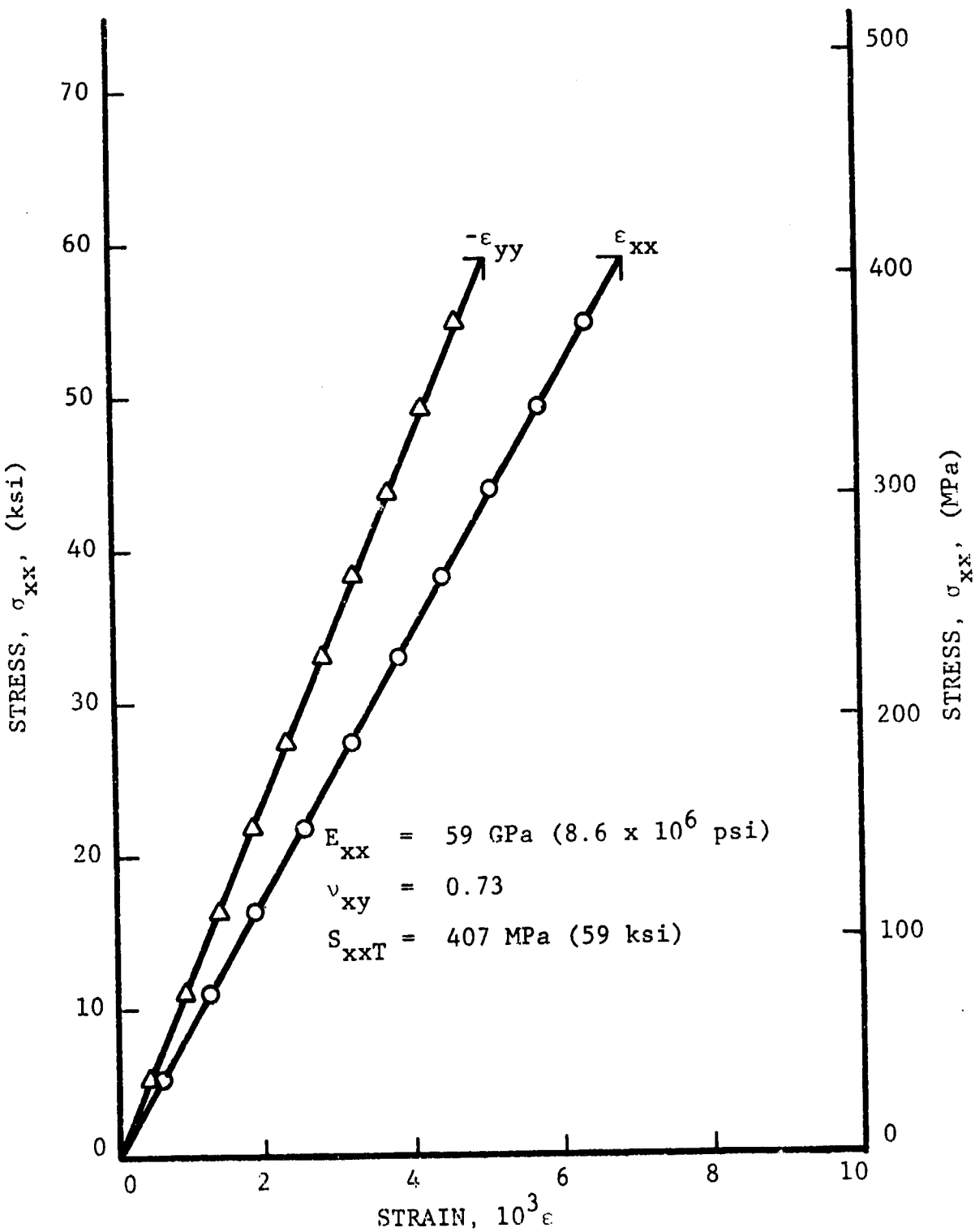

Fig. 11 STRAINS IN UNIAXIALLY LOADED FLAT COUPON OF $[\pm 45/0]_s$ HT-GRAPHITE/EPOXY

Table 2

RESULTS OF STATIC TENSILE TESTS OF FLATTENED TUBULAR SPECIMENS

Material	Specimen Layup	Tensile Failure Stress MPa	(ksi)	Failure Strain ε_{xx} (10-3 m/m)	Tensile Modulus E_{xx} GPa	(10^6 psi)	Poisson's Ratio ν_{xy}
S-Glass/Epoxy	$[\pm 45/0_2]_s$	865	(126)	30.4	37	(5.3)	0.38
		858	(124)	29.5	36	(5.3)	0.44
		834	(121)	30.3	37	(5.3)	0.40
PRD-49-III/ Epoxy	$[\pm 45/0_2]_s$	699	(101)	17.3	41	(5.9)	0.70
		659	(96)	15.4	45	(6.5)	0.79
		628	(91)	16.0	42	(6.1)	0.85
HT-Graphite/ Epoxy	$[\pm 45/0_2]_s$	798	(116)	7.2	110	(16.0)	0.63
		768	(111)	6.8	112	(16.3)	0.64
		630	(91)	6.1	101	(14.7)	0.66
HT-Graphite/ S-Glass/Epoxy	$[\pm 45^C/0^G]_s$	433*	(63)*	13.8	41	(5.9)	0.62
		424*	(61)*	15.6	32	(4.7)	0.66
		407*	(59)*	21.2	37	(5.3)	0.68
HT-Graphite/ S-Glass/Epoxy	$[\pm 45^C/0_2^G]_s$	632	(92)	22.1	39	(5.6)	0.61
		598*	(87)*	20.4	36	(5.2)	0.52
		506*	(73)*	13.8	41	(5.9)	0.63
PRD-49-III/ S-Glass/Epoxy	$[\pm 45^P/0_2^G]_s$	642	(93)	24.5	30	(4.3)	0.50
		611	(88)	15.6	40	(5.7)	0.70
		564*	(82)*	21.2	31	(4.5)	0.63
PRD-49-III/ S-Glass/Epoxy	$[\pm 45^P/0_4^G]_s$	933	(135)	28.2	36	(5.2)	0.57
		877	(127)	25.6	36	(5.2)	0.45
		689*	(100)*	20.0	37	(5.3)	0.50

*Failure at or near tab

- - - continued - - -

Table 2 (continued)

RESULTS OF STATIC TENSILE TESTS OF FLATTENED TUBULAR SPECIMENS

Material	Specimen Layup	Tensile Failure Stress MPa	Tensile Failure Stress (ksi)	Failure Strain, ε_{xx} (10^{-3} m/m)	Tensile Modulus E_{xx} GPa	Tensile Modulus E_{xx} (10^6 psi)	Poisson's Ratio ν_{xy}
HT-Graphite/ PRD-49-III/Epoxy	$[\pm 45^C/0^P]_s$	457*	(66)*	11.7	46	(6.7)	0.71
		447*	(65)*	12.1	47	(6.8)	0.75
		400*	(58)*	12.6	39	(5.6)	0.58
HT-Graphite/ PRD-49-III/Epoxy	$[\pm 45^C/0_2^P]_s$	635*	(92)*	13.7	54	(7.8)	0.70
		623*	(90)*	13.6	51	(7.4)	0.70
		443*	(64)*	9.3	52	(7.5)	0.78
H-Graphite/ Epoxy	$[\pm 45/0]_s$	459	(67)	8.3	57	(8.3)	0.70
		442	(64)	8.6	51	(7.4)	0.57
		454	(66)	-	-	-	-

*Failure at or near tab

reinforcing plies under the outer plies of the specimen was conceived and applied late in the program. Consequently not all static tests produced failures in the test section. Those specimens which failed at the tabs or in close proximity to them are indicated by an asterisk in the failure stress column of Table 2. This type of failure most likely indicates that the full strength of the specimen is higher than that obtained in the test.

Uniaxial static tension tests were also performed on flat coupons of S-glass/epoxy, PRD-49-III/epoxy and HT graphite/epoxy of $[\pm 45/0_2]_s$ construction. These were performed in order to compare their static properties with those of corresponding flattened tubular specimens. The results for these flat coupon static tests, including those of the previously discussed HT graphite/epoxy $[\pm 45/0]_s$ coupons, are shown in Table 3.

Typical failure modes of flattened tubular specimens which failed in the test section are shown in Figs. 12 and 13. The stretch-pinch mode of failure illustrated in Fig. 13 was characteristic of those specimens whose outer plies were either $\pm$45-degree S-glass/epoxy or PRD-49-III/epoxy. This failure mode is a consequence of the continuous character of the $\pm$45-degree fibers in an edgeless specimen. It is more pronounced for the S-glass and PRD-49-III fibers than for the HT graphite fibers because the former have a much lower modulus and higher elongation capability than the HT graphite fibers.

The stress-strain curves for three statically tested flattened tubular specimens of $[\pm 45/0_2]_s$ S-glass/epoxy are shown in Figs. 14, 15 and 16. All three specimens show mild nonlinear behavior to failure. They all failed in the characteristic stretch-pinch mode which was illustrated in Fig. 13. The failures occurred partially in the test section and partially under the tab overdrape

Table 3

RESULTS OF STATIC TENSILE TESTS OF FLAT COUPONS

Material	Specimen Layup	Tensile Failure Stress MPa	Tensile Failure Stress (ksi)	Failure Strain, ε_{xx} (10^{-3} m/m)	Tensile Modulus E_{xx} GPa	Tensile Modulus E_{xx} (10^6 psi)	Poisson's Ratio ν_{xy}
S-Glass/Epoxy	$[\pm 45/0_2]_s$	977	(142)	34.3	38	(5.5)	0.42
		909	(132)	34.0	37	(5.4)	0.42
PRD-49-III/ Epoxy	$[\pm 45/0_2]_s$	701	(102)	17.0	41	(6.0)	0.86
		687	(100)	17.9	39	(5.6)	0.82
HT-Graphite/ Epoxy	$[\pm 45/0_2]_s$	776	(112)	6.2	125	(18.2)	0.74
		638	(93)	5.5	119	(17.2)	0.71
HT-Graphite/ Epoxy	$[\pm 45/0]_s$	428	(62)	7.4	58	(8.4)	0.74
		407	(59)	6.9	59	(8.6)	0.73

Fig. 12 TYPICAL FAILURE MODES OF FLATTENED TUBULAR SPECIMENS

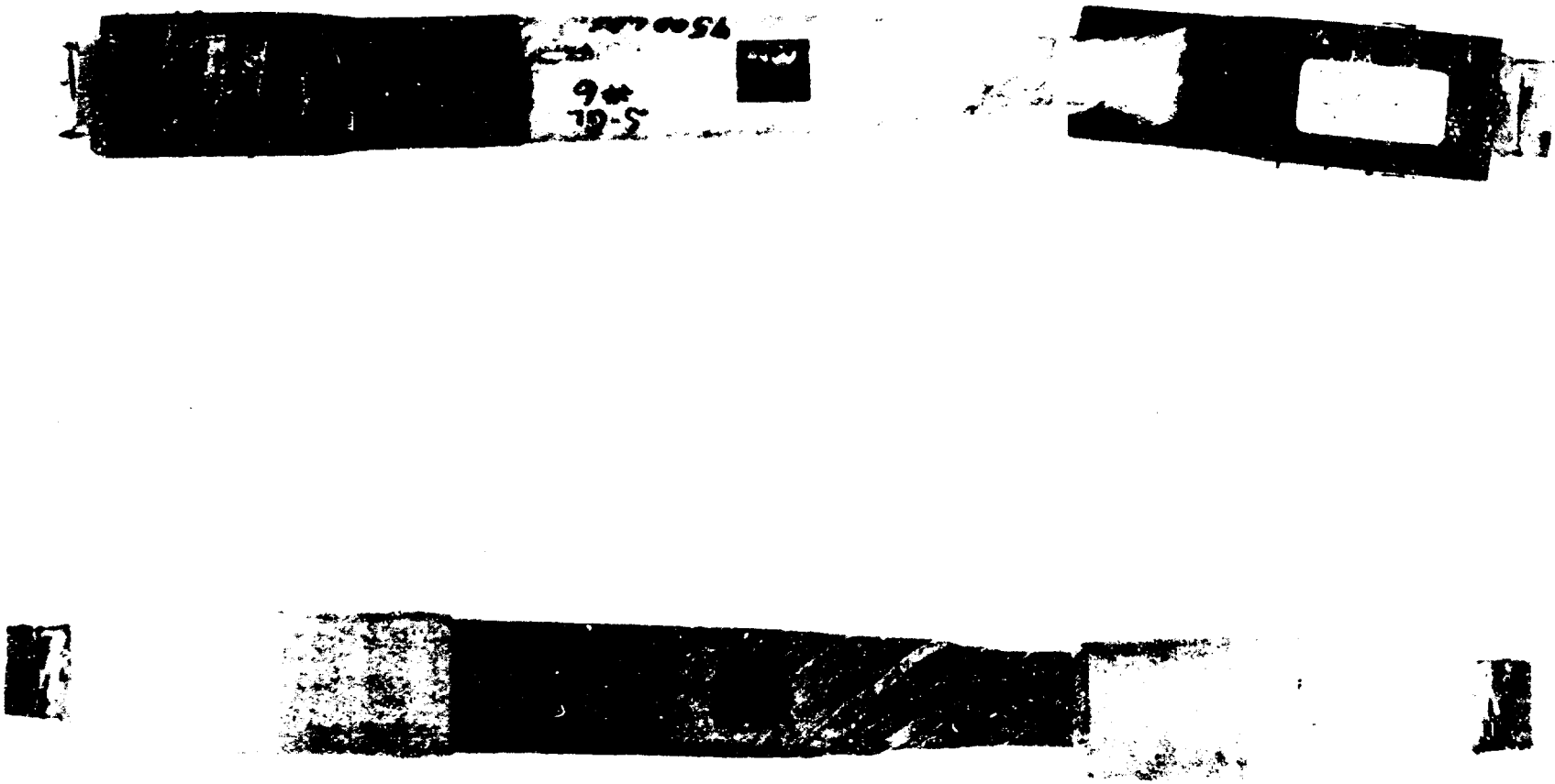

Fig. 13 FAILURE MODES OF FLATTENED TUBULAR SPECIMENS OF S-GLASS/ EPOXY AND PRD-49-III/EPOXY

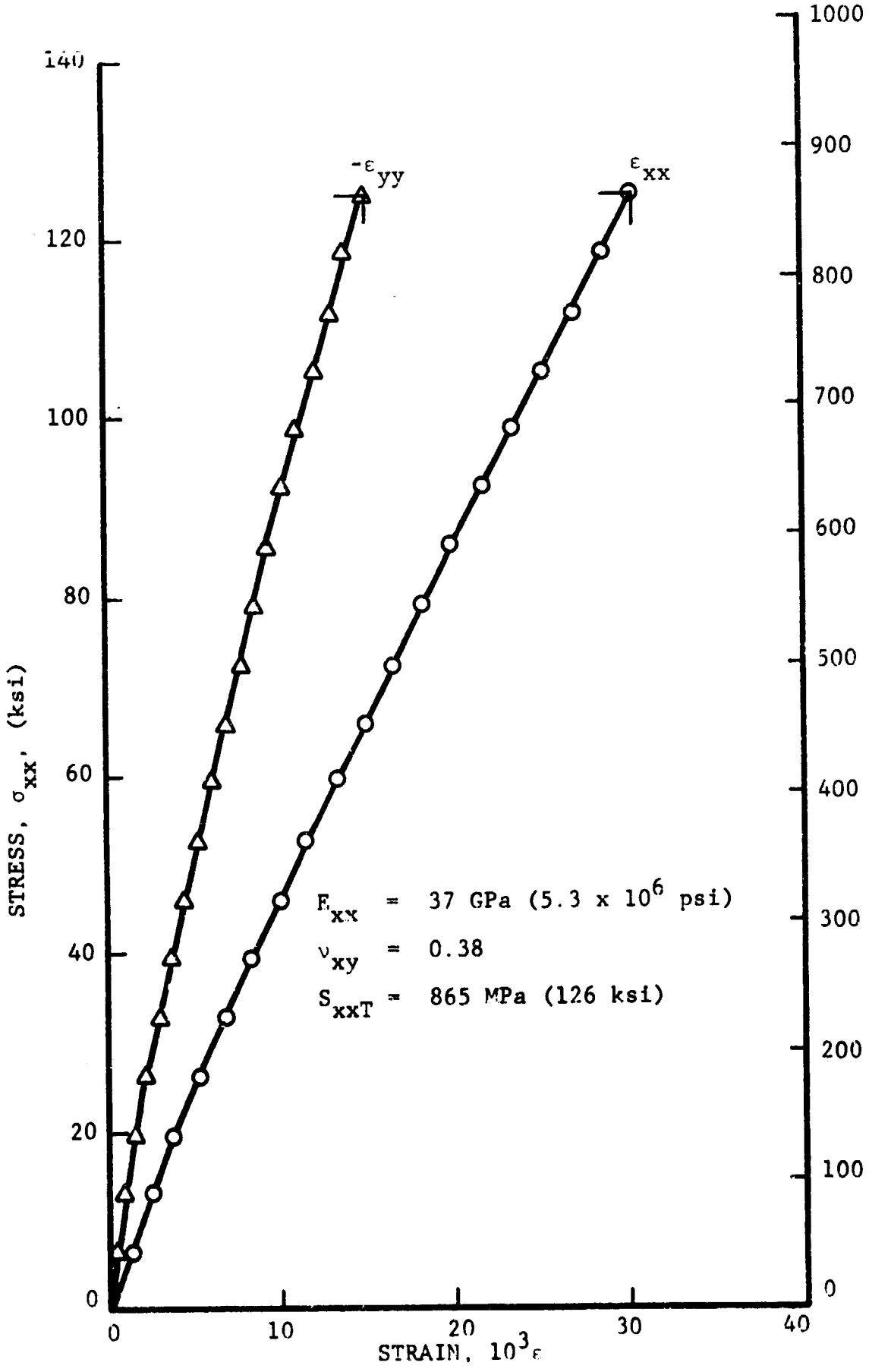

Fig. 14 STRAINS IN UNIAXIALLY LOADED FLATTENED TUBE OF $[\pm 45/0_2]_s$ S-GLASS/EPOXY

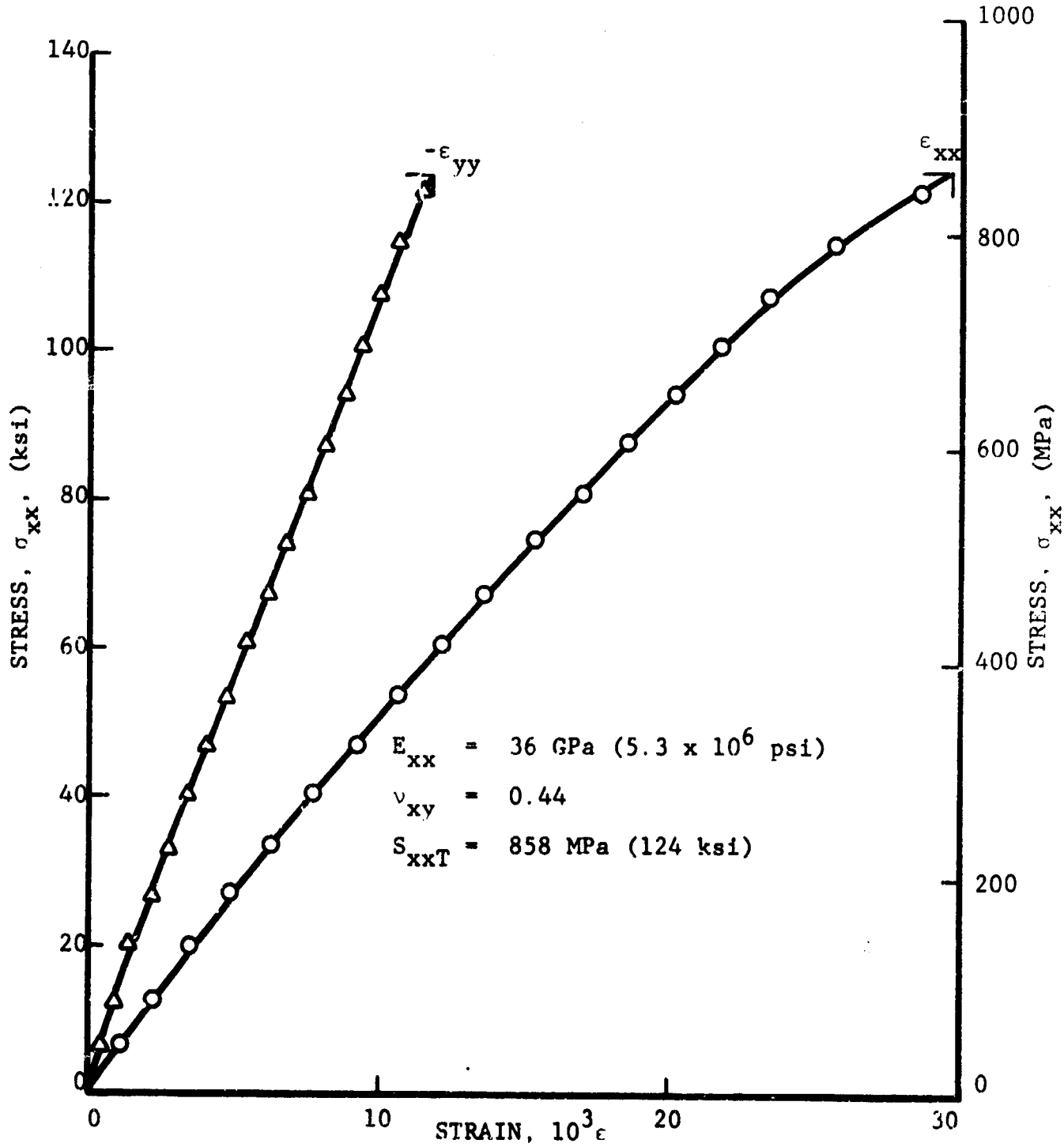

Fig. 15 STRAINS IN UNIAXIALLY LOADED FLATTENED TUBE OF $[\pm 45/0_2]_s$ S-GLASS/EPOXY

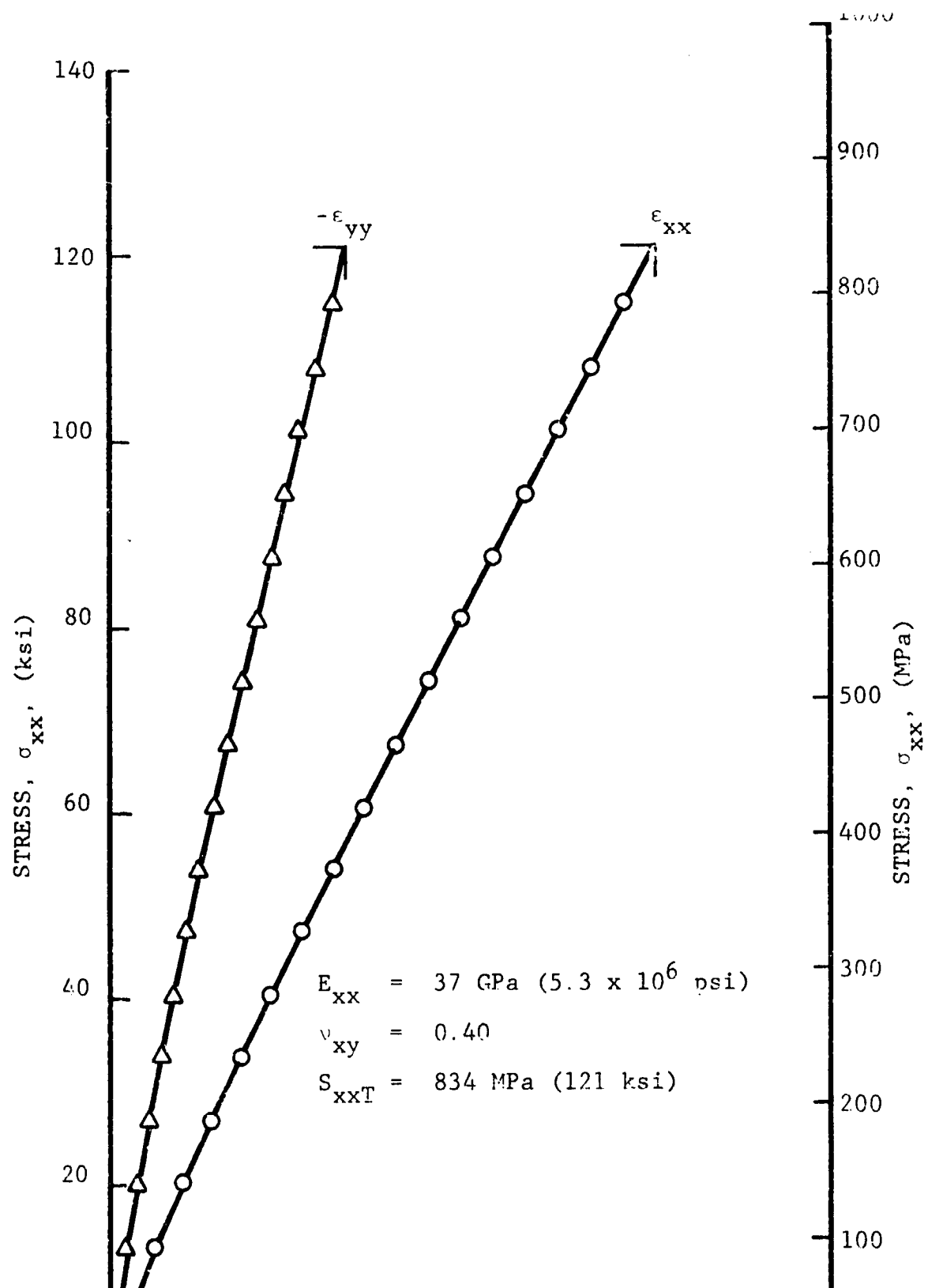

Fig. 16 STRAINS IN UNIAXIALLY LOADED FLATTENED TUBE OF $[\pm 45/0_2]_s$ S-GLASS/EPOXY

near one tab. All specimens showed close correspondence of properties as can be seen from the data in the figures. Average property values for these specimens are:

$$E_{xx} = 37 \text{ GPa } (5.3 \times 10^6 \text{ psi})$$

$$\nu_{xy} = 0.41$$

$$S_{xxT} = 852 \text{ MPa } (124 \text{ ksi})$$

$$\varepsilon^u_{xx} = 30.0 \times 10^{-3}$$

Stress-strain curves for the flat coupons of $[\pm 45/0_2]_s$ S-glass/epoxy are shown in Figs. 17 and 18. They exhibit similar nonlinear stress-strain behavior to failure as the corresponding flattened tubular specimens. Both coupons show close correspondence of properties and failure loads as can be seen from the data listed on the figures. Average property values for the two specimens are:

$$E_{xx} = 37.5 \text{ GPa } (5.45 \times 10^6 \text{ psi})$$

$$\nu_{xy} = 0.42$$

$$S_{xxT} = 943 \text{ MPa } (137 \text{ ksi})$$

$$\varepsilon^u_{xx} = 34.1 \times 10^{-3}$$

Both the strength and ultimate strains of the flat coupons are higher than those for the flattened tubular specimens. This is contrary to what can be expected based on the results obtained for the HT graphite/epoxy and PRD-49-III/epoxy specimens. It has been caused most likely by nonoptimal tubular specimen quality combined with the nonoptimal tab reinforcement procedure, as manifested by the failures occurring partially under the tab overdrapes.

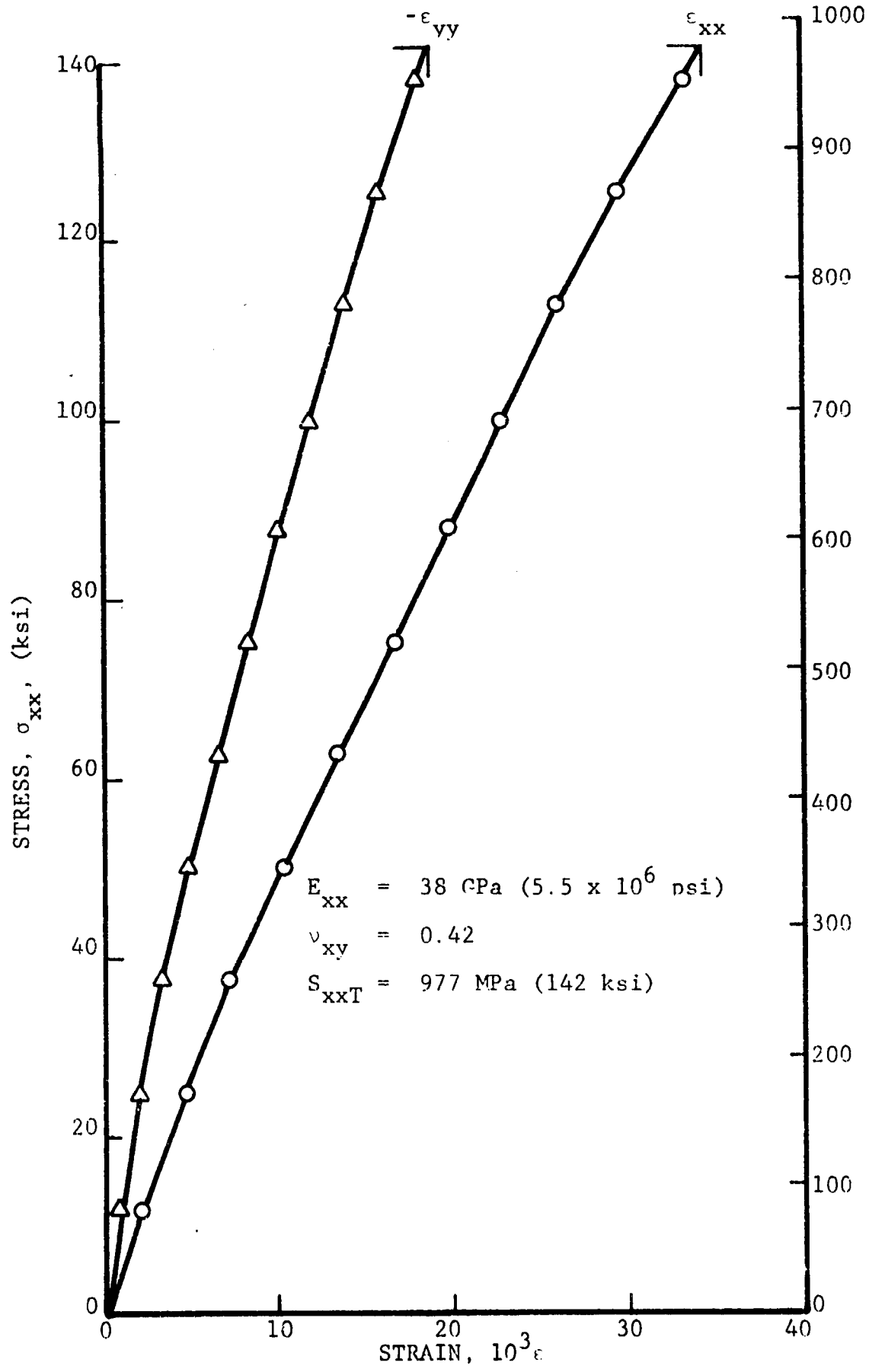

Fig. 17 STRAINS IN UNIAXIALLY LOADED FLAT COUPON OF $[\pm 45/0_2]_s$ S-GLASS/EPOXY

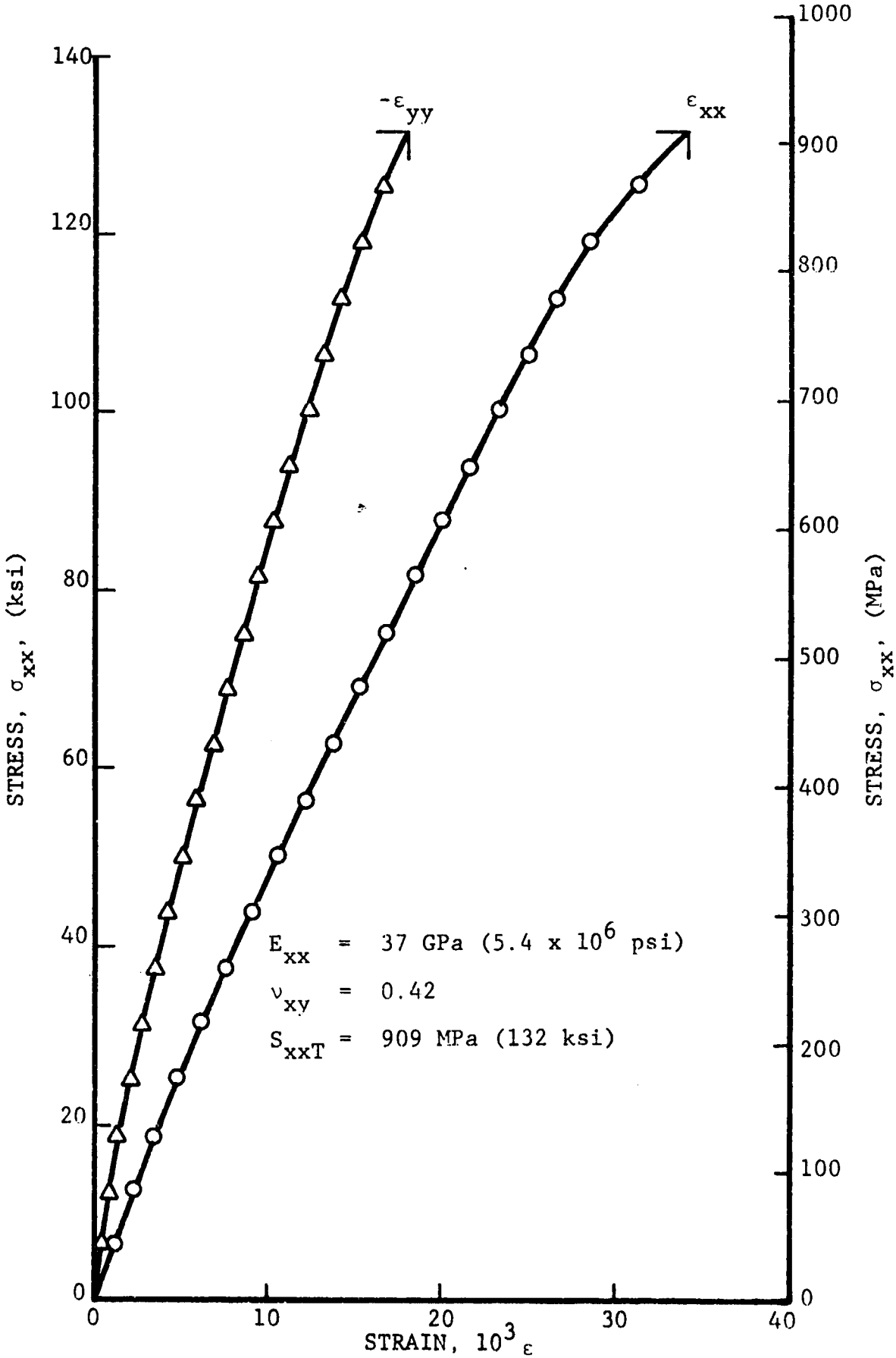

Fig. 18 STRAINS IN UNIAXIALLY LOADED FLAT COUPON OF $[\pm 45/0_2]_s$ S-GLASS/EPOXY

The stress-strain curves for the three statically tested flattened tubular specimens of $[\pm 45/0_2]_s$ PRD-49-III/epoxy are shown in Figs. 19, 20 and 21. The specimens of Figs. 20 and 21 show a small bend in the longitudinal strain at about 103 to 138 MPa (15 to 20 ksi) of load, but otherwise the longitudinal strains are linear. The bend probably indicates early nonprogressive damage in the specimen. The sharp change in curvature of the transverse strain in Fig. 20 is due to partial debonding of one of the transverse gages. All three specimens failed in the characteristic stretch-pinch mode partly in the test section and partly under the tab overdrape near one tab. The average properties of these specimens are:

$$E_{xx} = 43 \text{ GPa } (6.2 \times 10^6 \text{ psi})$$

$$\nu_{xy} = 0.78$$

$$S_{xxT} = 662 \text{ MPa } (96 \text{ ksi})$$

$$\varepsilon^u_{xx} = 16.2 \times 10^{-3}$$

Stress-strain curves for the flat coupons of $[\pm 45/0_2]_s$ PRD-49-III/epoxy are shown in Figs. 22 and 23. They show nonlinear stress-strain behavior to failure, and have close correspondence of properties. Average values for the properties of the two specimens are:

$$E_{xx} = 40.0 \text{ GPa } (5.8 \times 10^6 \text{ psi})$$

$$\nu_{xy} = 0.84$$

$$S_{xxT} = 694 \text{ MPa } (101 \text{ ksi})$$

$$\varepsilon^u_{xx} = 17.5 \times 10^{-3}$$

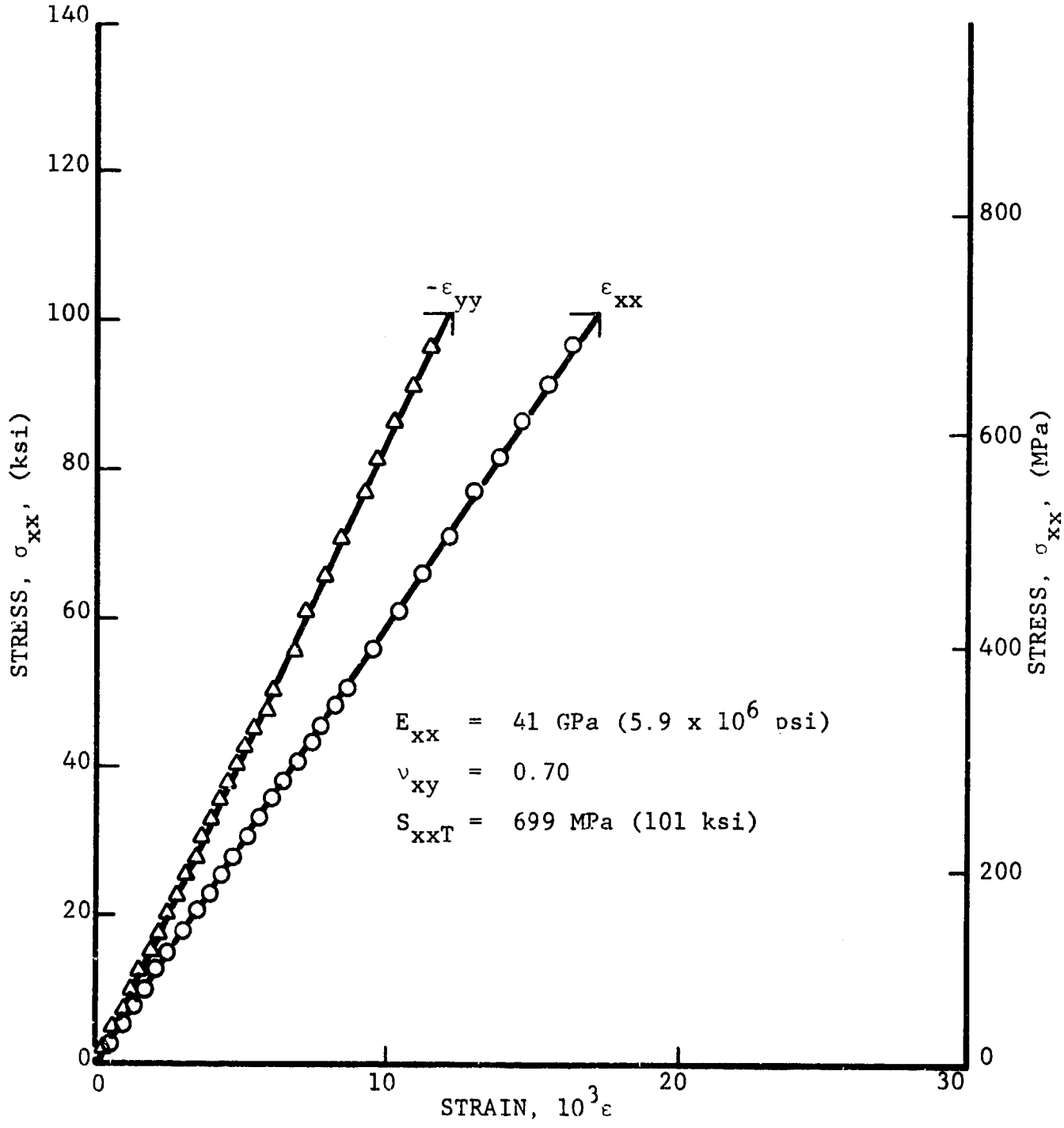

Fig. 19 STRAINS IN UNIAXIALLY LOADED FLATTENED TUBE OF $[\pm 45/0_2]_s$ PRD-49/EPOXY

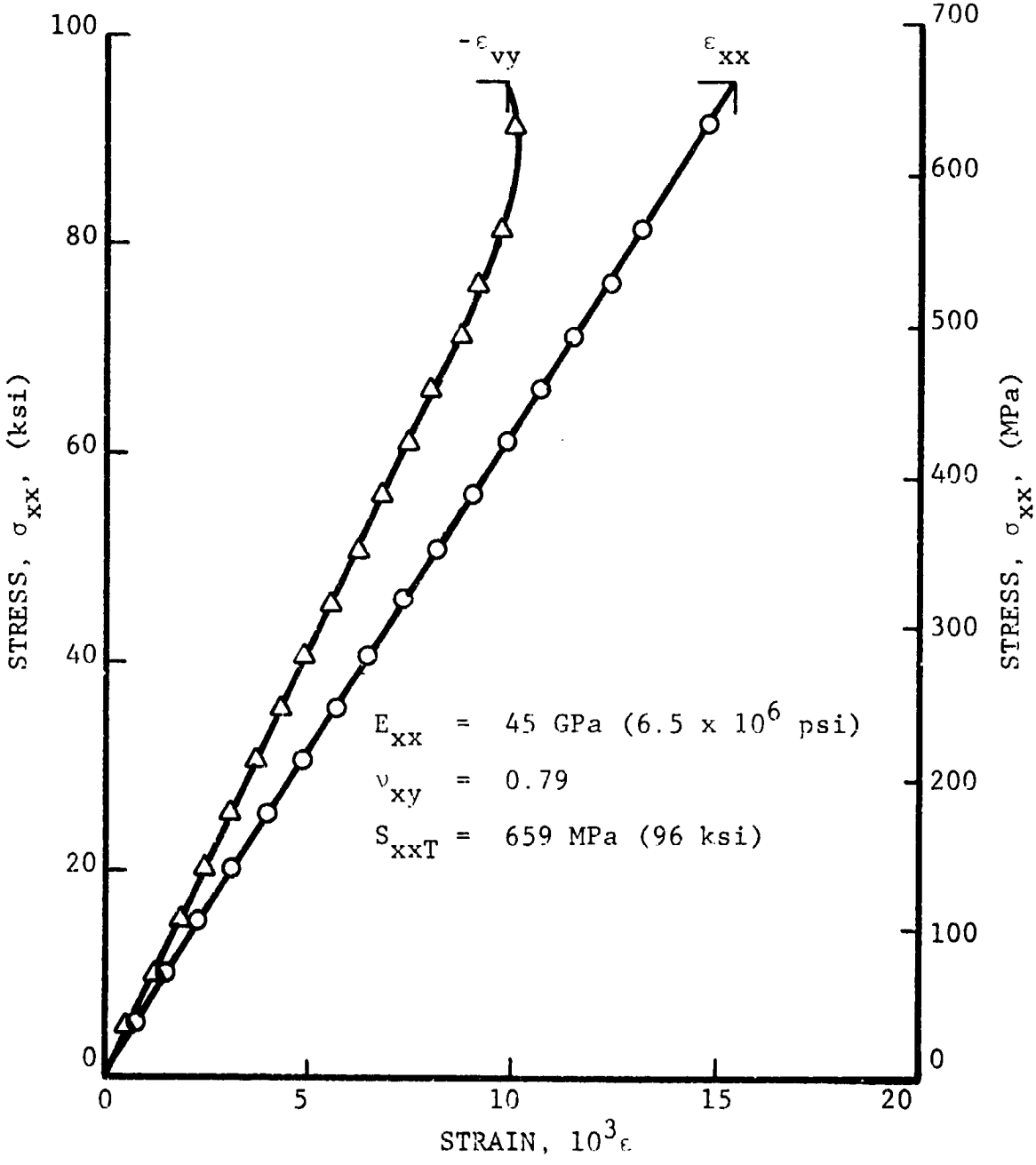

Fig. 20 STRAINS IN UNIAXIALLY LOADED FLATTENED TUBE OF $[\pm 45/0_2]_s$ PRD-49/EPOXY

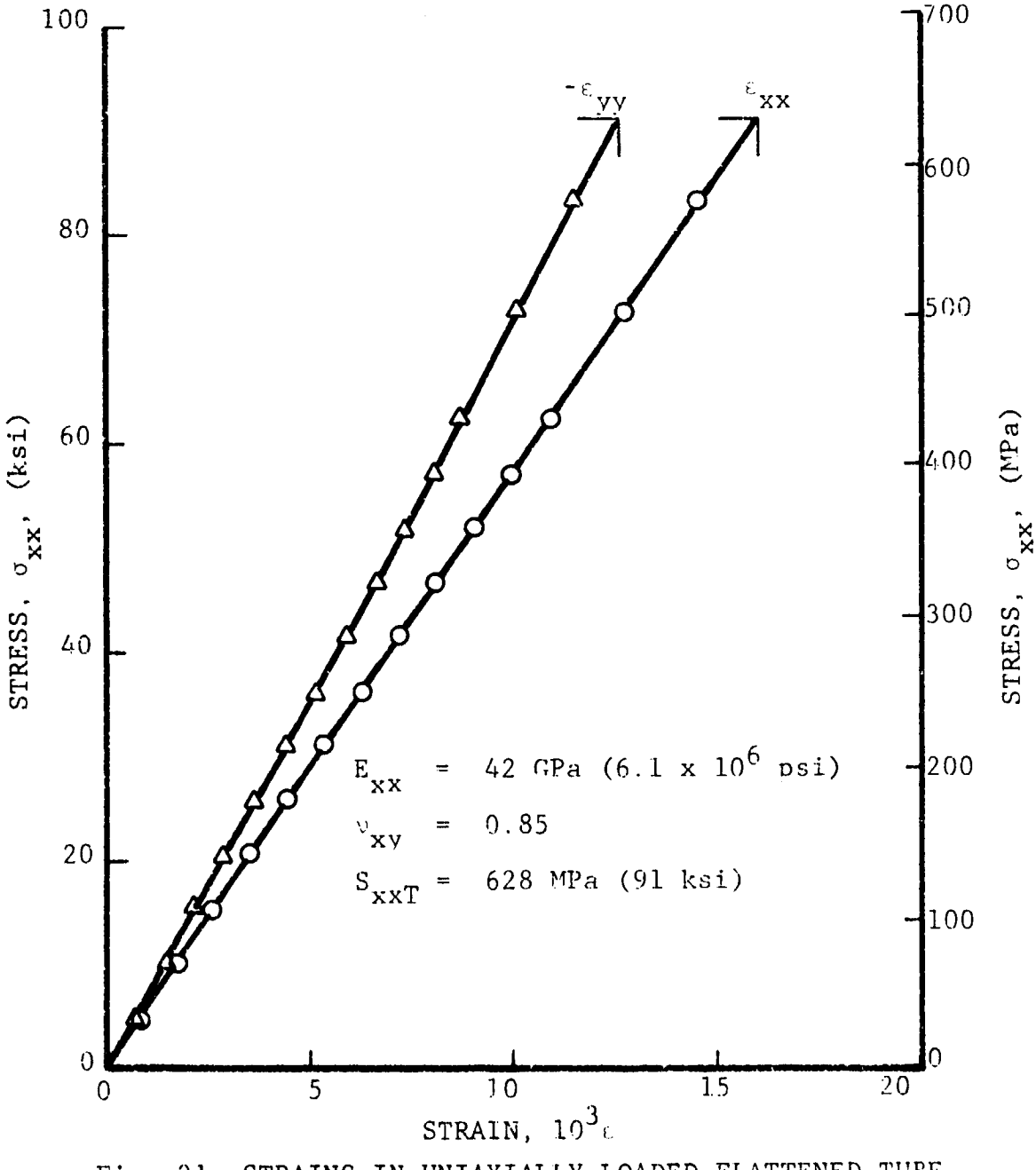

Fig. 21 STRAINS IN UNIAXIALLY LOADED FLATTENED TUBE OF $[\pm 45/0_2]_s$ PRD-49/EPOXY

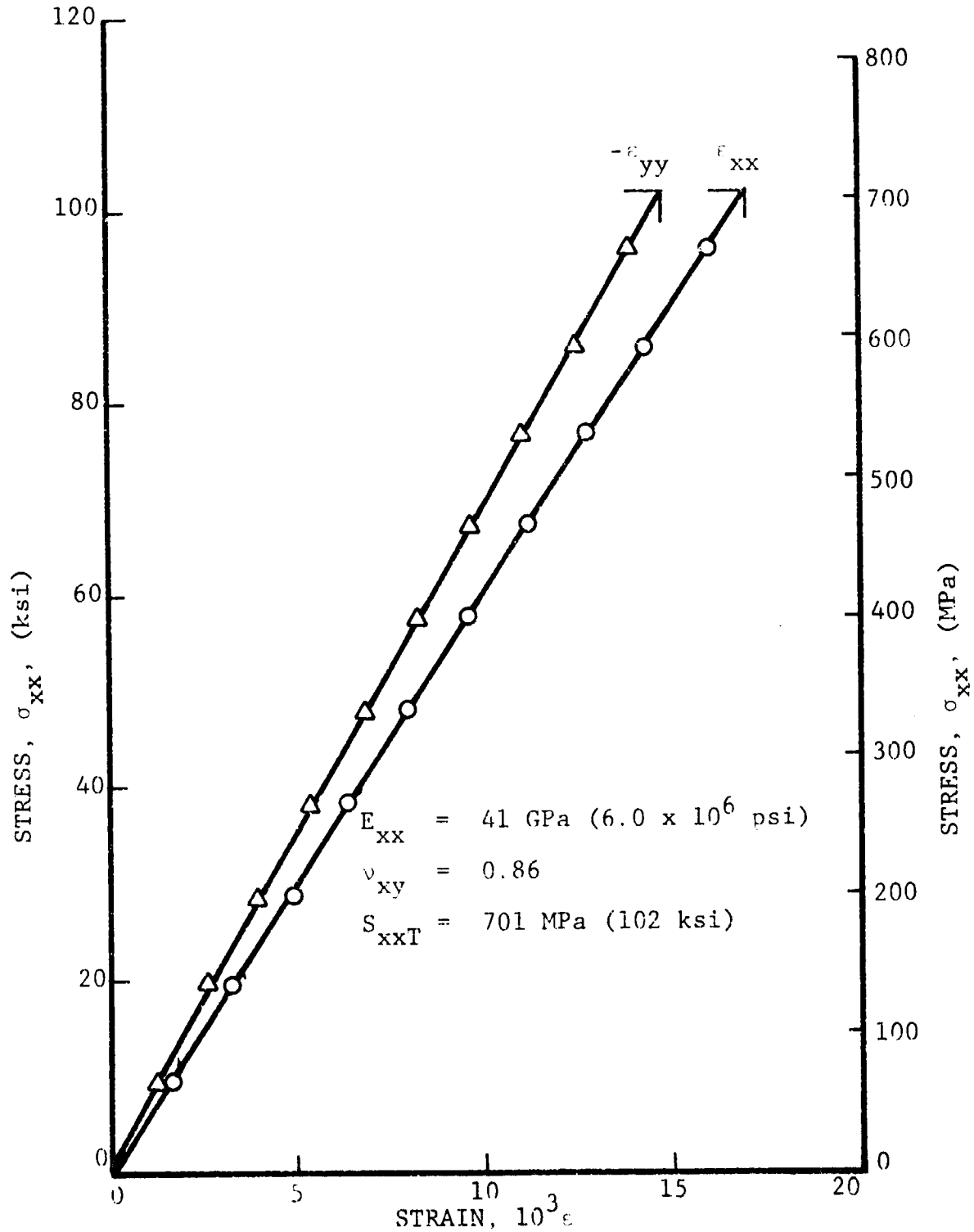

Fig. 22 STRAINS IN UNIAXIALLY LOADED FLAT COUPON OF $[\pm 45/0_2]_s$ PRD-49/EPOXY

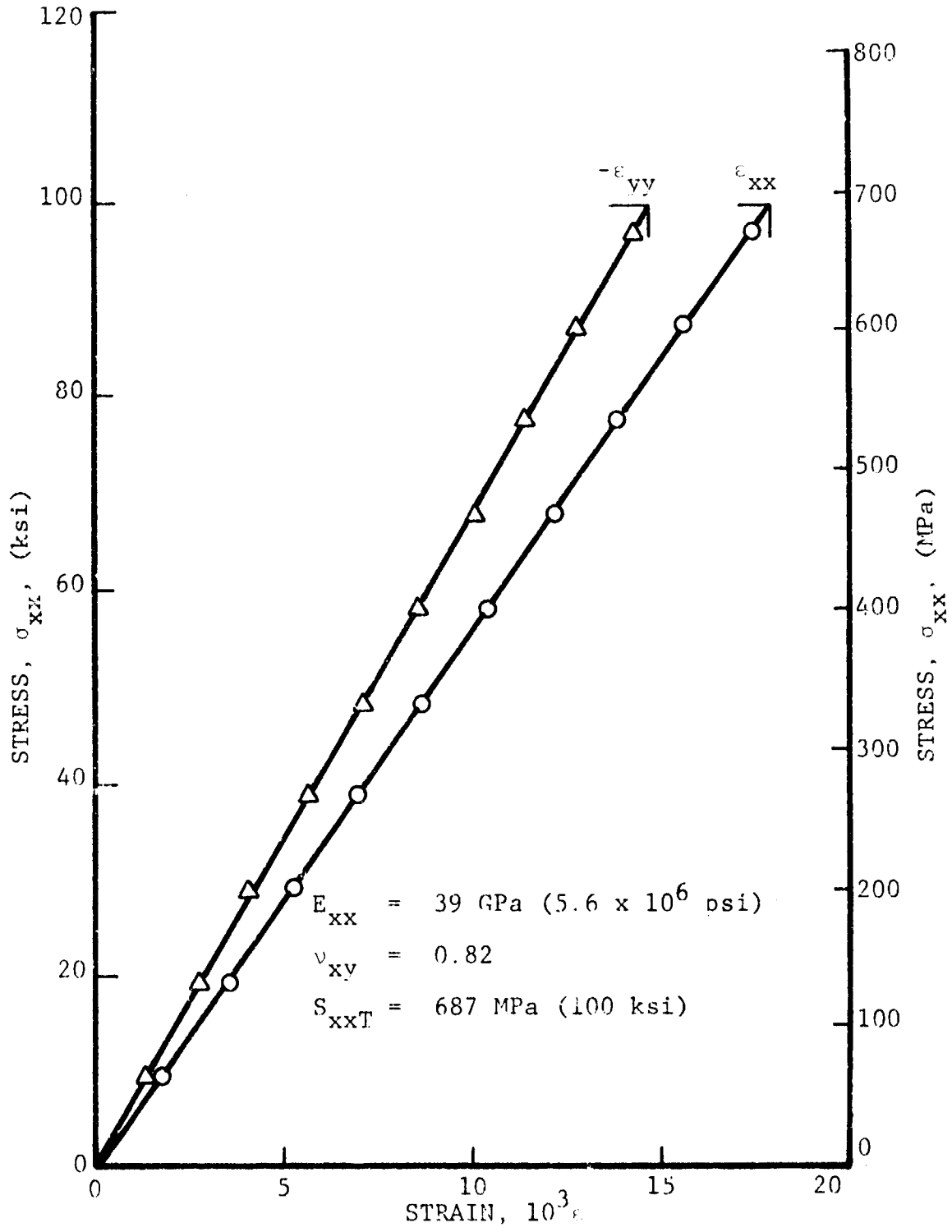

Fig. 23 STRAINS IN UNIAXIALLY LOADED FLAT COUPON OF $[\pm 45/0_2]_s$ PRD-49/EPOXY

These values are not significantly different from those of the flattened tubular specimens. Final conclusions cannot be drawn from these results since overdraping was used as the tab reinforcing technique which did not prove to be the best technique (see Section 2.4).

The stress-strain curves for the three statically tested flattened tubular specimens of $[\pm 45/0_2]_s$ HT graphite/epoxy are shown in Figs. 24, 25 and 26. The stress-strain curves are linear to failure showing no early or progressive degradation of properties. The low strength and modulus of the specimen of Fig. 26 is likely due to the fact that it was one of the early specimens made before the improved specimen fabrication technique was introduced as described in Section 2.2. The average properties of the three specimens are:

E_{xx} = 108 GPa (15.7 x 10^6 psi)

ν_{xy} = 0.64

S_{xxT} = 732 MPa (106 ksi)

ε^u_{xx} = 6.7 x 10^{-3}

Stress-strain curves for flat coupons of $[\pm 45/0_2]_s$ HT graphite/epoxy are shown in Figs. 27 and 28. As in the flattened tubular specimens they are linear to failure. Average values for their properties are:

E_{xx} = 122 GPa (17.7 x 10^6 psi)

ν_{xy} = 0.73

S_{xxT} = 707 MPa (103 ksi)

ε^u_{xx} = 5.9 x 10^{-3}

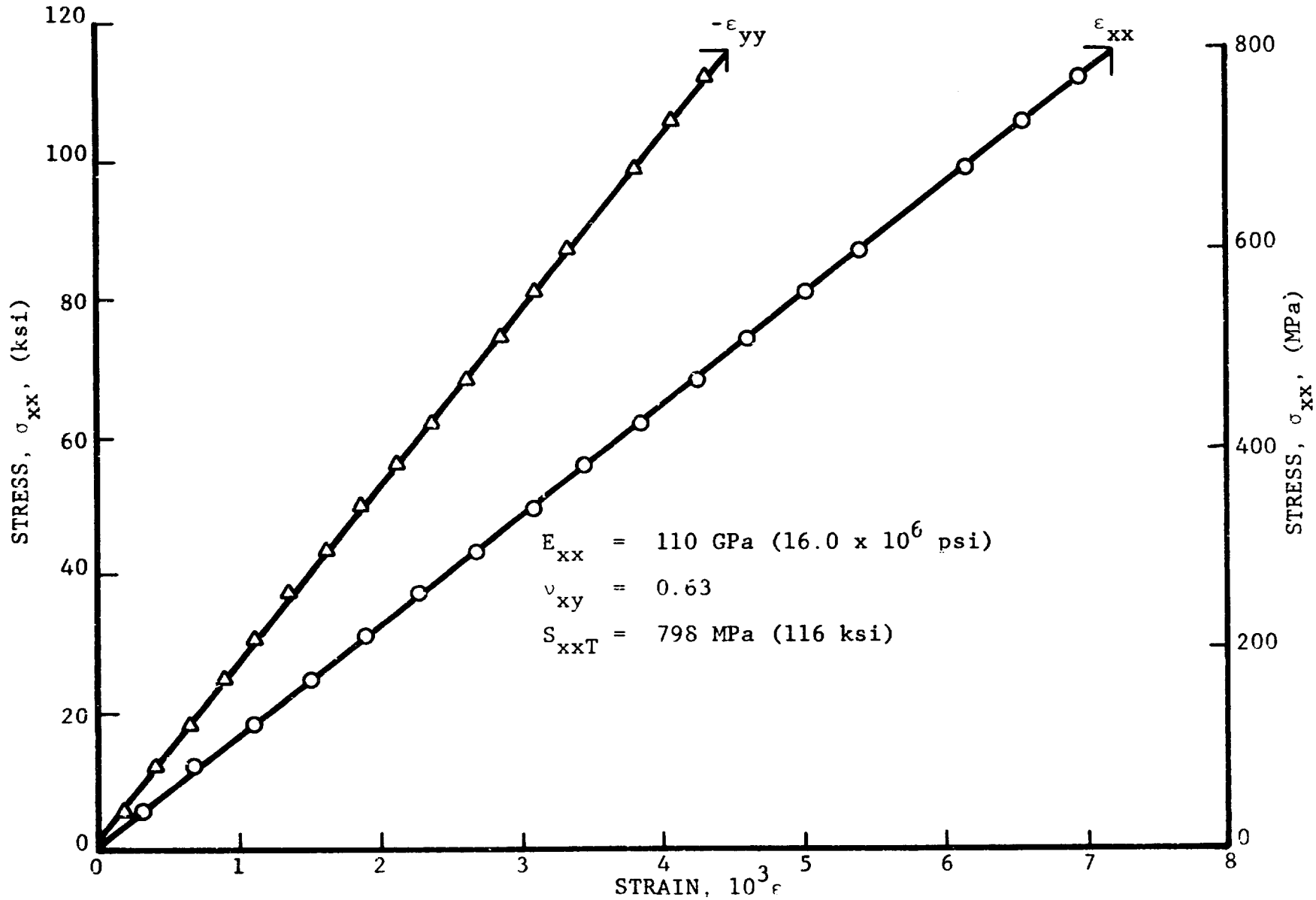

Fig. 24 STRAINS IN UNIAXIALLY LOADED FLATTENED TUBE OF $[\pm 45/0_2]_s$ GRAPHITE/EPOXY

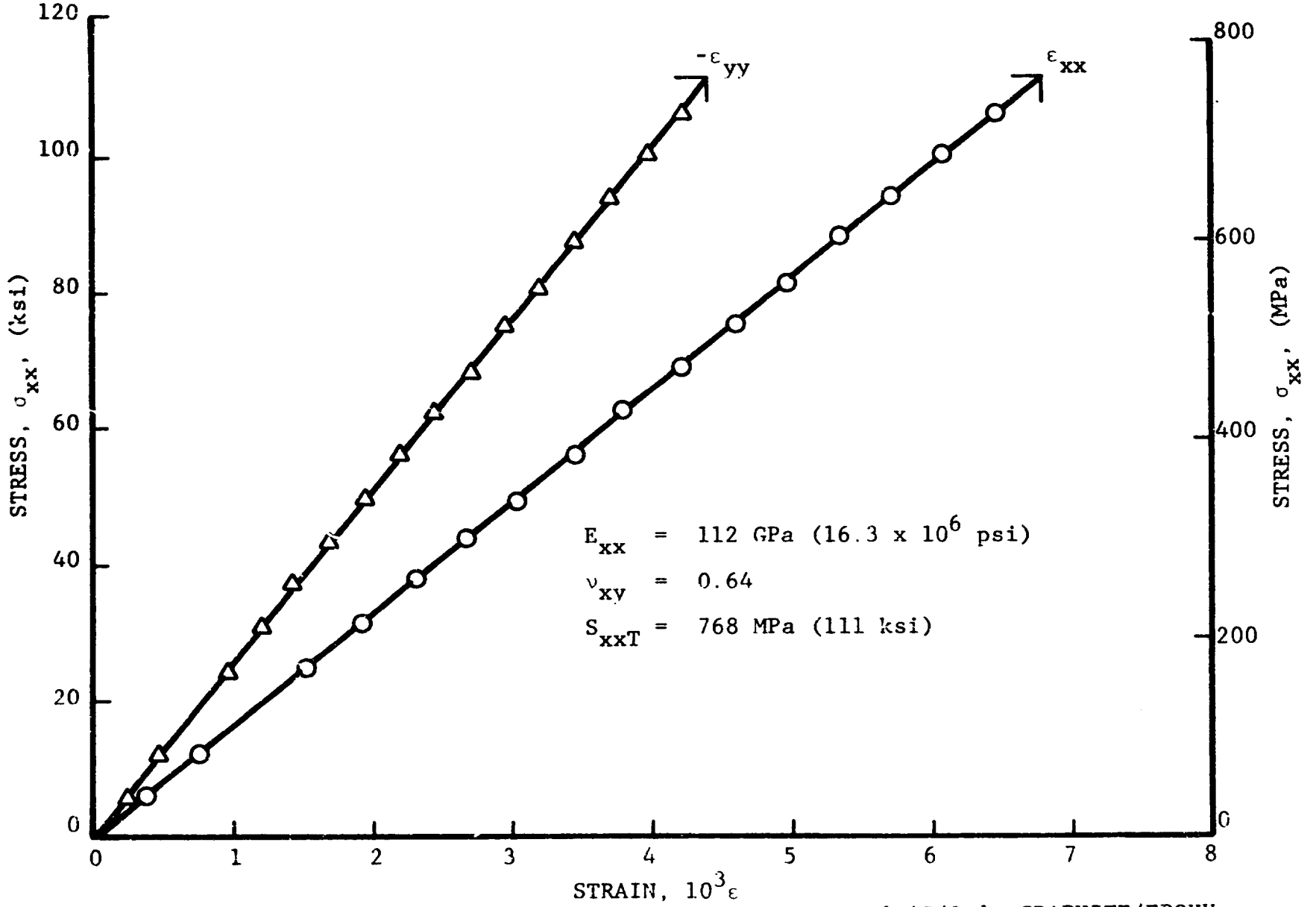

Fig. 25 STRAINS IN UNIAXIALLY LOADED FLATTENED TUBE OF $[\pm 45/0_2]_s$ GRAPHITE/EPOXY

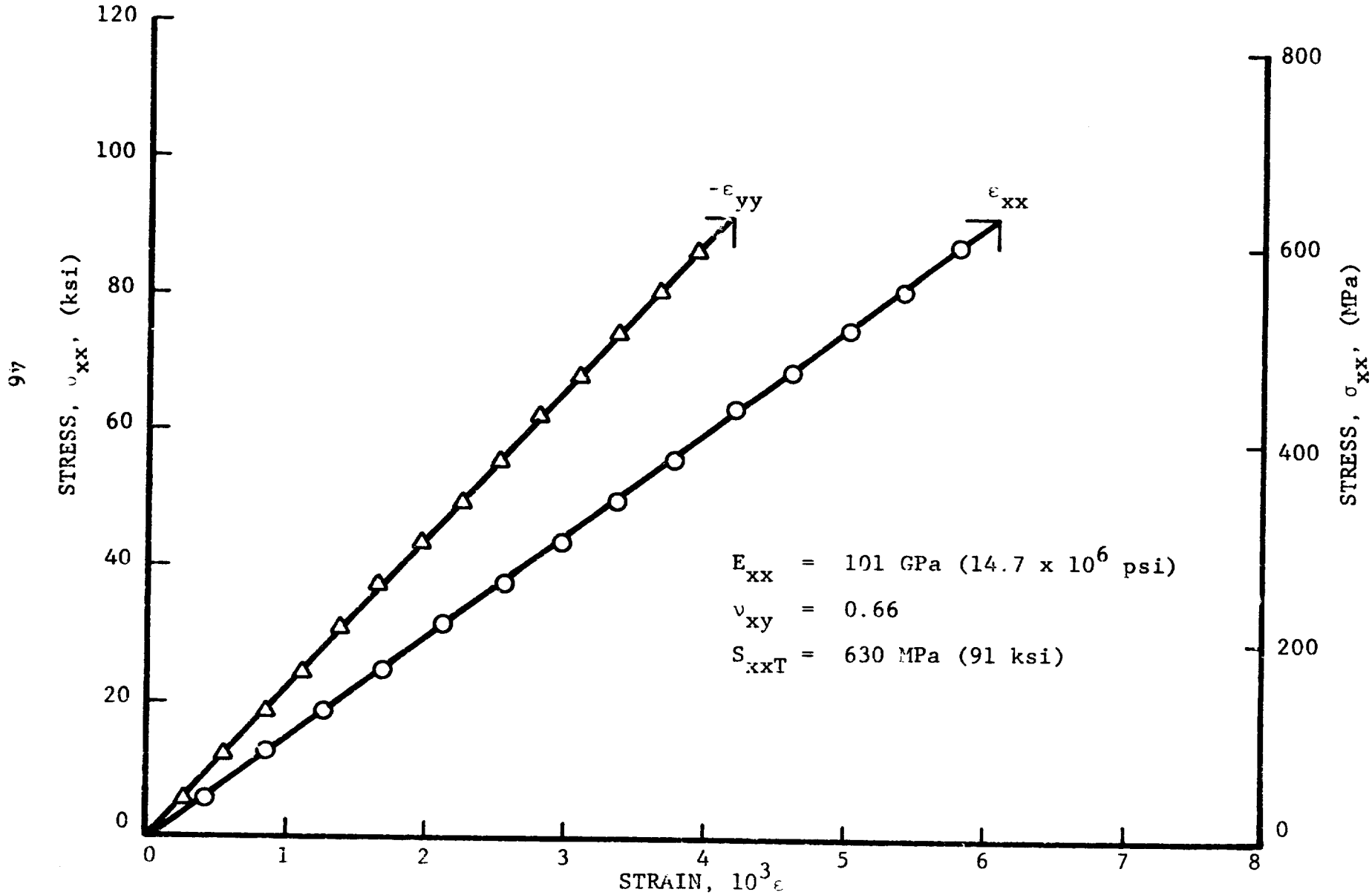

Fig. 26 STRAINS IN UNIAXIALLY LOADED FLATTENED TUBE OF $[\pm 45/0_2]_s$ GRAPHITE/EPOXY

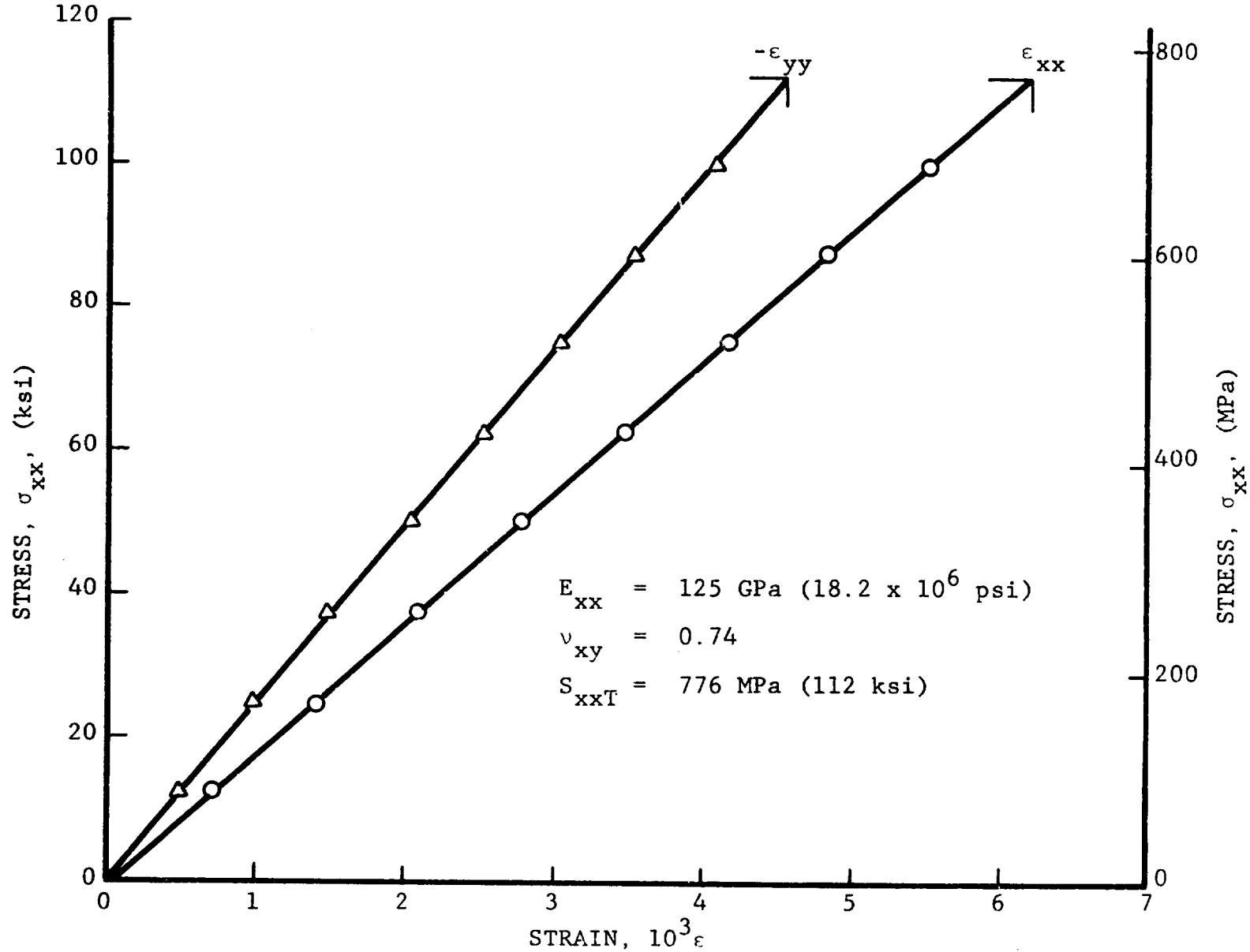

Fig. 27 STRAINS IN UNIAXIALLY LOADED FLAT COUPON OF $[\pm 45/0_2]_s$ GRAPHITE/EPOXY

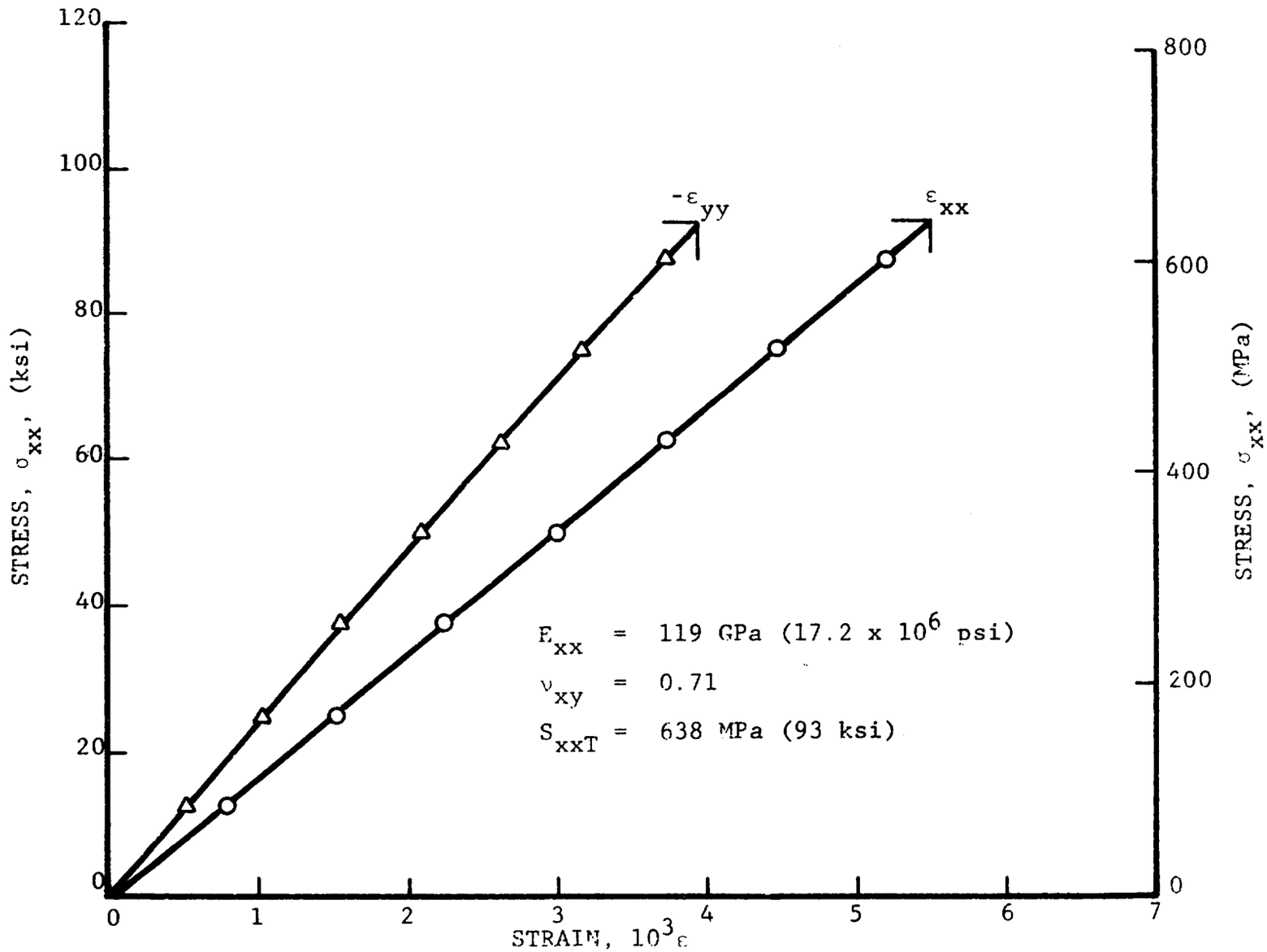

Fig. 28 STRAINS IN UNIAXIALLY LOADED FLAT COUPON OF $[\pm 45/0_2]_s$ GRAPHITE/EPOXY

It can be seen that the strength of the flattened tubular specimens is higher than for the flat coupons, although not significantly so. However, it is believed that the higher strength is a systematic trend which would be amplified with improved specimen quality. The same trend was found for the $[\pm 45/0]_s$ graphite/epoxy specimens.

Figures 29, 30 and 31 show the stress-strain curves for the hybrid flattened tubular specimens of $[\pm 45^C/0^G]_s$ HT graphite/S-glass/epoxy (C=graphite, G=S-glass). All specimens had tab overdrapes as tab reinforcement and all failed at the tabs. Hence the full strength of the material can be assumed to be higher than indicated by the test results. The stress-strain curves are nonlinear. The severe nonlinear effect occurring after 241 MPa (35 ksi) in Fig. 31 is very likely due to specimen degradation. Average property values for these specimens are:

E_{xx} = 37 GPa (5.3×10^6 psi)

ν_{xy} = 0.65

S_{xxT} = 421 MPa (61 ksi)

ε^u_{xx} = 14.7×10^{-3} (Figs. 29 and 30 only)

Figures 32, 33 and 34 are the stress-strain curves for the hybrid specimens of $[\pm 45^C/0_2^G]_s$ HT graphite/S-glass/epoxy. The specimen of Fig. 32 failed in the test section. The other two specimens failed at the tabs hence their strengths do not represent the effective strength of the material. The stress-strain curves are nonlinear to failure. In Fig. 32 some specimen degradation is evident after 517 MPa (75 ksi) from the more severe changes in slope. The average property values for these specimens are:

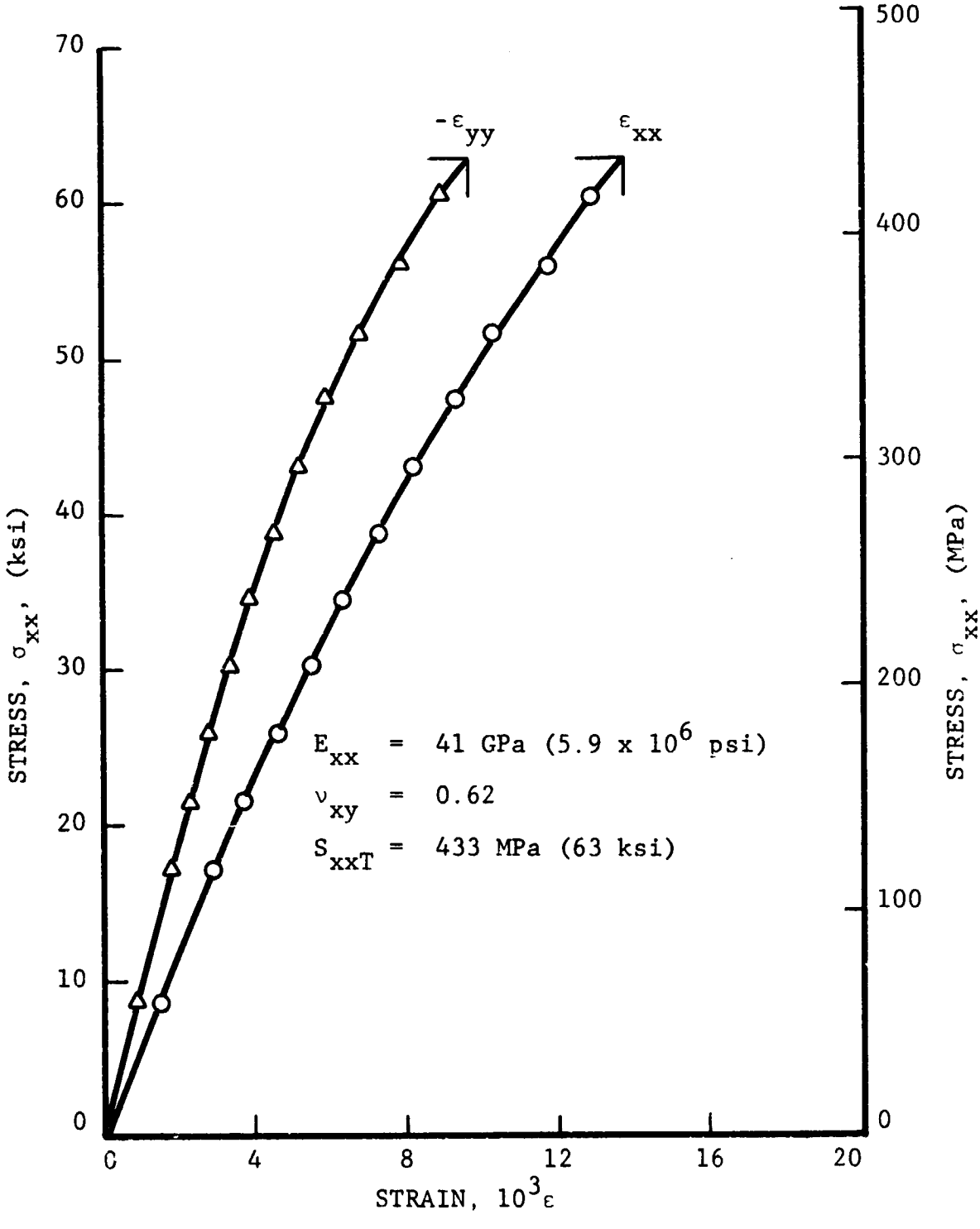

Fig. 29 STRAINS IN UNIAXIALLY LOADED FLATTENED TUBE OF $[\pm 45^C/0^G]_s$ GRAPHITE/S-GLASS/EPOXY

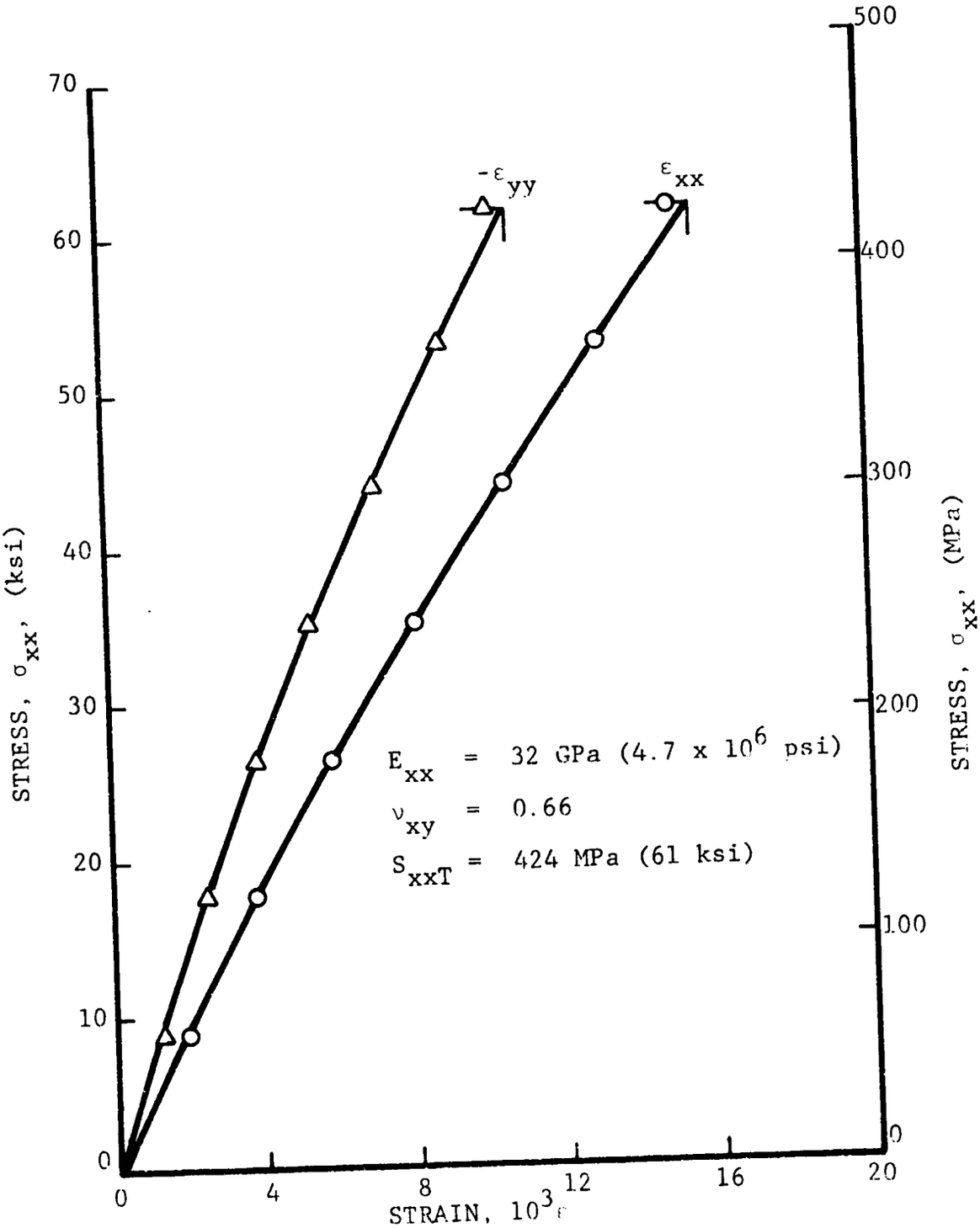

Fig. 30 STRAINS IN UNIAXIALLY LOADED FLATTENED TUBE OF $[\pm 45^G/0^G]_s$ GRAPHITE/S-GLASS/EPOXY

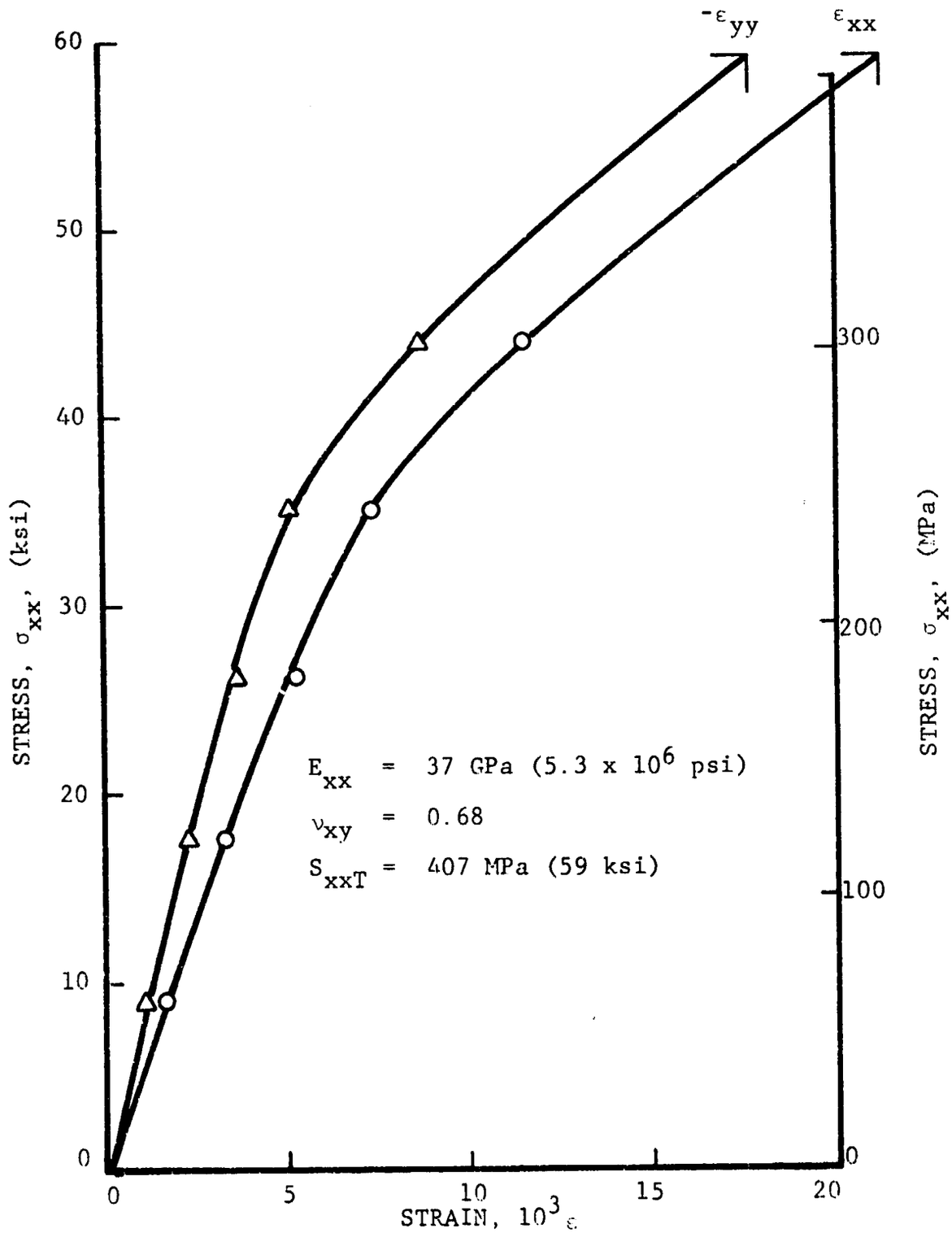

Fig. 31 STRAINS IN UNIAXIALLY LOADED FLATTENED TUBE OF $[\pm 45^C/0^G]_s$ GRAPHITE/S-GLASS/EPOXY

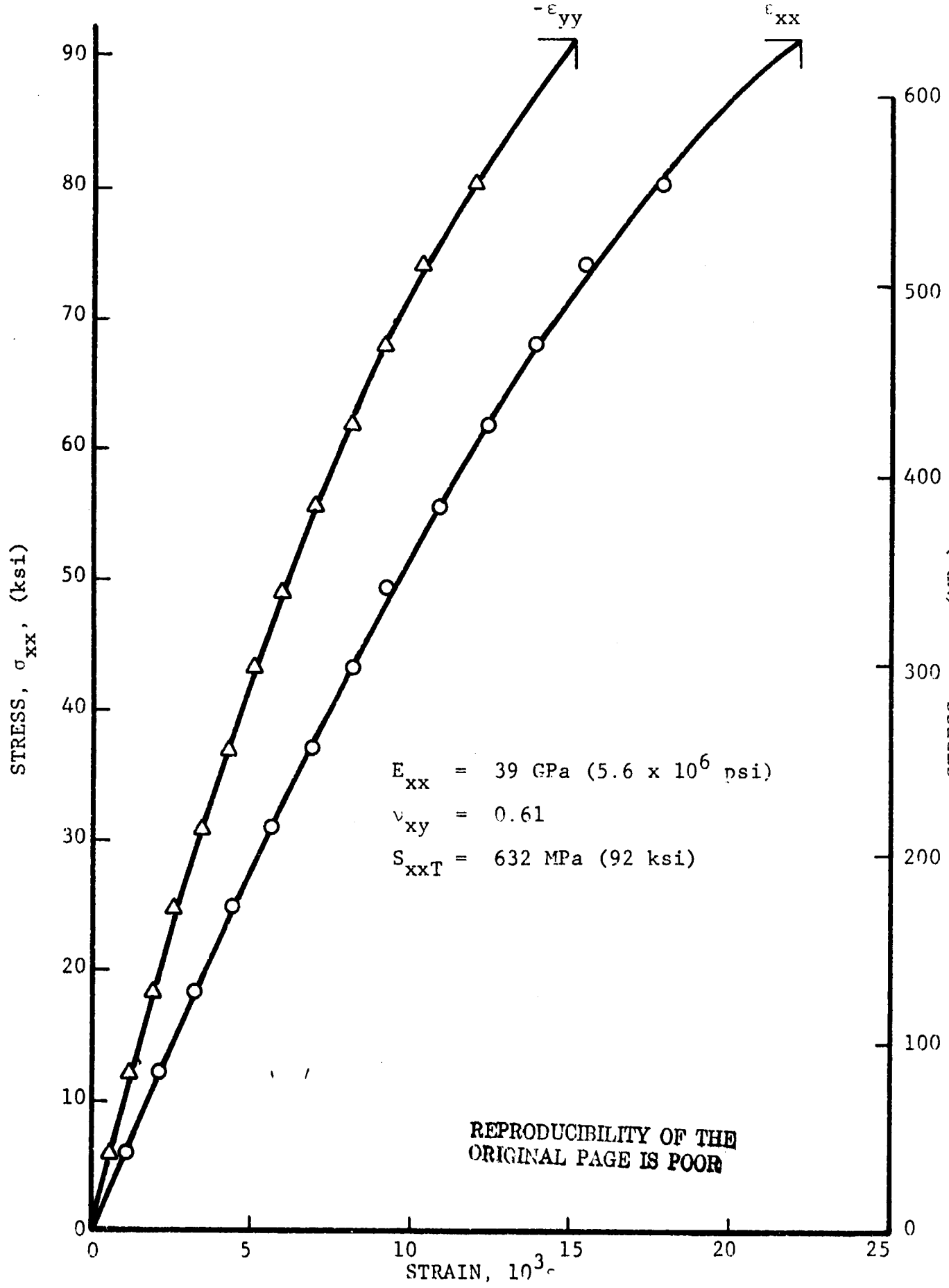

Fig. 32 STRAINS IN UNIAXIALLY LOADED FLATTENED TUBE OF $[\pm 45^{C}/0_2{}^{G}]_s$ GRAPHITE/S-GLASS/EPOXY

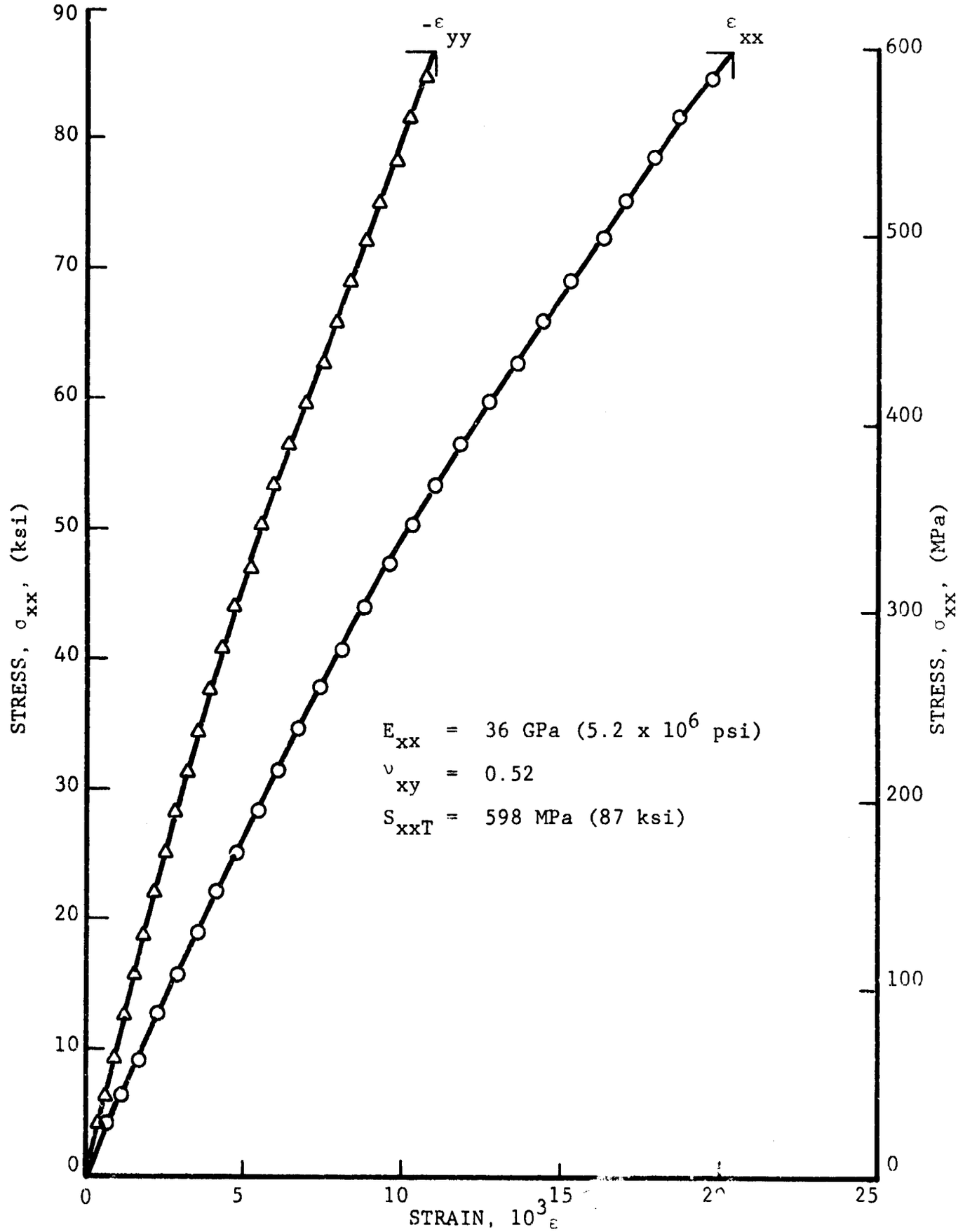

Fig. 33 STRAINS IN UNIAXIALLY LOADED FLATTENED TUBE OF $[\pm 45^C/0_2^G]$ GRAPHITE/S-GLASS EPOXY

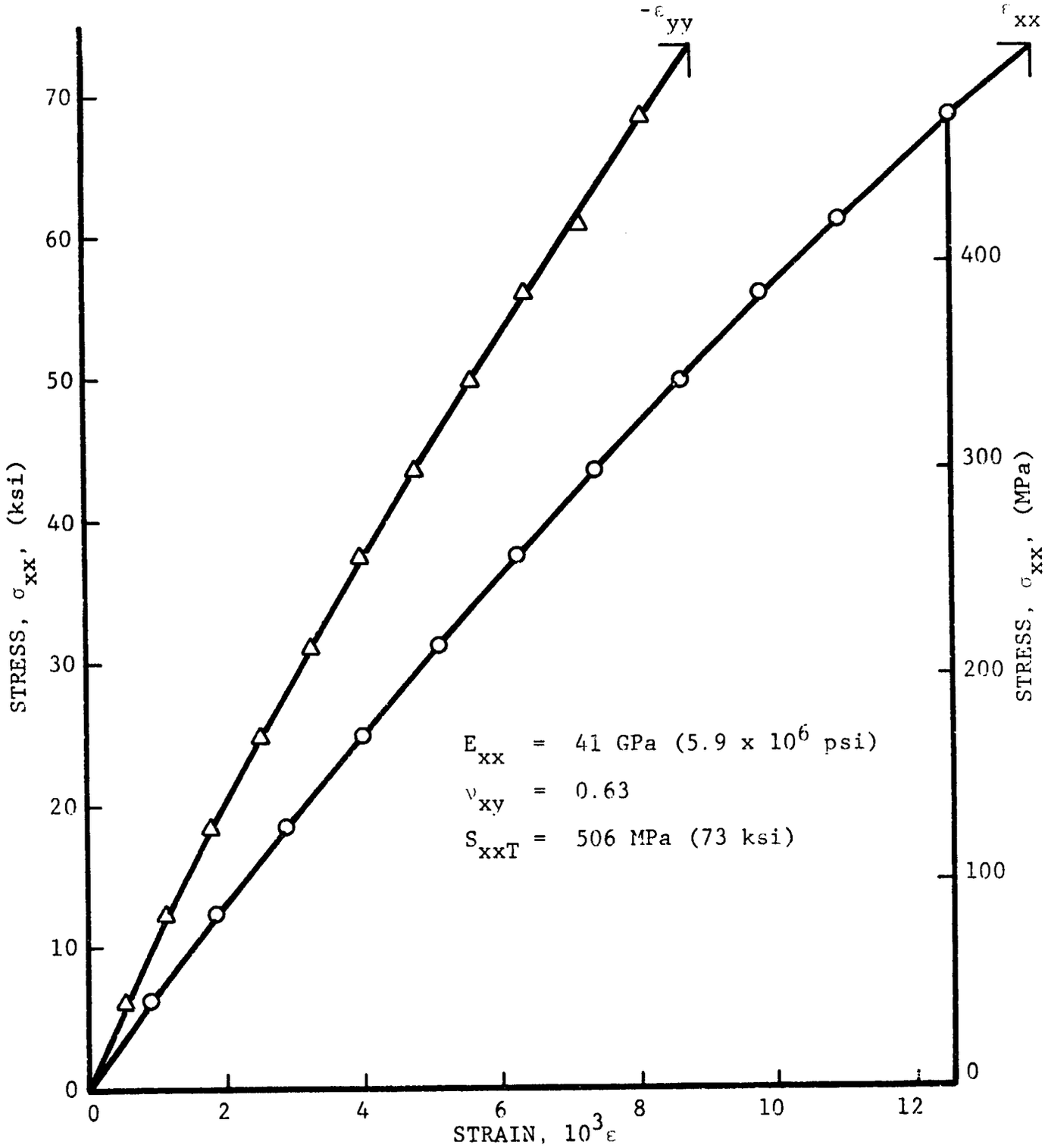

Fig. 34 STRAINS IN UNIAXIALLY LOADED FLATTENED TUBE OF $[\pm 45^C/0_2^G]_s$ GRAPHITE/S-GLASS/EPOXY

E_{xx} = 39 GPa (5.6 x 10^6 psi)

ν_{xy} = 0.59

S_{xxT} = 632 (92 ksi) (Fig. 32 only)

ε^u_{xx} = 21.3 x 10^{-3} (Figs. 32 and 33)

The stress-strain curves for the hybrid flattened tubular specimens of $[\pm 45^P/0_2^G]_s$ PRD-49-III/S-glass/epoxy (P=PRD-49-III) are shown in Figs. 35, 36 and 37. The specimens of Figs. 35 and 36 failed in the test section, that of Fig. 37 failed at the tab. The stress-strain curves are nonlinear to failure. The sudden change in transverse strain manifested in Fig. 37 is likely due to instrumentation error since no corresponding effect is evident in the longitudinal strain. The average property values for these specimens are:

E_{xx} = 34 GPa (4.8 x 10^6 psi)

ν_{xy} = 0.61

S_{xxT} = 627 MPa (91 ksi) (Figs. 35 and 36)

ε^u_{xx} = 20.0 x 10^{-3} (Figs. 35 and 36)

The stress-strain curves for the three hybrid flattened tubular specimens of $[\pm 45^P/0_4^G]_s$ PRD-49-III/S-glass/epoxy are shown in Figs. 38, 39 and 40. The specimens of Figs. 38 and 39 failed in the test section. For the specimen of Fig. 40 the tabs debonded prematurely during the test resulting in the low strength recorded. Tab repair and retest of this specimen gave an even lower strength indicating that the specimen was damaged during its first tab failure. All three specimens show essentially linear behavior to failure and close correspondence in modulus. A slight knee can be discerned in the curves at stresses between 138 and 207 MPa (20 to 30 ksi). Average values of the properties of these specimens are:

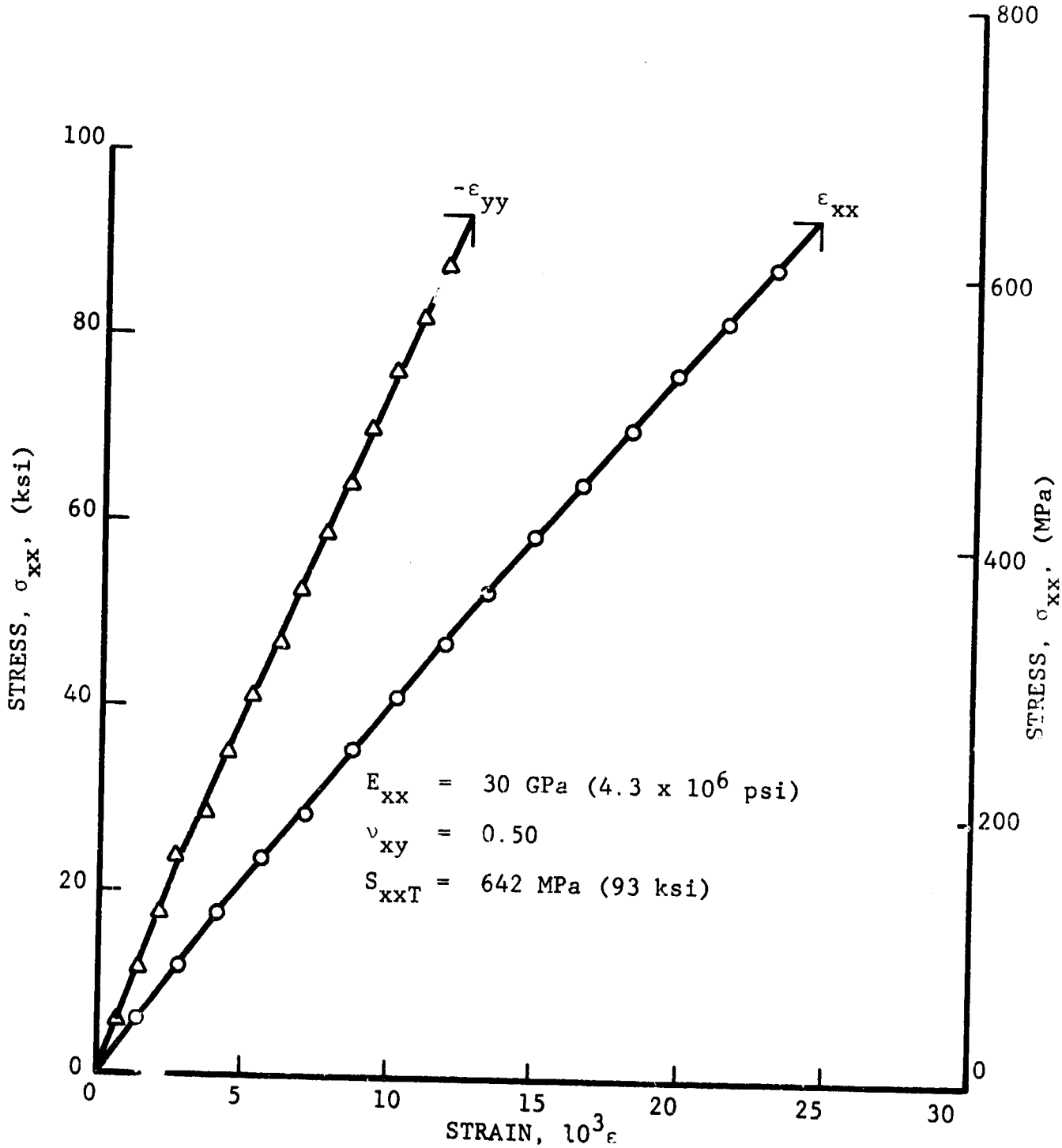

Fig. 35 STRAINS IN UNIAXIALLY LOADED FLATTENED TUBE OF $[\pm 45_2^P/0_2^G]_s$ PRD-49/S-GLASS/EPOXY

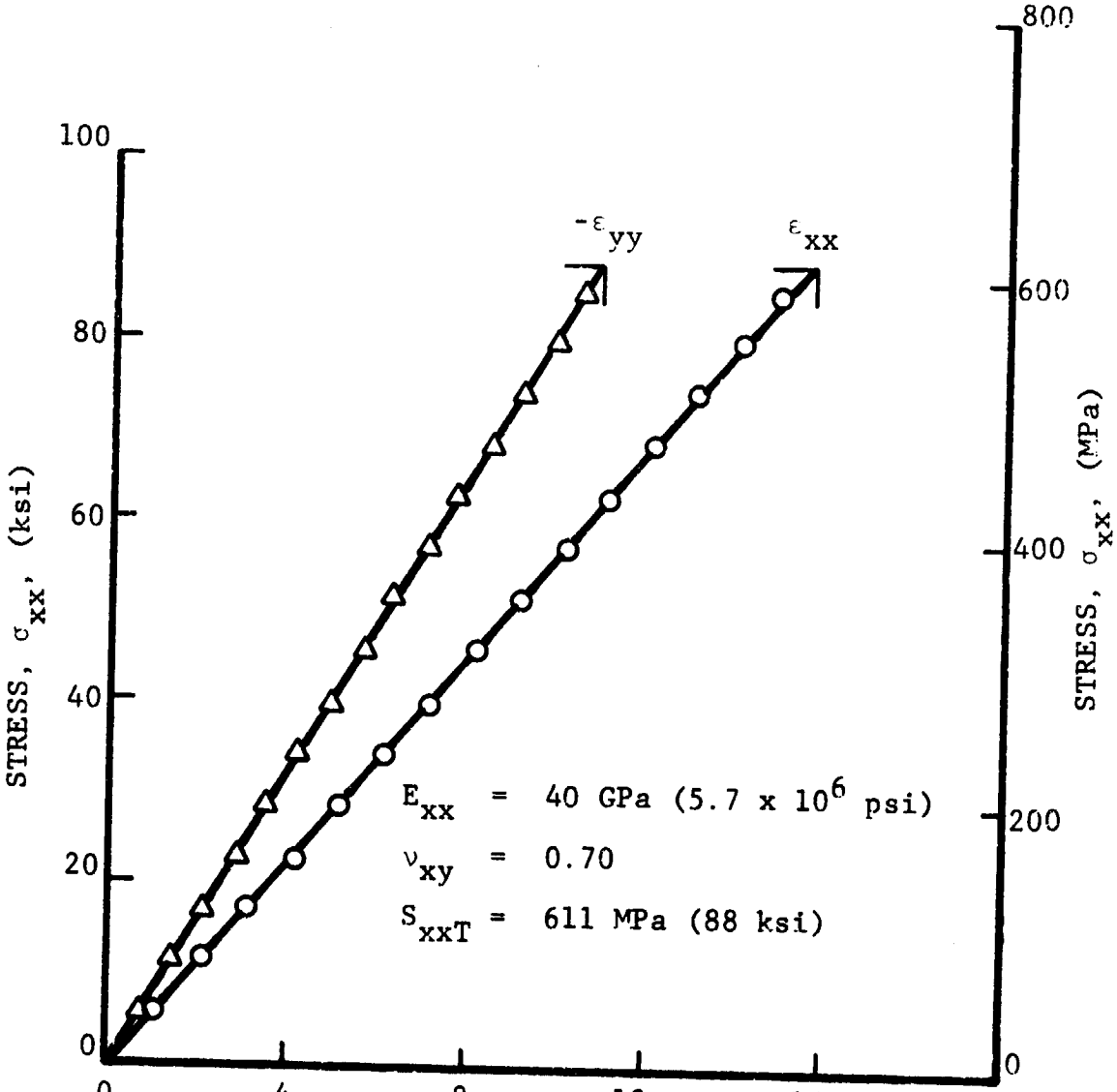

Fig. 36 STRAINS IN UNIAXIALLY LOADED FLATTENED TUBE OF $[\pm 45^P/0_2{}^G]_s$ PRD-49/S-GLASS/EPOXY

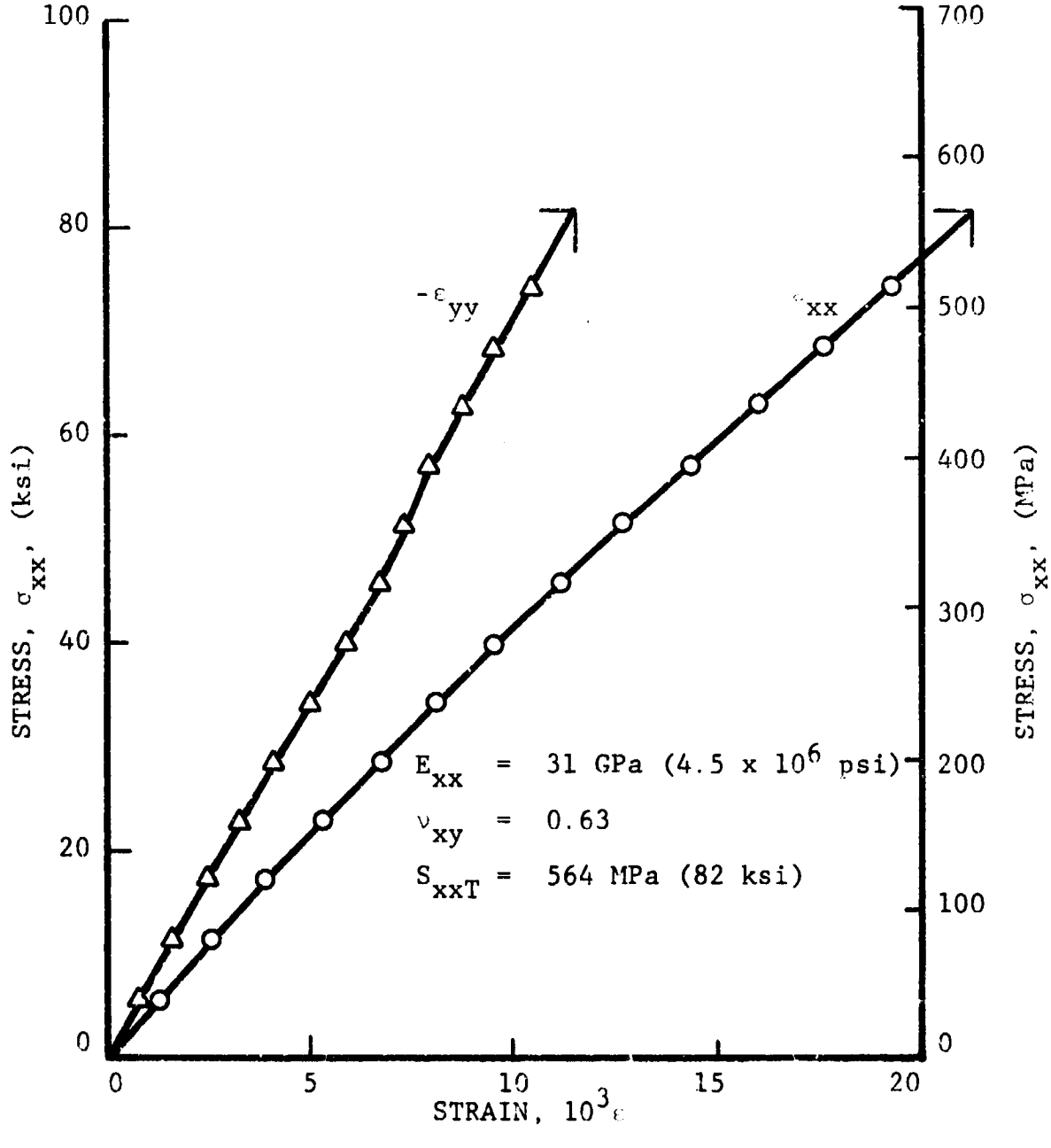

Fig. 37 STRAINS IN UNIAXIALLY LOADED FLATTENED TUBE OF $[\pm 45^P/0_2^G]_s$ PRD-49/S-GLASS/EPOXY

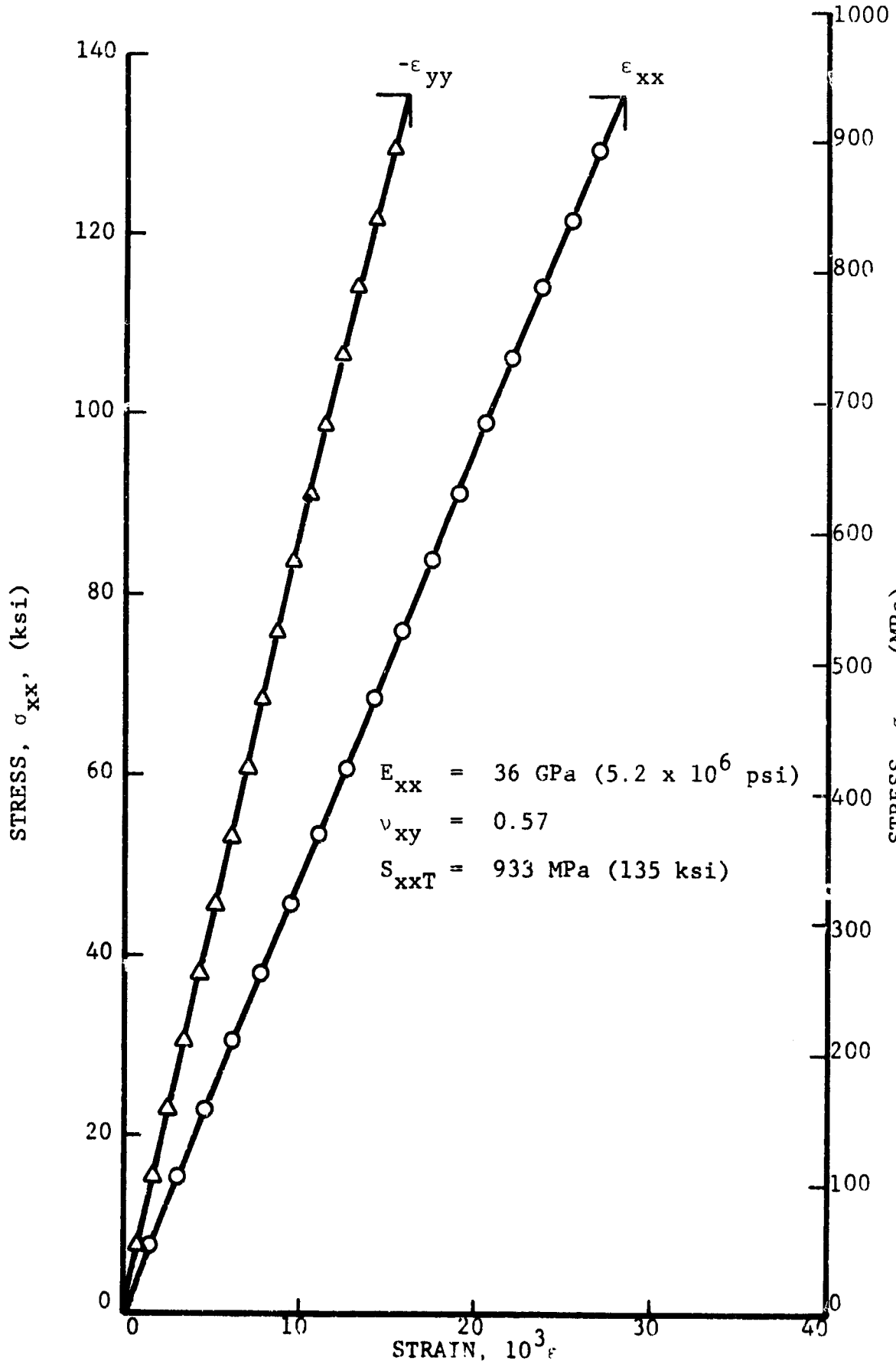

Fig. 38 STRAINS IN UNIAXIALLY LOADED FLATTENED TUBE OF $[\pm 45^P/0_4^G]_s$ PRD-49/S-GLASS/EPOXY

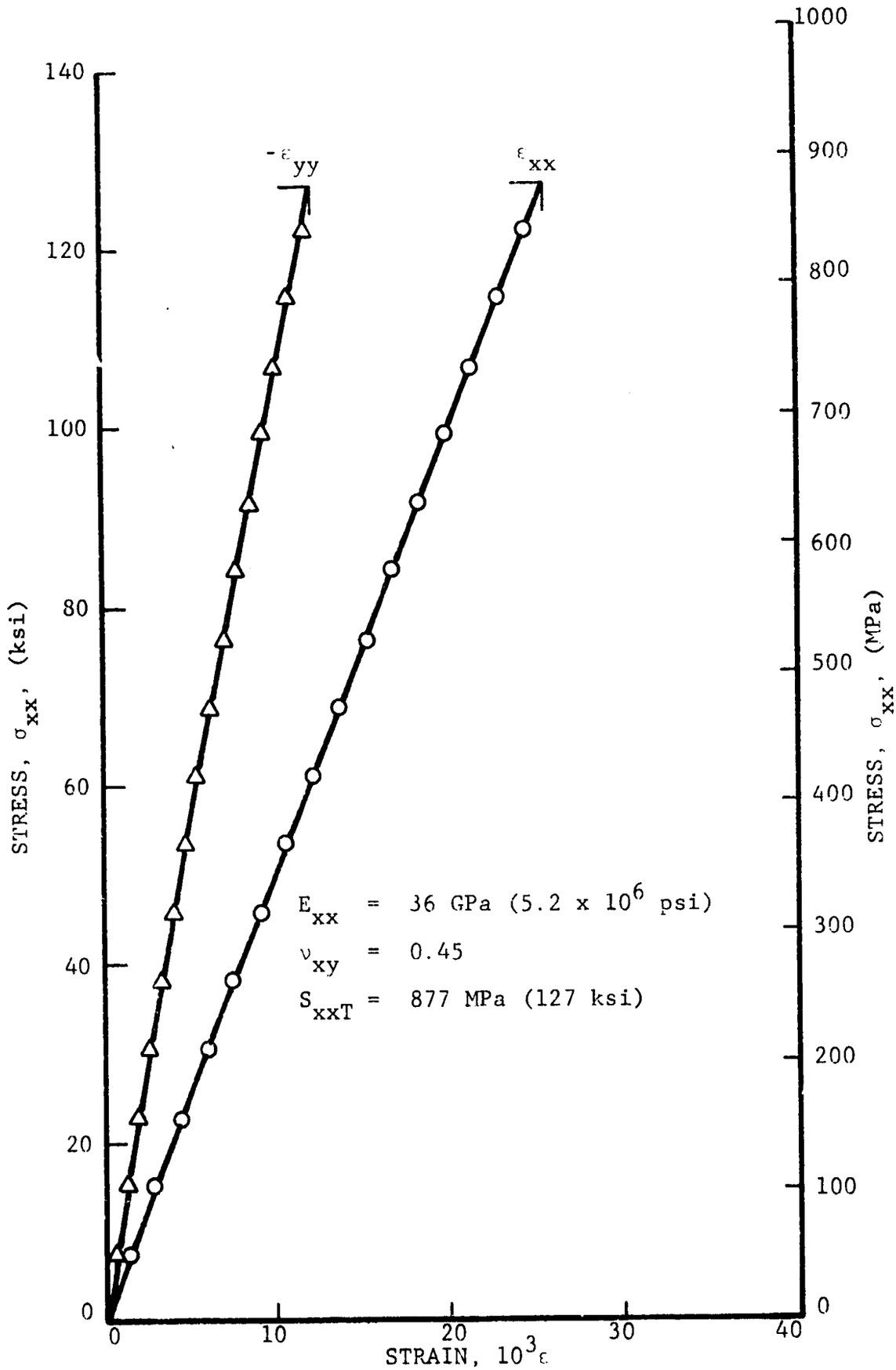

Fig. 39 STRAINS IN UNIAXIALLY LOADED FLATTENED TUBE OF $[\pm 45^P/0_4{}^G]_s$ PRD-49/S-GLASS/EPOXY

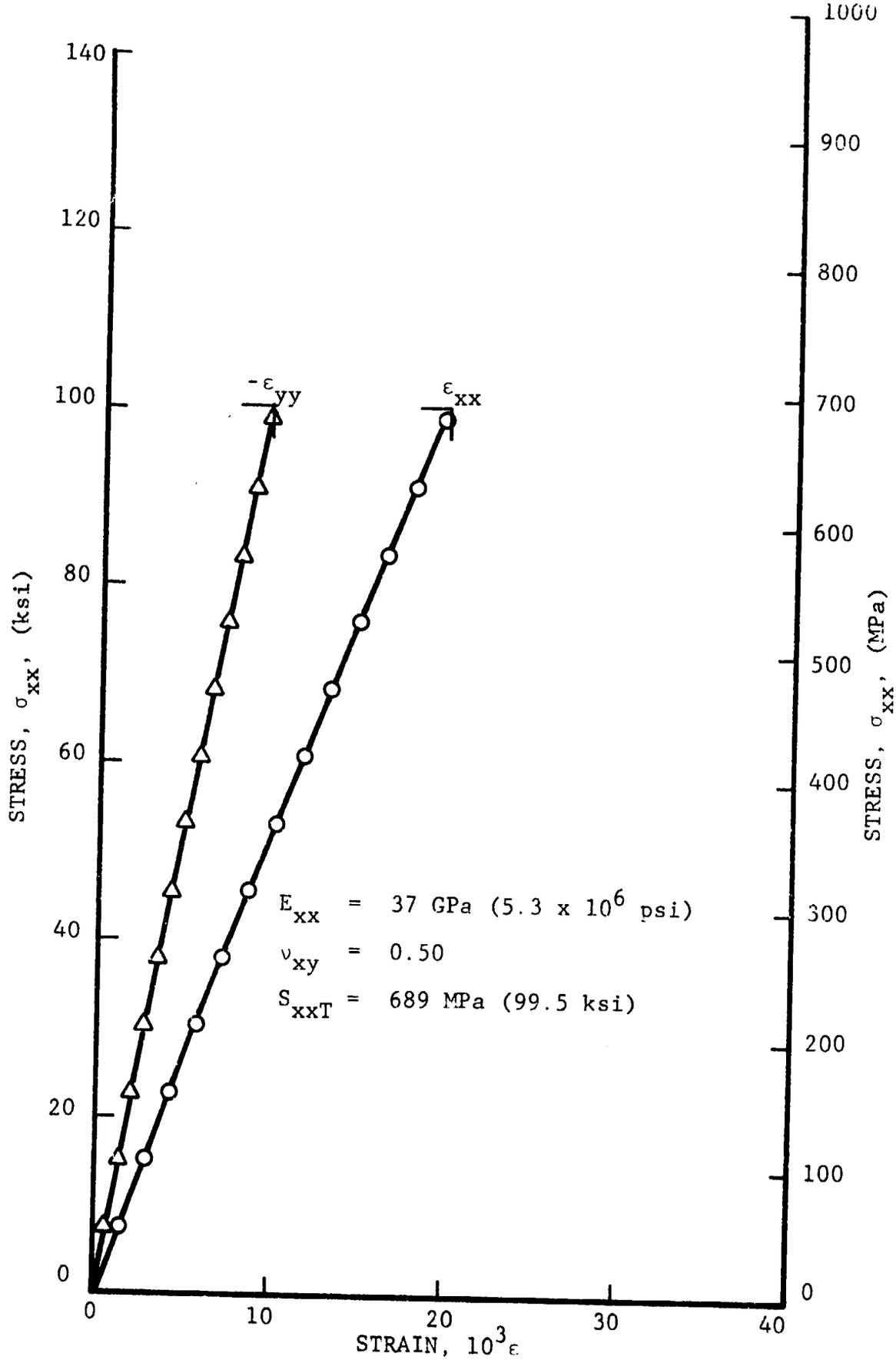

Fig. 40 STRAINS IN UNIAXIALLY LOADED FLATTENED TUBE OF $[\pm 45^P/0_4^G]_s$ PRD-49/S-GLASS/EPOXY

E_{xx} = 36 GPa (5.2 x 10^6 psi)

ν_{xy} = 0.51

S_{xxT} = 905 MPa (131 ksi) (Fig. 38 and 39)

ε_u^{xx} = 26.9 x 10^{-3} (Fig. 38 and 39)

The stress-strain curves for the three hybrid flattened tubular specimens of $[\pm 45^C/0^P]$ HT graphite/PRD-49-III/epoxy are shown in Figs. 41, 42 and 43. All specimens had tab overdrapes as reinforcement and all failed at the tabs. These conditions and failures are entirely similar to those of the HT graphite/S-glass/epoxy hybrid specimens. They indicate that the tabbing technique is more critical with hybrids with graphite outer layers than those with S-glass or PRD outer layer in contact with the tabs. Since all three specimens failed at the tabs, the values obtained do not represent the full strength of the material. All specimens show nonlinear behavior to failure without evidence of intermediate degradation. Average property values for these specimens are:

E_{xx} = 44 GPa (6.4 x 10^6 psi)

ν_{xy} = 0.68

S_{xxT} = 435 MPa (63 ksi)

ε_{xx}^u = 12.1 x 10^{-3}

Figures 44, 45 and 46 show the stress-strain curves for the hybrid flattened tubular specimens of $[\pm 45^C/0_2^P]_s$ HT graphite/PRD-49-III/epoxy. Here again all specimens failed at the tabs indicating the criticality of the tabbing technique in this type of hybrid. Because of the failures at the tabs the test results do not represent the full strength of the material. The stress-strain curves are nonlinear to failure and show no intermediate degradation. Average property values for these specimens are:

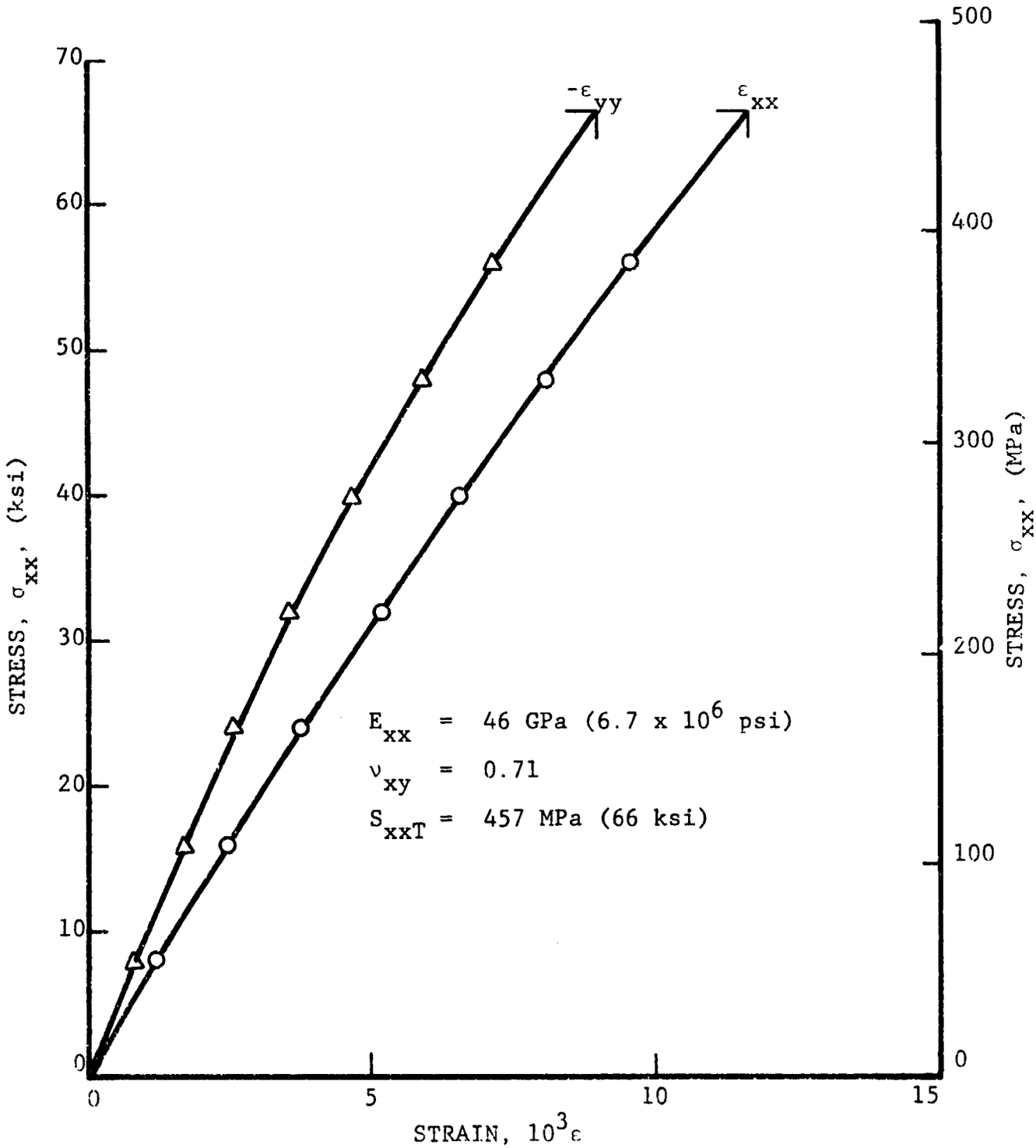

Fig. 41 STRAINS IN UNIAXIALLY LOADED FLATTENED TUBE OF $[\pm 45^C/0^P]_s$ HT-GRAPHITE/PRD-49/EPOXY

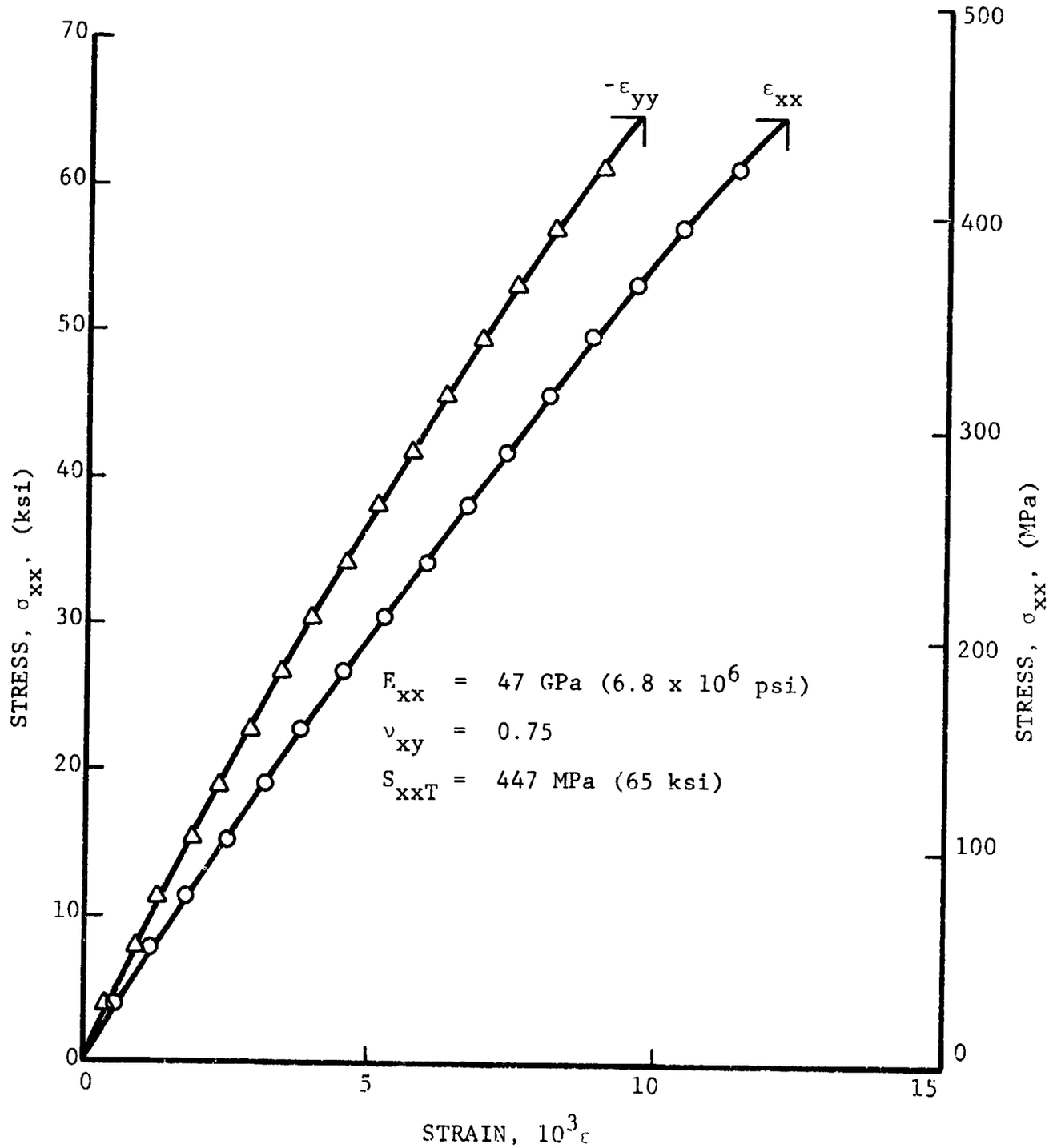

Fig. 42 STRAINS IN UNIAXIALLY LOADED FLATTENED TUBE OF $[\pm 45^C/0^P]_s$ HT-GRAPHITE/PRD-49/EPOXY

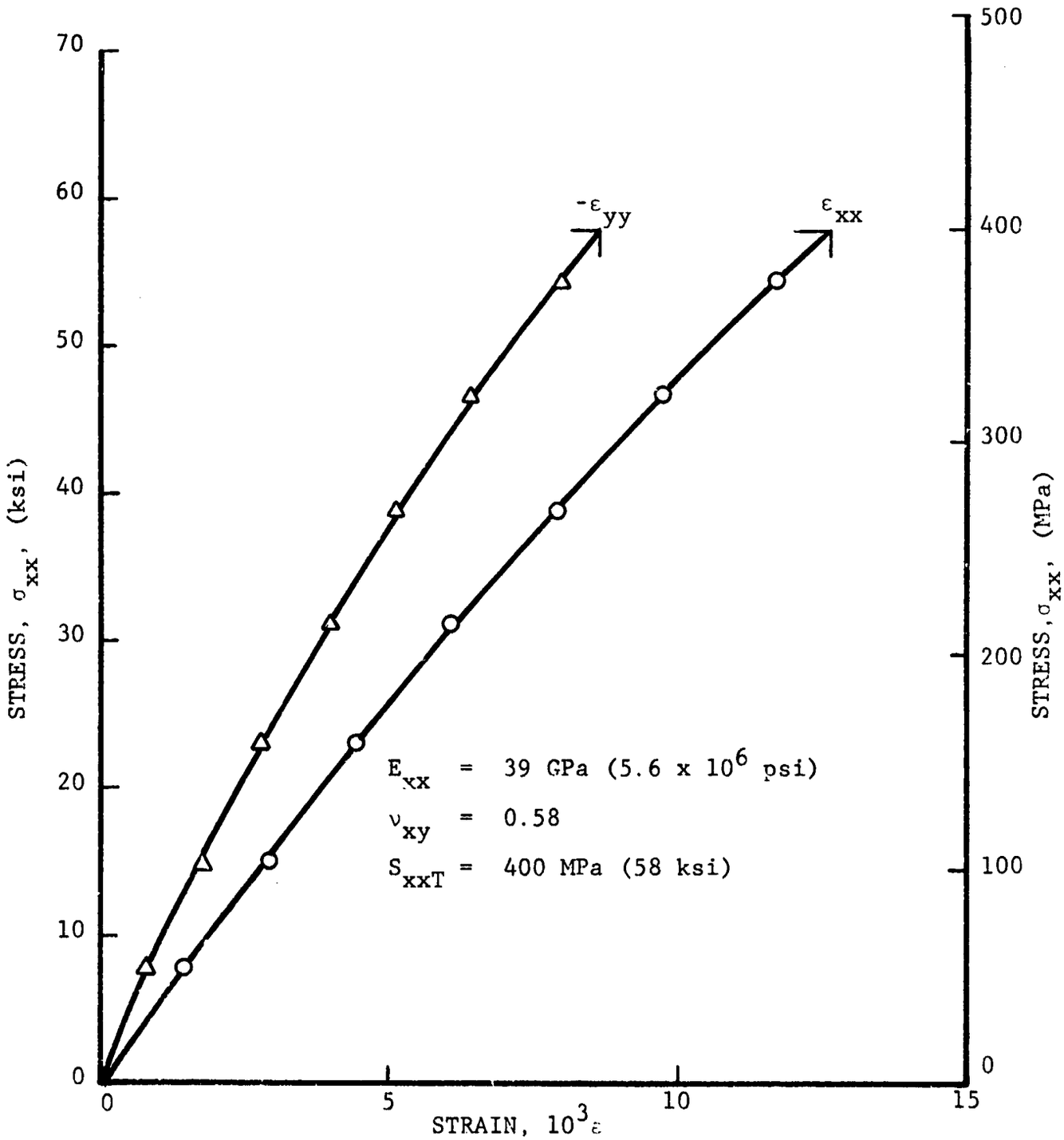

Fig. 43 STRAINS IN UNIAXIALLY LOADED FLATTENED TUBE OF $[\pm 45^C/0^P]_s$ HT-GRAPHITE/PRD-49/EPOXY

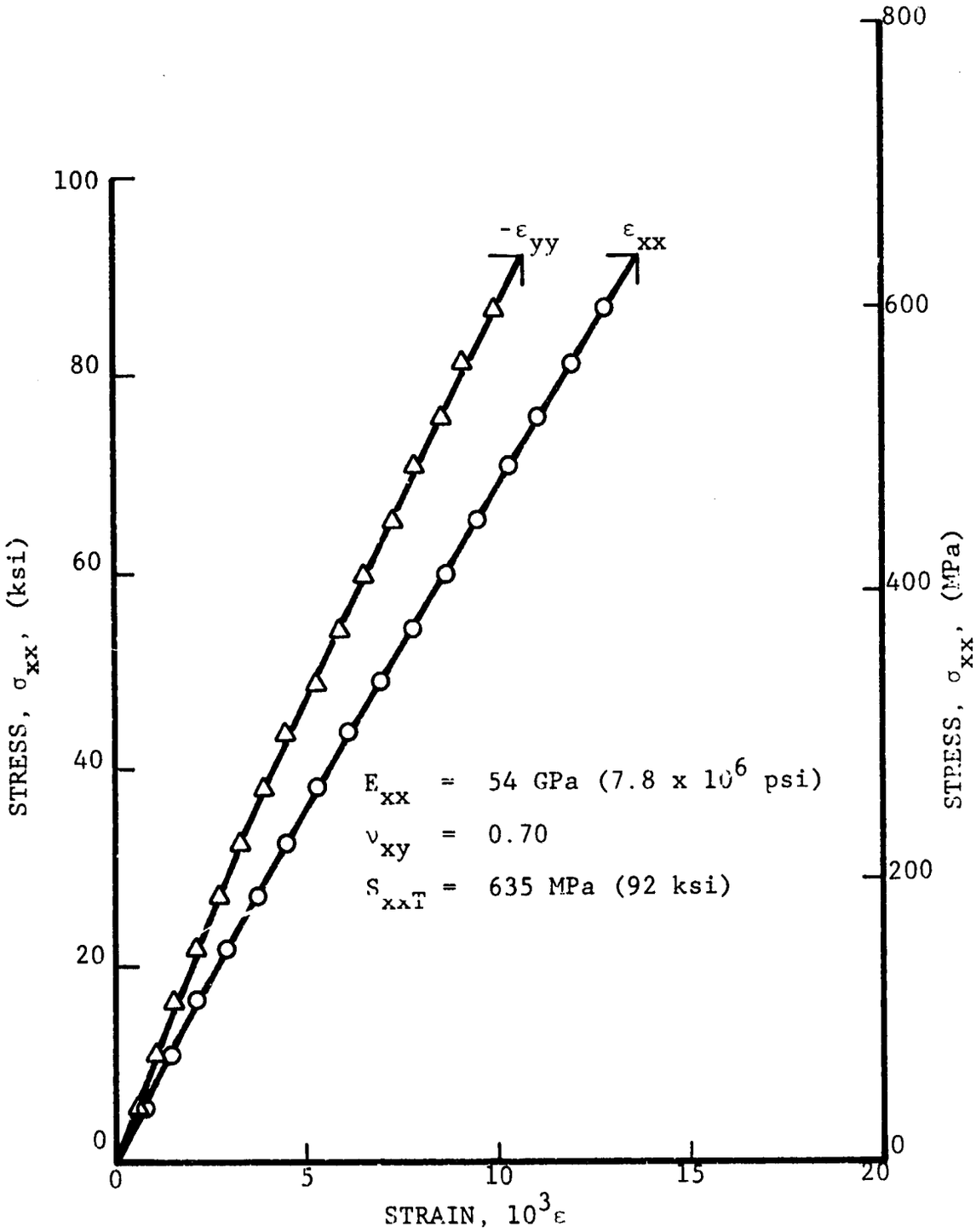

Fig. 44 STRAINS IN UNIAXIALLY LOADED FLATTENED TUBE OF $[\pm 45^C/0_2^P]_s$ HT-GRAPHITE/PRD-49/ EPOXY

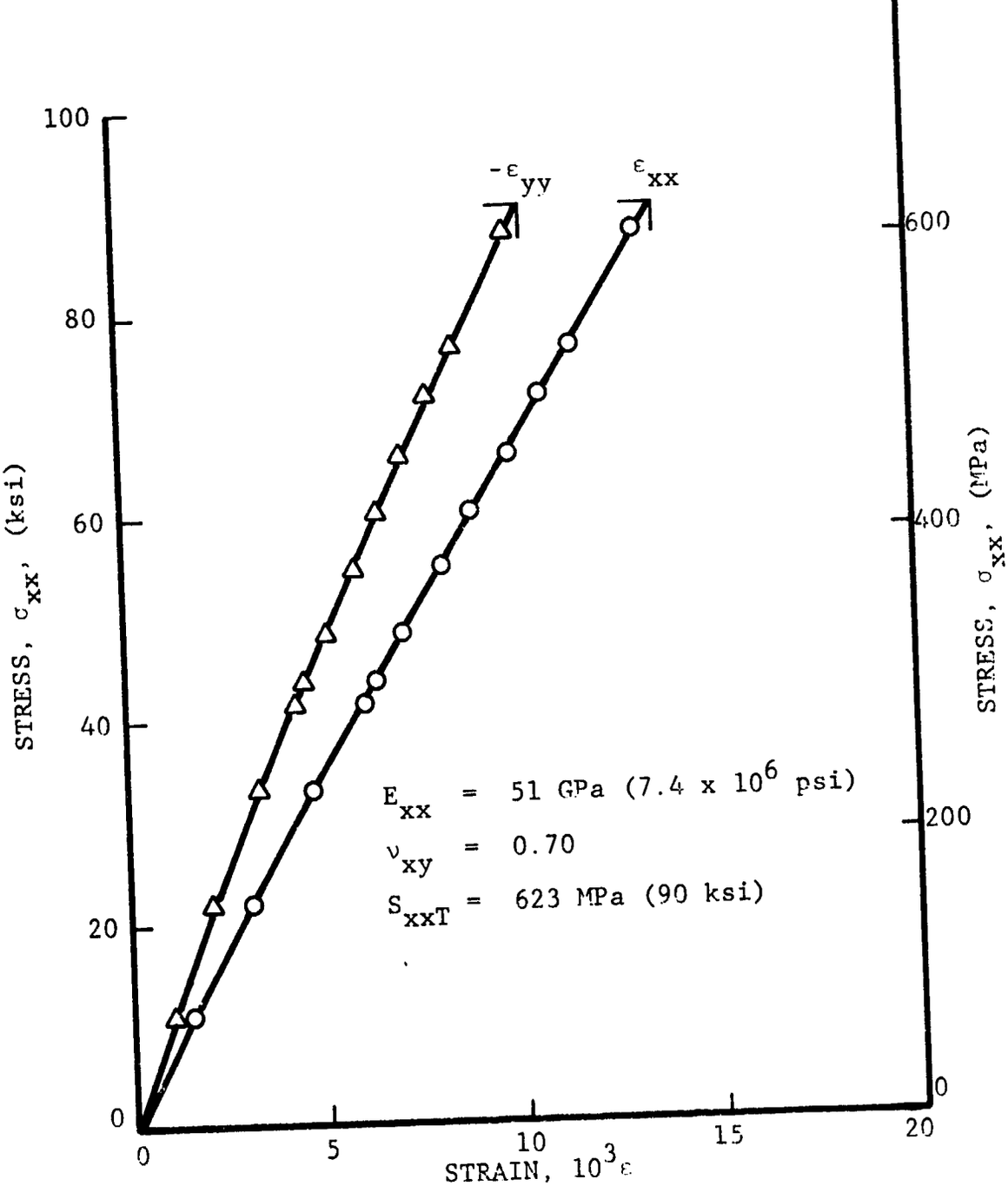

Fig. 45 STRAINS IN UNIAXIALLY LOADED FLATTENED TUBE OF $[\pm 45^C/0_2^P]_s$ HT-GRAPHITE/PRD-49/EPOXY

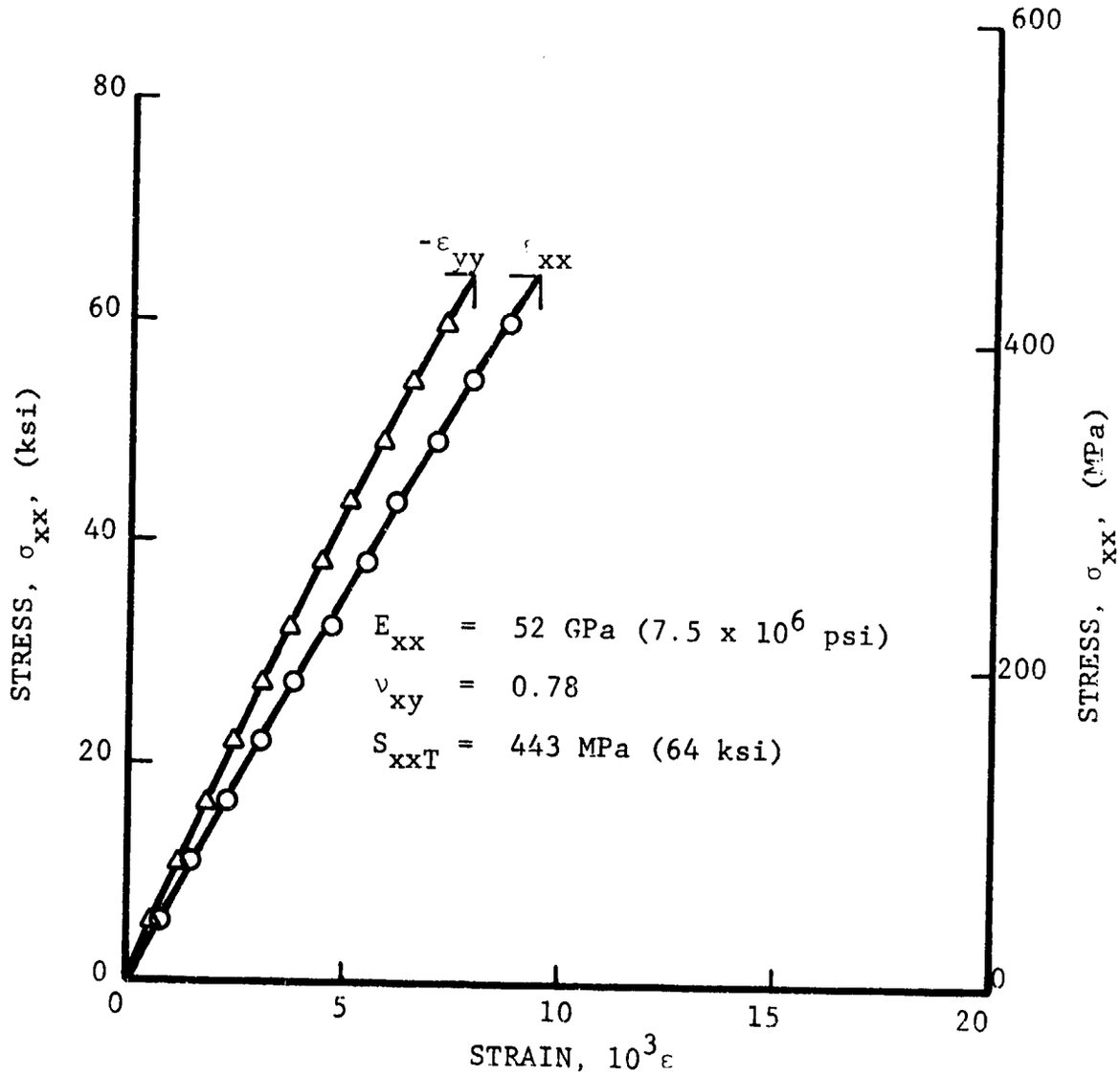

Fig. 46 STRAINS IN UNIAXIALLY LOADED FLATTENED TUBE OF $[\pm 45^C/0_2^P]_s$ HT-GRAPHITE/PRD-49/EPOXY

E_{xx} = 52 GPa (7.6×10^6 psi)

ν_{xy} = 0.73

S_{xxT} = 567 MPa (82 ksi)

ε^u_{xx} = 12.2×10^{-3}

4.2 Fatigue Tests

Table 4 shows the results obtained in the tensile cycling fatigue tests performed on the flattened tubular specimens of the nine different layups listed in Table 1. As was the case with the static tests and for similar reasons not all specimens failed in the test section. Such specimens are indicated by an asterisk in the "Cycles to Failure" column. In those cases the true number of cycles to failure is most likely higher than that obtained in the test.

Most tab type of failures appear to have been caused by tab overdrape or underdrape. This external tab reinforcement had the tendency to have its exposed ends separate from the specimen as the cycling progressed. This gave rise to a mechanical scrubbing and flapping action of the loosened draping against the specimen, very likely resulting in local heating and weakening of the specimen.

Figures 47 through 55 show graphically the fatigue strength vs cycles to failure of the flattened tubular specimens. They are based on the data of Table 4. The ordinates of the graphs are presented in terms of percentages of static strength where static strengths, listed on every graph, are the average values reported in Section 4.1. All data points have been plotted regardless of type of failure. Curves have been drawn between the data points to indicate trends.

Table 4

RESULTS OF TENSILE CYCLING FATIGUE TESTS OF FLATTENED TUBULAR SPECIMENS

Material	Specimen Layup	Maximum Cyclic Stress MPa	(ksi)	Cycles to Failure
S-Glass/Epoxy	$[\pm 45/0_2]_s$	142	(20.6)	1.555×10^6*
		145	(21.0)	4.169×10^6*
		163	(23.6)	1.297×10^6
		165	(23.9)	8.23×10^5 *
		210	(30.5)	1.44×10^5
PRD-49-1II/Epoxy	$[\pm 45/0_2]_s$	284	(41.2)	8.40×10^5 *
		284	(41.2)	6.659×10^6*
		320	(46.4)	2.555×10^6*
		397	(57.6)	5.52×10^5 *
HT-Graphite/Epoxy	$[\pm 45/0_2]_s$	499	(72.4)	1.4714×10^7 Runout
		540	(78.3)	1.0170×10^7 Runout
		568	(82.4)	$<1.0 \times 10^3$ *
		576	(83.6)	5.2×10^4 *
HT-Graphite/ S-Glass/Epoxy	$[\pm 45^C/0^G]_s$	133	(19.2)	1.0030×10^7 Runout
		145	(21.0)	4.055×10^6*
		157	(22.7)	1.241×10^6*
		169	(24.5)	3.94×10^5 *
HT-Graphite/ S-Glass/Epoxy	$[\pm 45^C/0_2^G]_s$	155	(22.5)	1.0312×10^7 Runout
		173	(25.1)	1.0300×10^7 Runout
		206	(29.9)	3.270×10^6*
		227	(32.9)	1.198×10^6
		242	(35.1)	2.77×10^5 *
PRD-49-III/ S-Glass/Epoxy	$[\pm 45^P/0_2^G]_s$	144	(20.9)	8.253×10^6
		158	(22.9)	3.413×10^6
		177	(25.6)	8.21×10^5
		188	(27.2)	3.90×10^5

*Failure at or near tab

Table 4 (Cont'd)

RESULTS OF TENSILE CYCLING FATIGUE TESTS OF FLATTENED TUBULAR SPECIMENS

Material	Specimen Layup	Maximum Cyclic Stress MPa	(ksi)	Cycles to Failure
PRD-49-III/ S-Glass/Epoxy	$[\pm 45^{P}/0_{4}^{G}]_{s}$	157	(22.8)	5.352×10^{6}
		184	(26.6)	2.949×10^{6}
		196	(28.5)	1.341×10^{6}*
		213	(30.9)	7.81×10^{5}
		227	(32.9)	4.00×10^{5} *
HT-Graphite/ PRD-49-III/Epoxy	$[\pm 45^{C}/0^{P}]_{s}$	259	(37.6)	1.0002×10^{7} Runout
		275	(39.9)	8.876×10^{6}*
		279	(40.4)	3.585×10^{6}
		294	(42.7)	1.274×10^{6}
HT-Graphite/ PRD-49-III/Epoxy	$[\pm 45^{C}/0_{2}^{P}]_{s}$	334	(48.5)	6.944×10^{5}
		342	(49.6)	7.869×10^{6}*
		362	(52.6)	2.297×10^{6}
		381	(55.3)	7.70×10^{5} *

*Failure at or near tab

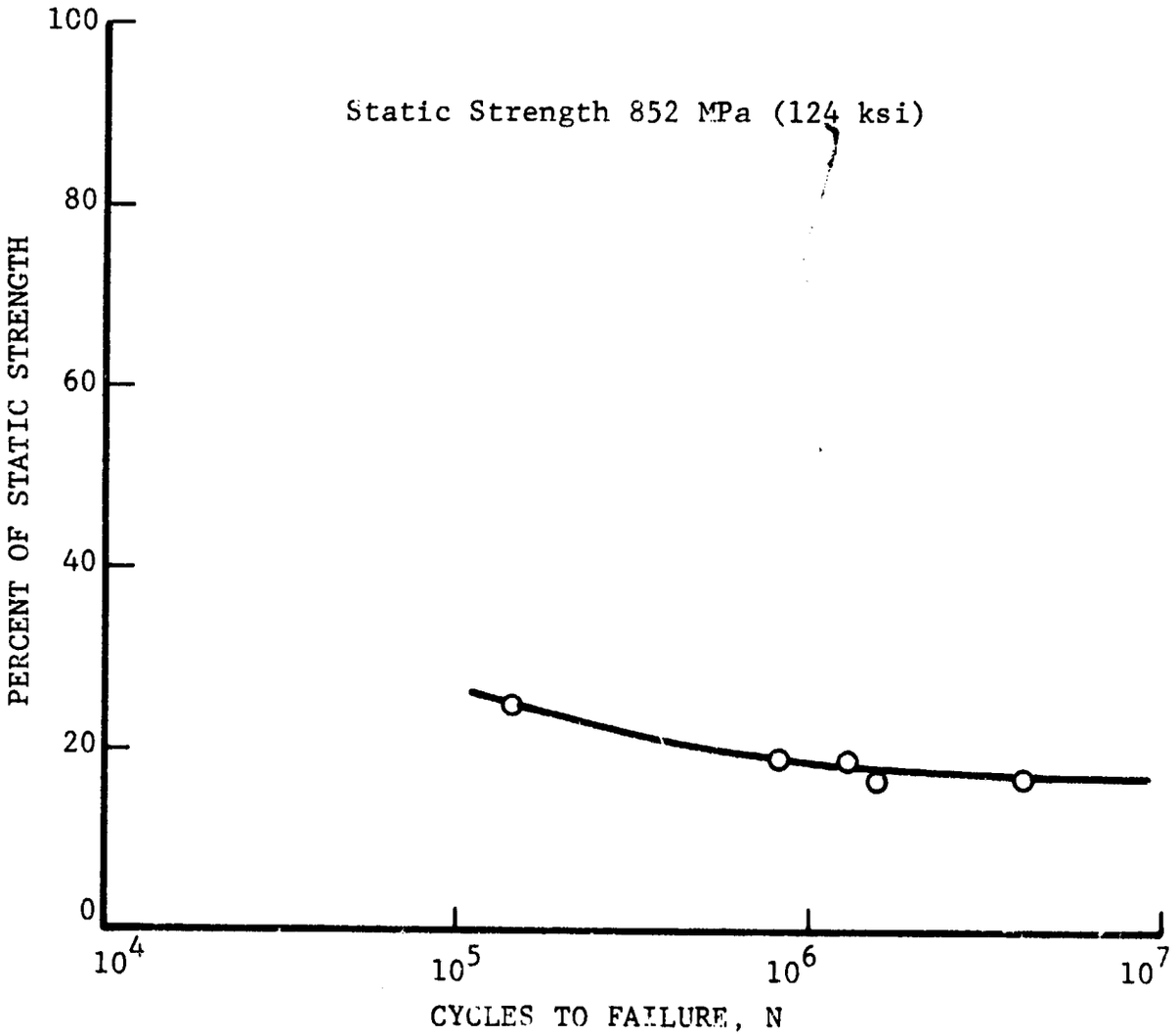

Fig. 47 TENSILE CYCLING FATIGUE STRENGTH OF FLATTENED TUBE SPECIMENS OF $[\pm 45/0_2]_s$ S-GLASS/EPOXY

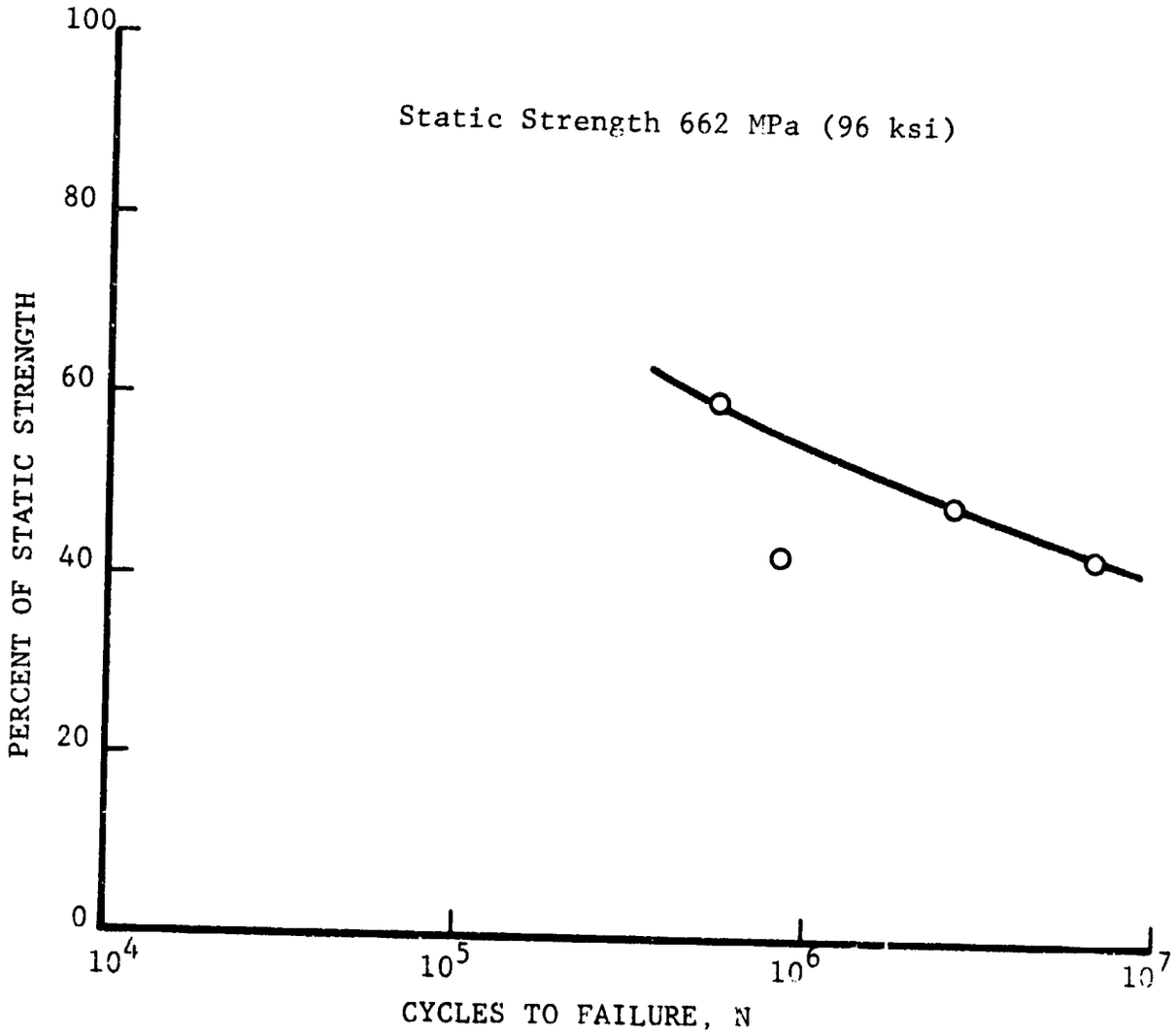

Fig. 48 TENSILE CYCLING FATIGUE STRENGTH OF FLATTENED TUBE SPECIMENS OF $[\pm 45/0_2]_s$ PRD-III/EPOXY

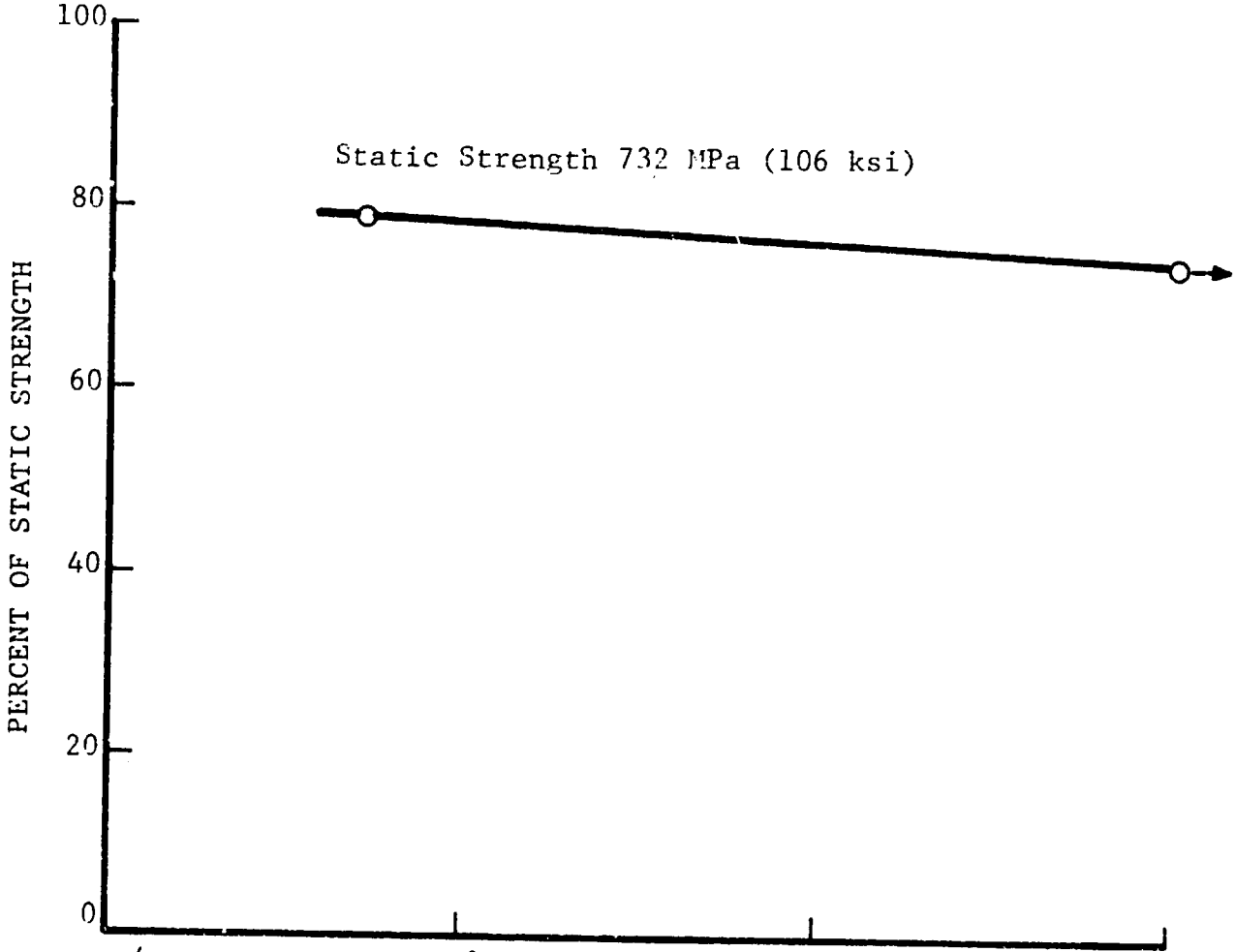

Fig. 49 TENSILE CYCLING FATIGUE STRENGTH OF FLATTENED TUBE SPECIMENS OF $[\pm 45/0_2]_s$ HT-GRAPHITE/EPOXY

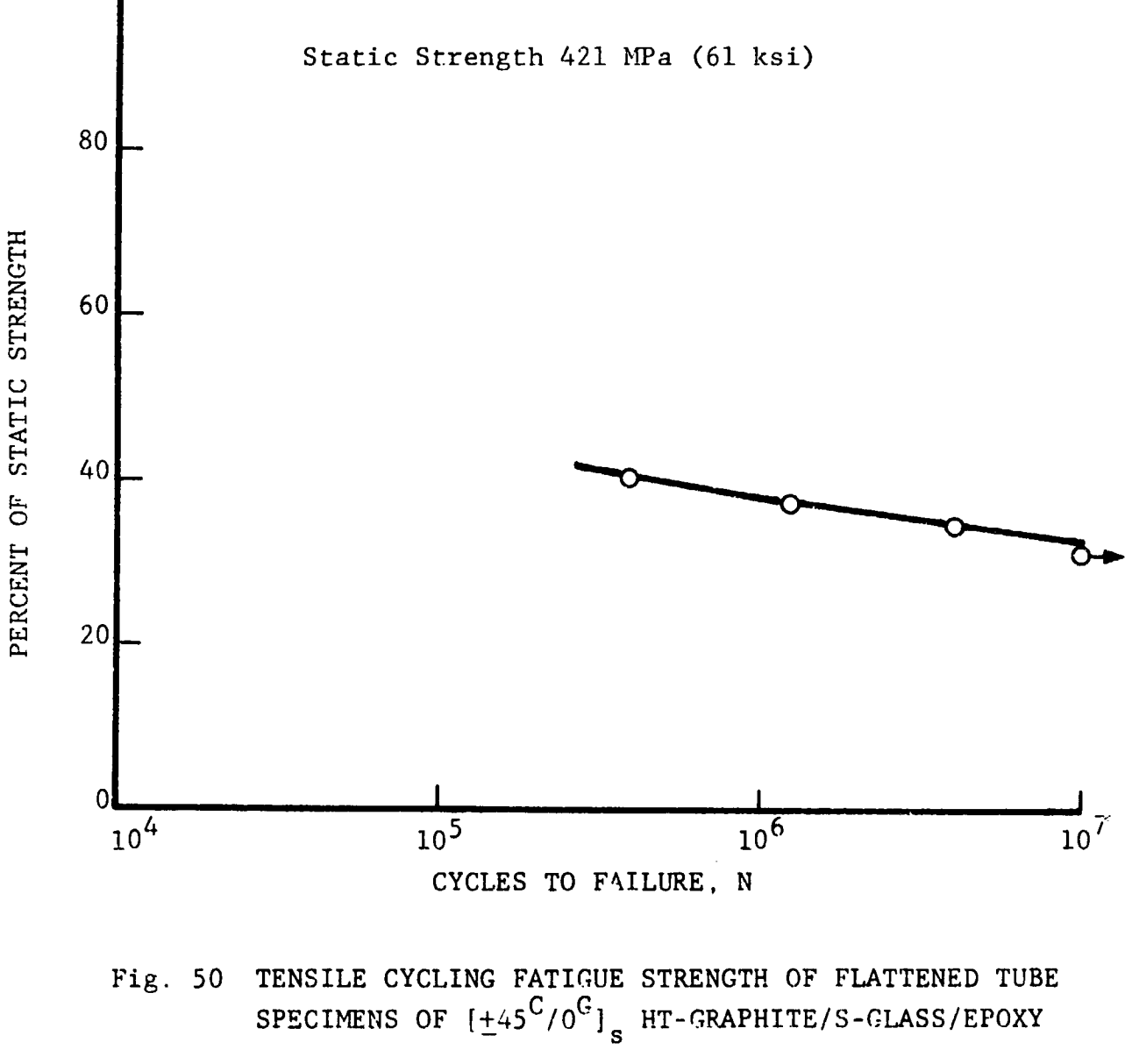

Fig. 50 TENSILE CYCLING FATIGUE STRENGTH OF FLATTENED TUBE SPECIMENS OF $[\pm 45^C/0^G]_s$ HT-GRAPHITE/S-GLASS/EPOXY

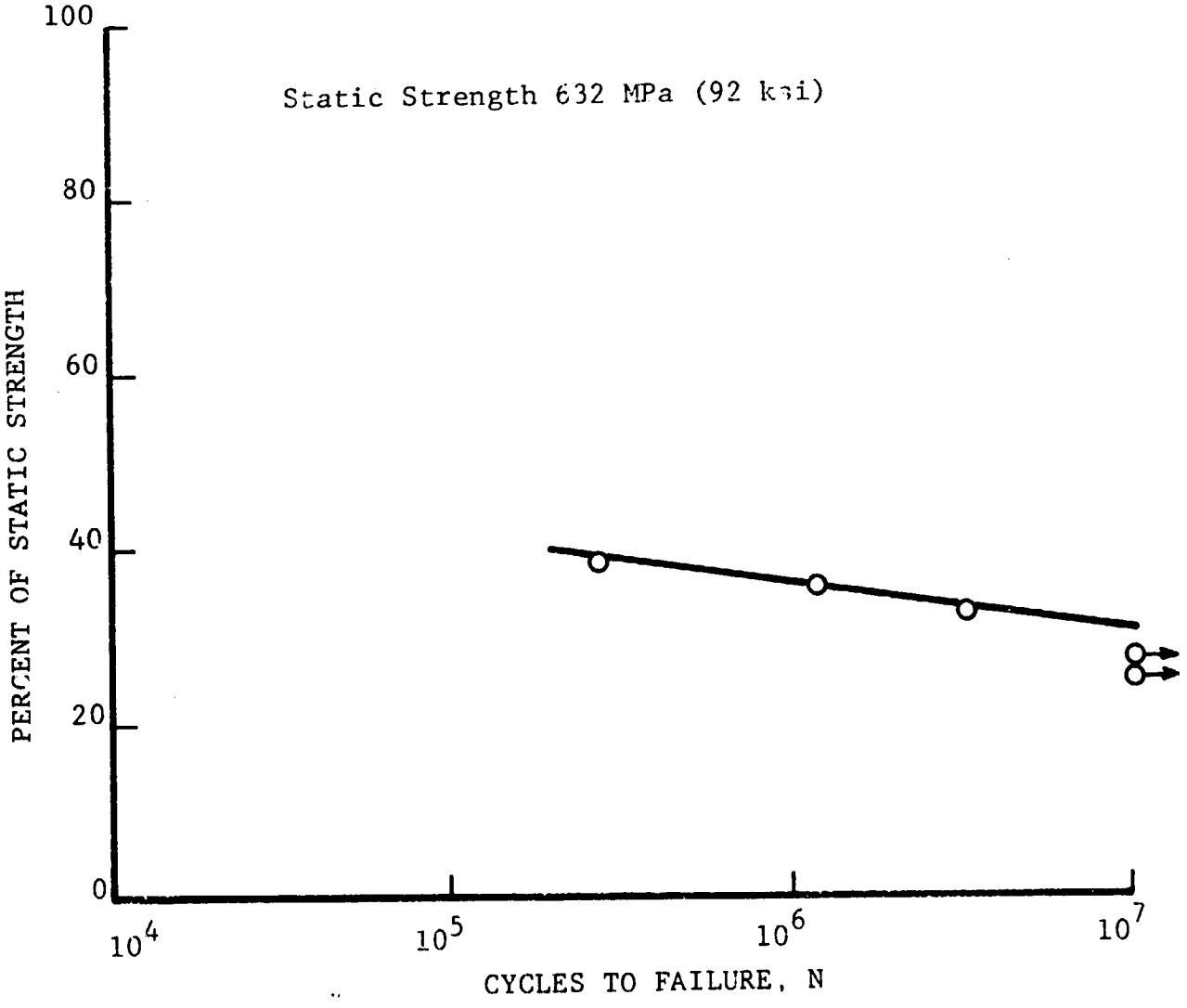

Fig. 51 TENSILE CYCLING FATIGUE STRENGTH OF FLATTENED TUBE SPECIMENS OF $[\pm 45^C/0_2^G]_s$ HT-GRAPHITE/S-GLASS/EPOXY

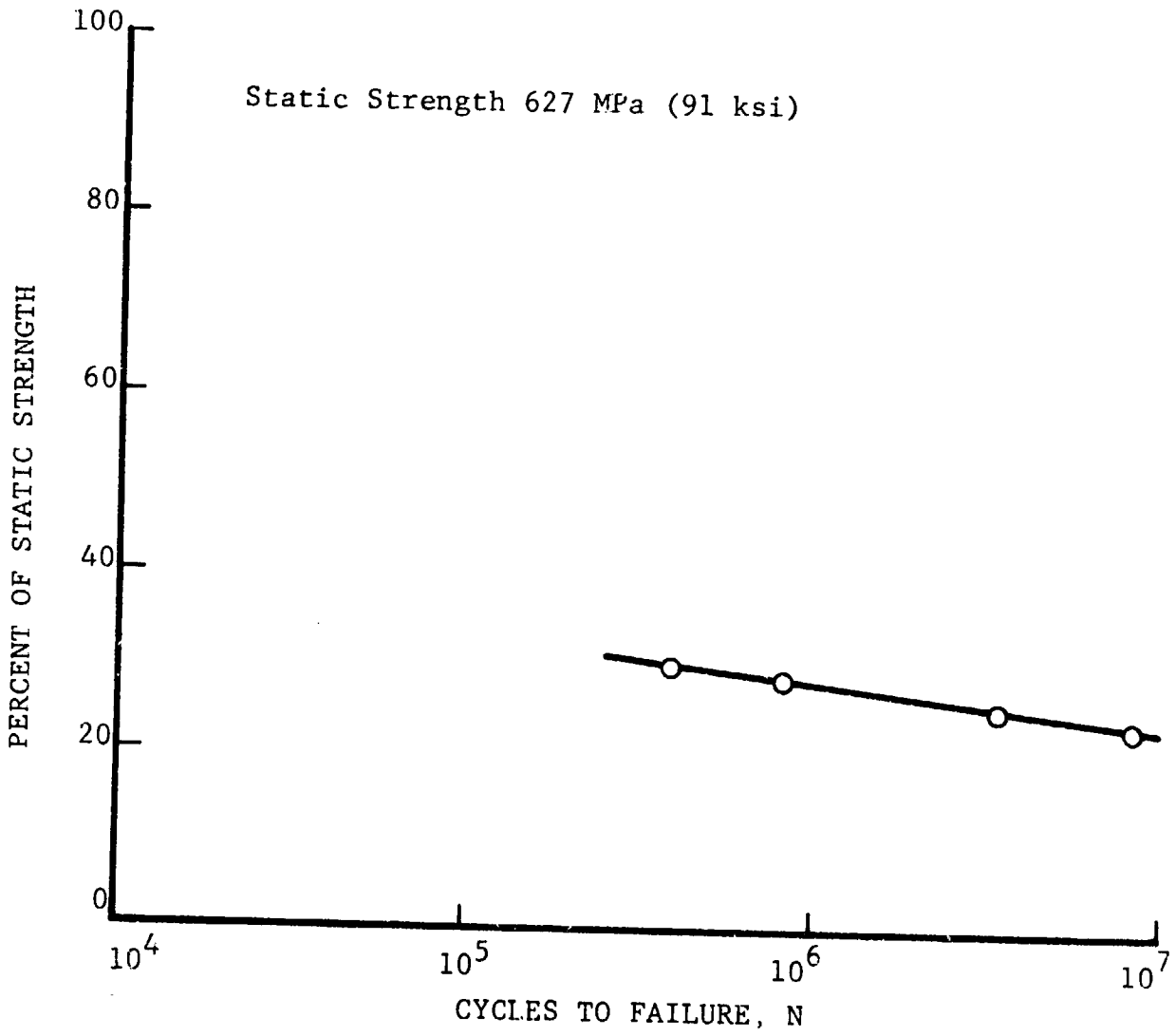

Fig. 52 TENSILE CYCLING FATIGUE STRENGTH OF FLATTENED TUBE SPECIMENS OF $[\pm 45^P/0_2^G]_s$ PRD-49/S-GLASS/EPOXY

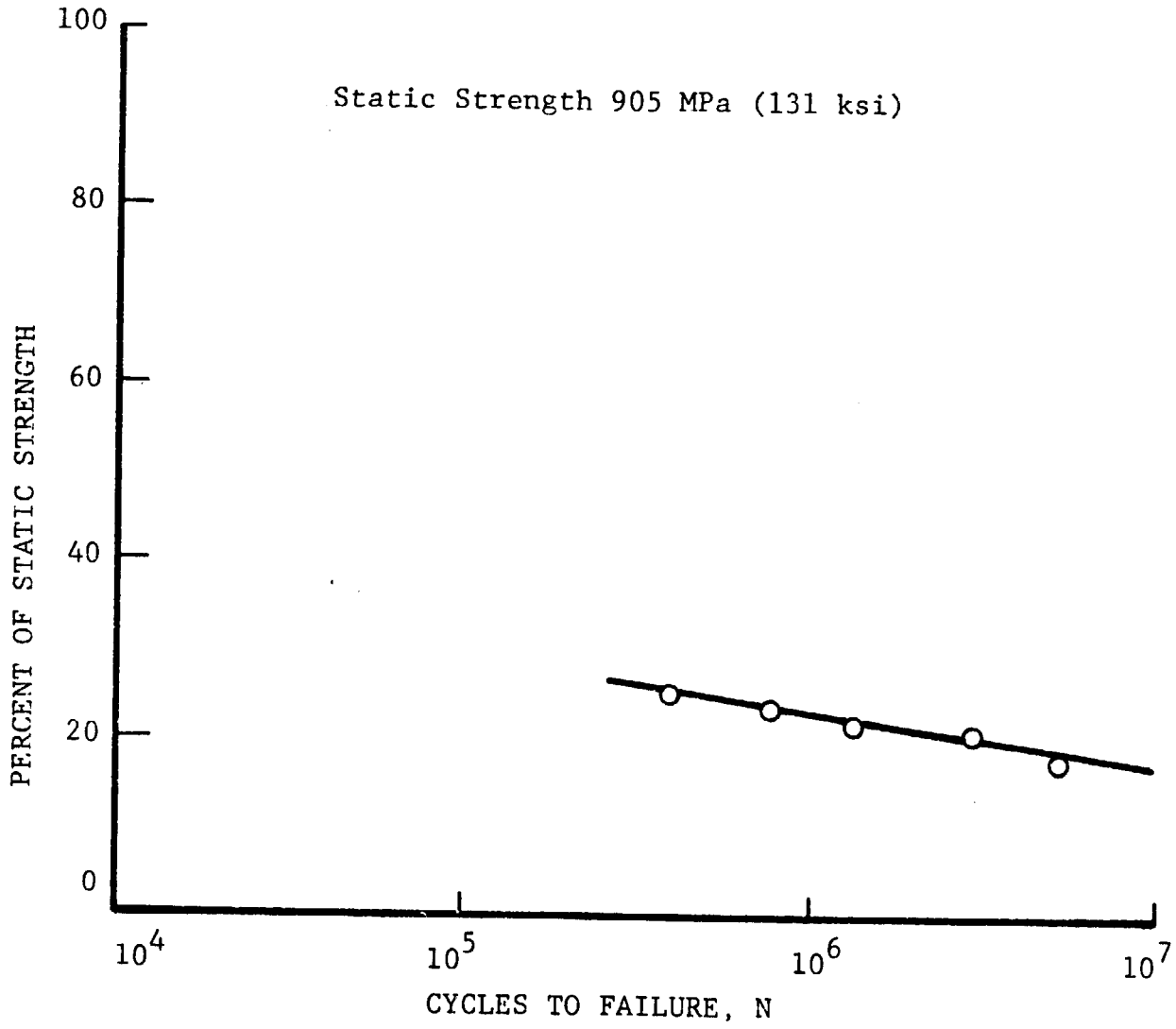

Fig. 53 TENSILE CYCLING FATIGUE STRENGTH OF FLATTENED TUBE SPECIMENS OF $[\pm 45^P/0_4^G]_s$ PRD-49/S-GLASS/EPOXY

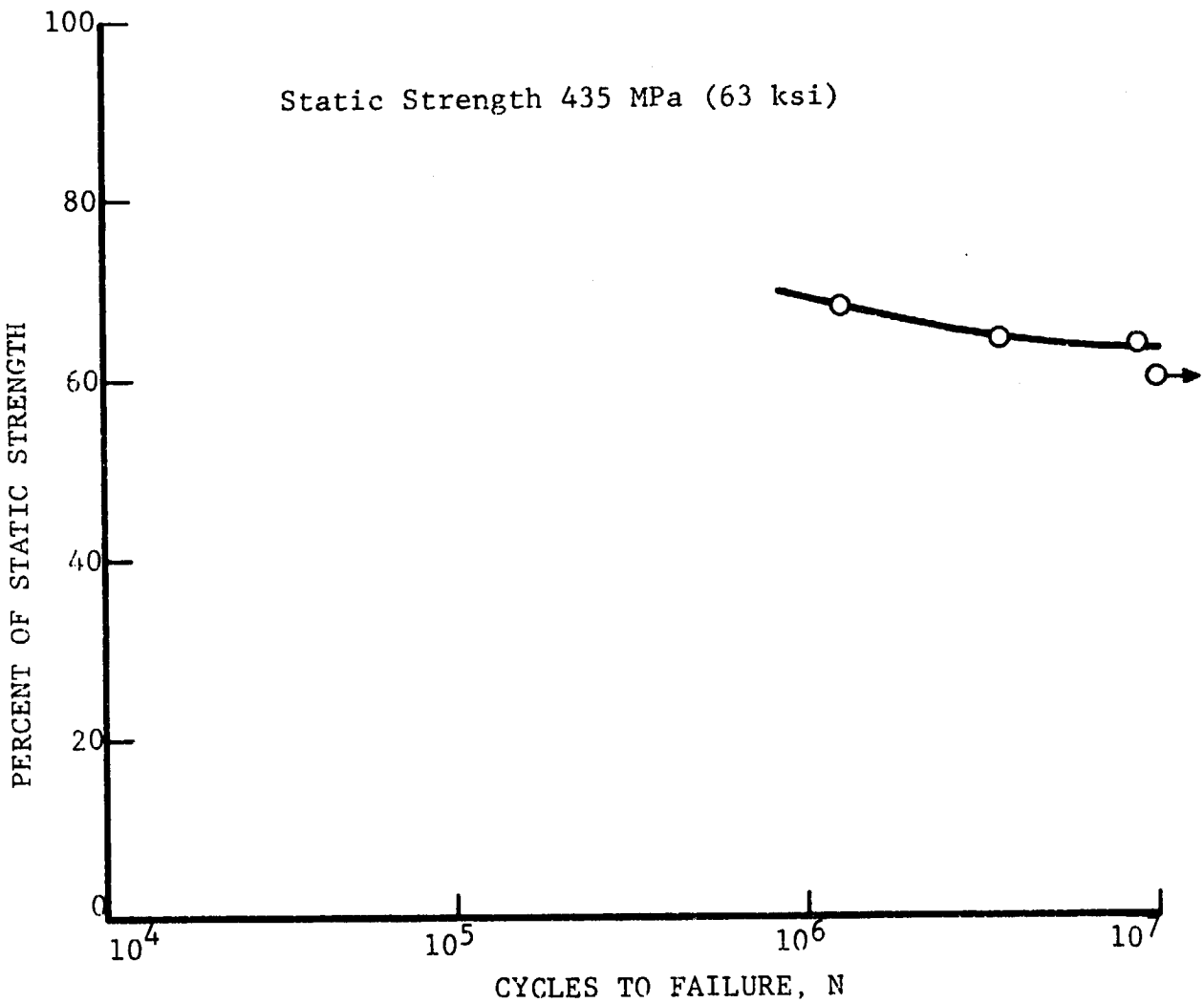

Fig. 54 TENSILE CYCLING FATIGUE STRENGTH OF FLATTENED TUBE SPECIMENS OF $[\pm 45^C/0^P]_S$ HT-GRAPHITE/PRD-49/EPOXY

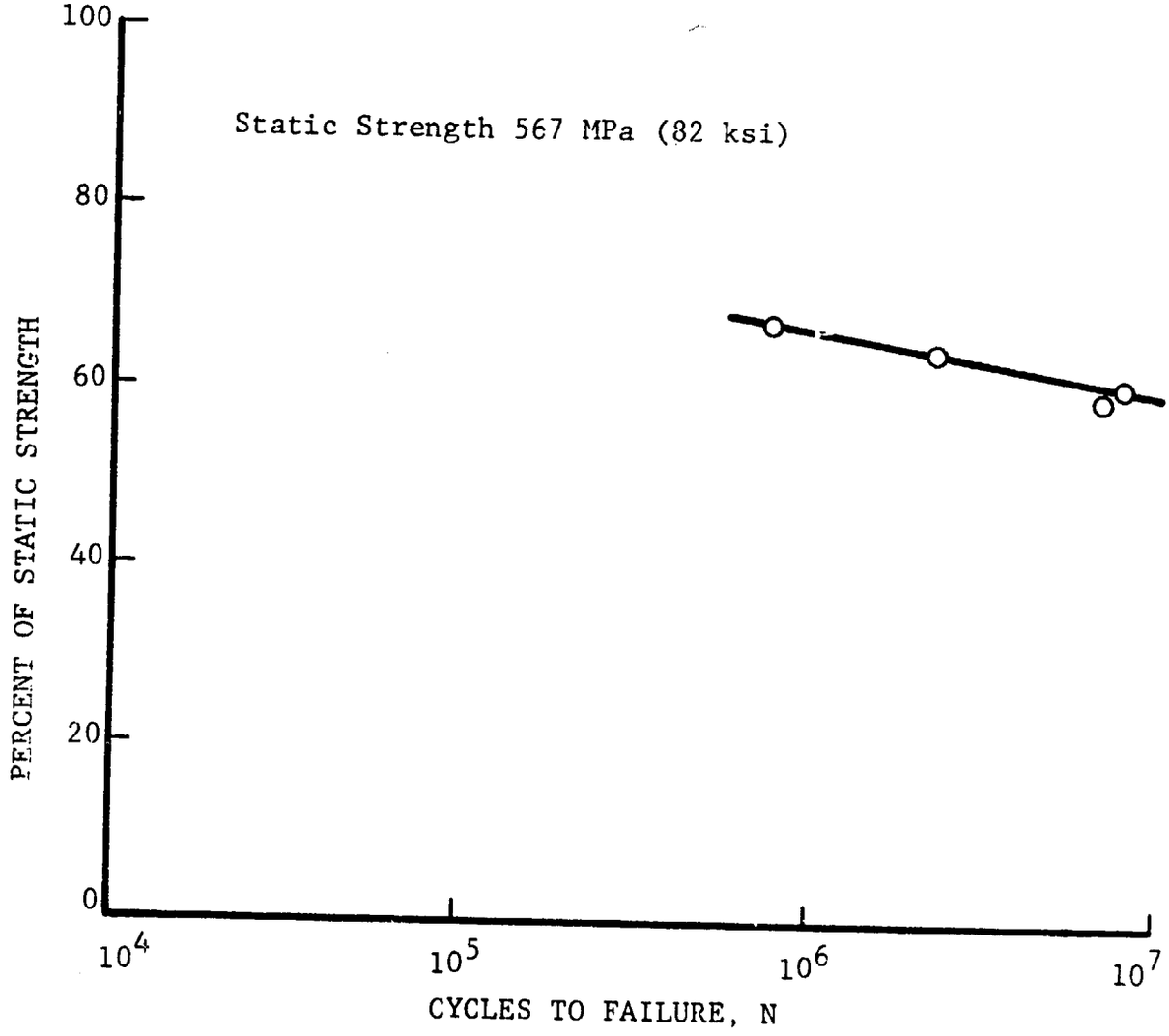

Fig. 55 TENSILE CYCLING FATIGUE STRENGTH OF FLATTENED TUBE SPECIMENS OF $[\pm 45^C/0_2^P]_s$ HT-GRAPHITE/PRD-49/EPOXY

In Fig. 47 for the $[\pm 45/0_2]_s$ S-glass/epoxy specimens the data fall around the 25 percent of static strength limit as expected.

Figure 48 presents the data for $[\pm 45/0_2]_s$ PRD-49-III/epoxy specimens. From past experience it was expected that the data would fall below 55 percent of static strength, but the specimens proved to be stronger. Since they all represent tab failures the endurance limit must be even higher than indicated in Fig. 48. It would be of interest to compare this with the behavior of flat coupons of the same material. Based on past experience with flat PRD-49/epoxy coupons (different resin) the region should be below 55 percent. Hence the flattened tubular specimens appear to have higher fatigue endurance.

In Fig. 49 for the $[\pm 45/0_2]_s$ HT graphite/epoxy specimens, it was expected that the data would fall above 60 percent of static strength with a runout of 10^7 cycles at about 60 percent of static strength, based on experience with similar graphite/epoxy material. The flattened tubular specimens exceeded the endurance limit expectation with a runout at 74 percent of static strength indicating superior endurance over flat coupons. It would be of interest to verify this against flat coupons of the same material.

Figure 50 shows the data for $[\pm 45^C/0^G]_s$ HT graphite/S-glass/epoxy. It appears that the data fall below 40 percent of static strength rather than below 25 percent as expected from the data for S-glass/epoxy shown in Fig. 47 and from past experience. This may possibly be deceptive, since the data in Fig. 50 are based on "static strength" of tab-failed specimens rather than on true static strength, which must be higher.

Figure 51 presents the data for $[\pm 45^{C}/0_2{}^{G}]_s$ HT graphite/S-glass/epoxy specimens. Here too, the data were expected to be governed by the usual behavior of the 0-degree glass/epoxy plies and fall below the 25 percent of static strength. The data, however, indicate the upper limit is nearer 40 percent of static strength and that the endurance limit of 10^7 cycles is probably in the neighborhood of 30 percent of static strength. Whether this unexpected superior performance is due to the edgeless specimen configuration, or the hybridization can only be established by comparison with tests of corresponding flat coupons.

The values in Fig. 52 for the $[\pm 45^{P}/0_2{}^{S}]_s$ PRD-49-III/S-glass/epoxy specimens were expected to fall below 25 percent of static strength based on past experience with S-glass/epoxy. The upper limit of the region is closer to 30 percent of static strength and superior to the pure S-glass/epoxy specimens of Fig. 47.

Figure 53 presents the data for $[\pm 45^{P}/0_4{}^{G}]_s$ PRD-49-III/S-glass/epoxy. The behavior of this layup parallels the results obtained for the related hybrid layup of Fig. 52 but is closer to the results obtained for the pure S-glass/epoxy specimen of Fig. 47 which may be due to the increased S-glass content.

In Figure 54 for the $[\pm 45^{C}/0^{P}]_s$ HT graphite/PRD-49-III/epoxy specimens it was expected that the data would be governed by the PRD-49/epoxy behavior and fall below the 55 percent of static strength. The data shown fall instead below 70 percent of static strength with a runout of 10^7 cycles at close to 60 percent of static strength. These results may be deceptive since the actual static strength may be higher than the one obtained here.

Figure 55 presents the data for the $[\pm 45^C/0_2^P]_s$ HT graphite/PRD-49-III/epoxy specimens. The behavior is essentially the same as that of the similar hybrid of Fig. 54.

4.3 Residual Properties

Static tensile tests to failure were performed on those flattened tube fatigue specimens which survived 10^7 cycles to determine their residual properties. Table 5 lists these residual properties. All specimens, except the $[\pm 45^C/0^P]_s$ specimen, failed at or near the tabs. The specimen which failed in the test section did not have external draping as tab reinforcement. The other surviving specimens had external draping. They must have sustained some damage near the tabs but not sufficient to fail the specimens during the cycling. At the higher loads applied during the static testing this damage became critical and produced failures at the tabs.

Stress-strain curves to failure for the surviving specimens are shown in Figs. 56 through 59. The $[\pm 45/0_2]_s$ HT graphite/epoxy specimen, Fig. 56, shows no intermediate degradation occurring during testing. The stress-strain curve is linear to failure which also was the case for the static specimens. The modulus and Poisson's ratio show no significant deviation from the average values for the static tests. Hence these material properties did not degrade due to cycling.

Figure 57 shows the stress-strain curve for the surviving specimen of $[\pm 45^C/0^G]_s$ HT graphite/S-glass/epoxy. The stress-strain to failure curve is nonlinear but not more so than was the case for the static specimens. The modulus and Poisson's ratio show no significant deviation from the average values obtained for the static tests. Thus, these material properties did not degrade due to cycling.

Table 5

RESIDUAL PROPERTIES OF FLATTENED TUBULAR SPECIMENS WHICH SURVIVED 10^7 CYCLES OF TENSILE CYCLING FATIGUE

Material	Specimen Layup	Maximum Cyclic Stress MPa	(ksi)	Tensile Failure Stress MPa	(ksi)	Failure Strain, ε_{xx} (10^{-3} m/m)	Tensile Modulus E_{xx} GPa	(10^6 psi)	Poisson's Ratio ν_{xy}
HT-Graphite/ Epoxy	$[\pm 45/0_2]_s$	540	(78.3)	831*	(121)*	7.8	108	(15.7)	0.60
HT-Graphite/ S-Glass/ Epoxy	$[\pm 45^C/0^G]_s$	133	(19.2)	323*	(47)*	10.6	36	(5.2)	0.63
HT-Graphite/ S-Glass/ Epoxy	$[\pm 45^C/0_2{}^G]_s$	155 173	(22.5) (25.1)	335* 454*	(49)* (66)*	11.2 -	35 -	(5.0) -	0.64 -
HT-Graphite/ PRD-49-III/ Epoxy	$[\pm 45^C/0^P]_s$	259	(37.6)	551	(80)	13.9	41	(5.0)	0.69

*Failure at tab

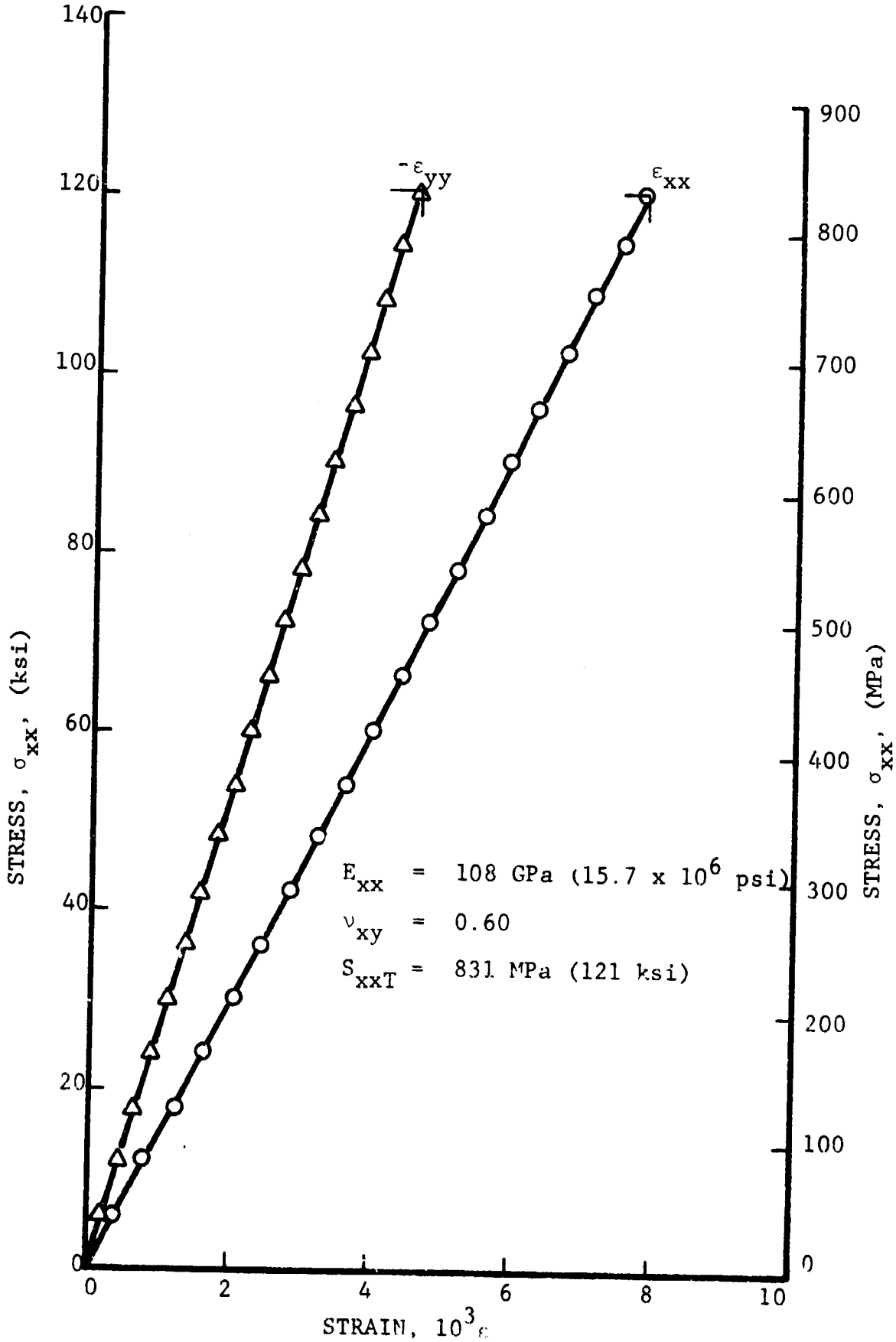

Fig. 56 STRAINS IN UNIAXIALLY LOADED FLATTENED TUBE OF $[+45/0_2]_s$ GRAPHITE/EPOXY AFTER SURVIVING 10^7 CYCLES OF TENSILE CYCLING FATIGUE TO 540 MPa (78.3 ksi)

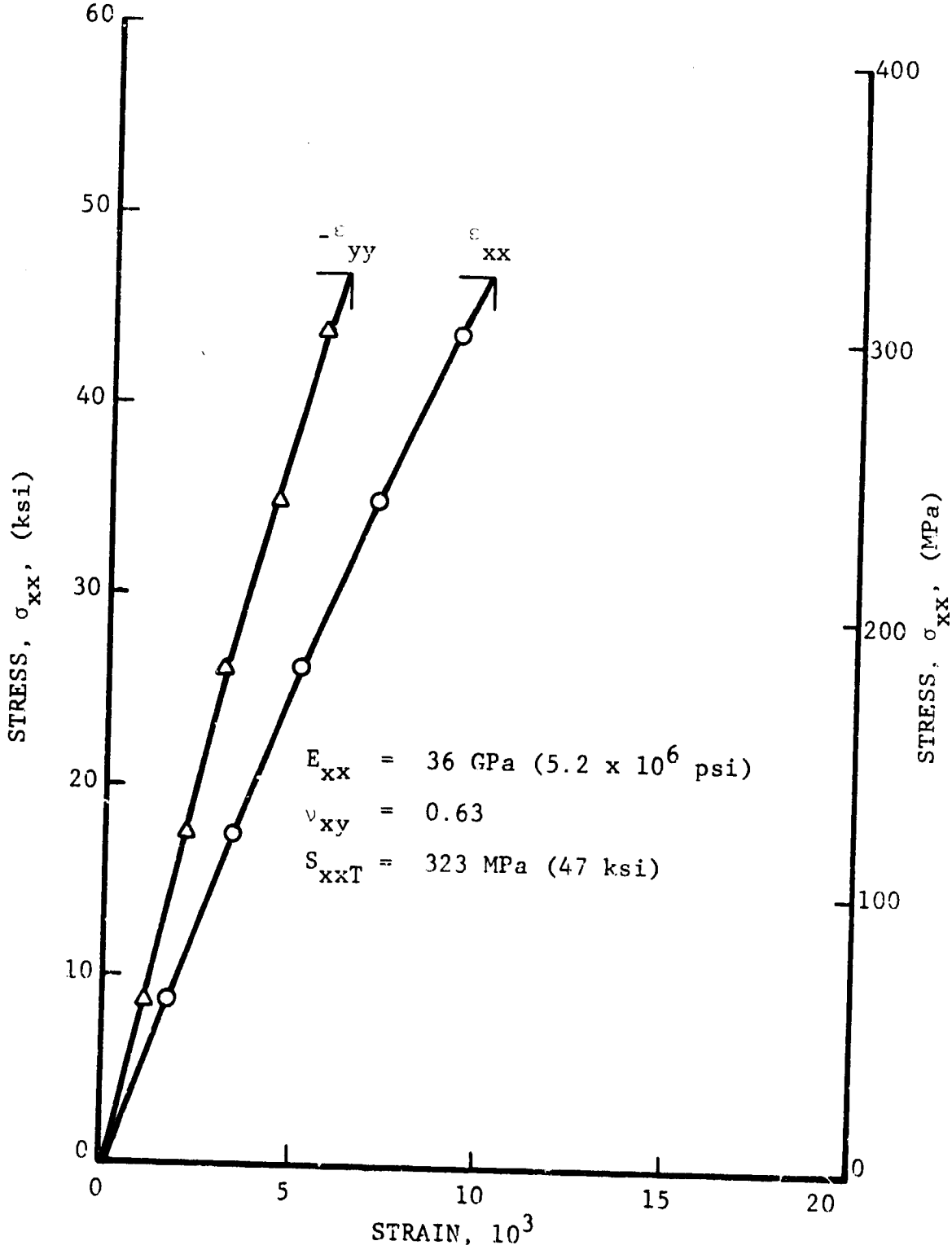

Fig. 57 STRAINS IN UNIAXIALLY LOADED FLATTENED TUBE OF $[+45^C/0^G]_s$ GRAPHITE/S-GLASS/EPOXY AFTER SURVIVING 10^7 CYCLES OF TENSILE CYCLING FATIGUE TO 133 MPa (19.2 ksi)

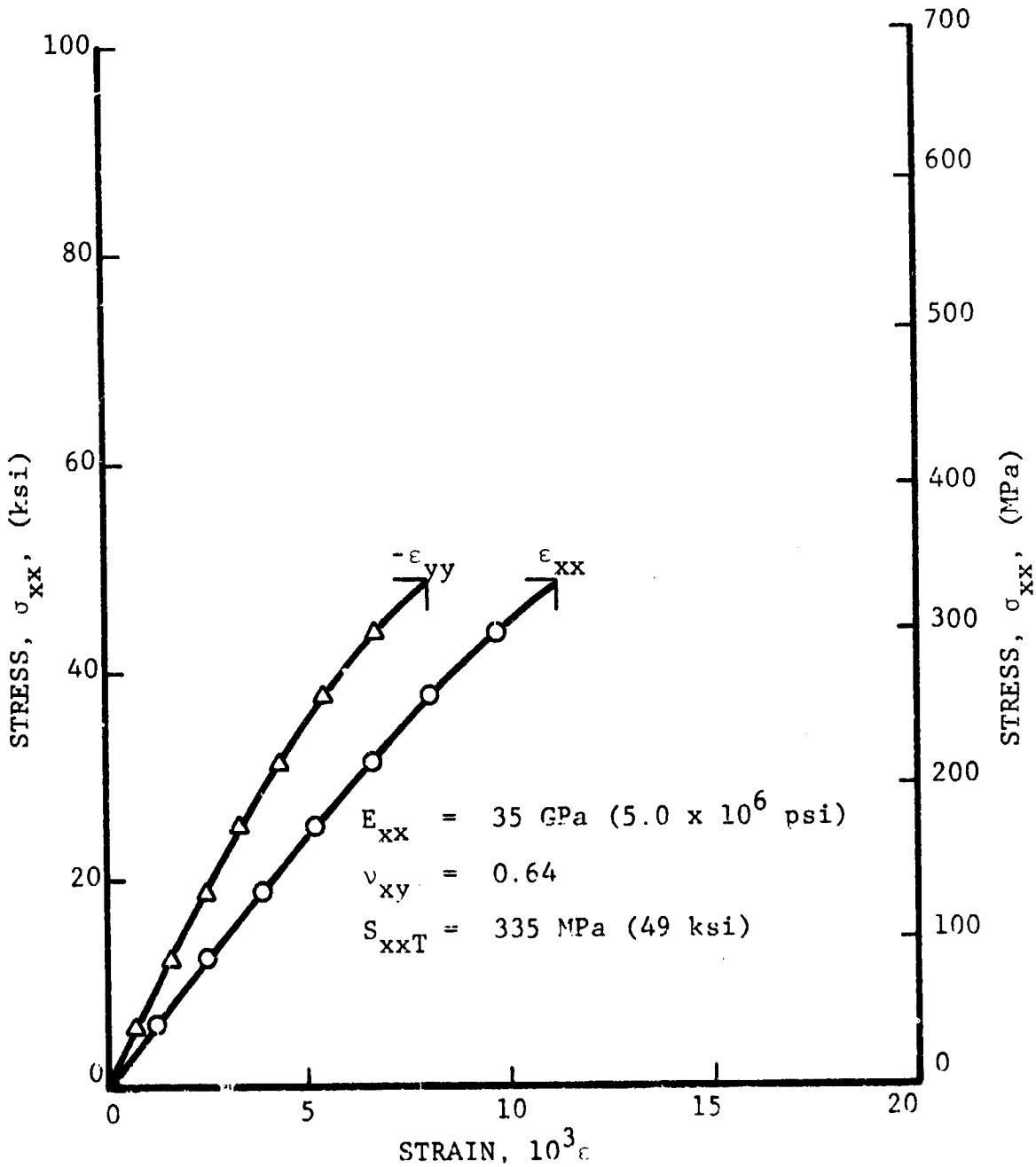

Fig. 58 STRAINS IN UNIAXIALLY LOADED FLATTENED TUBE OF $[+45^C/0_2^G]_s$ GRAPHITE/S-GLASS/EPOXY AFTER SURVIVING 10^7 CYCLES OF TENSILE CYCLING FATIGUE TO 155 MPa (22.5 ksi)

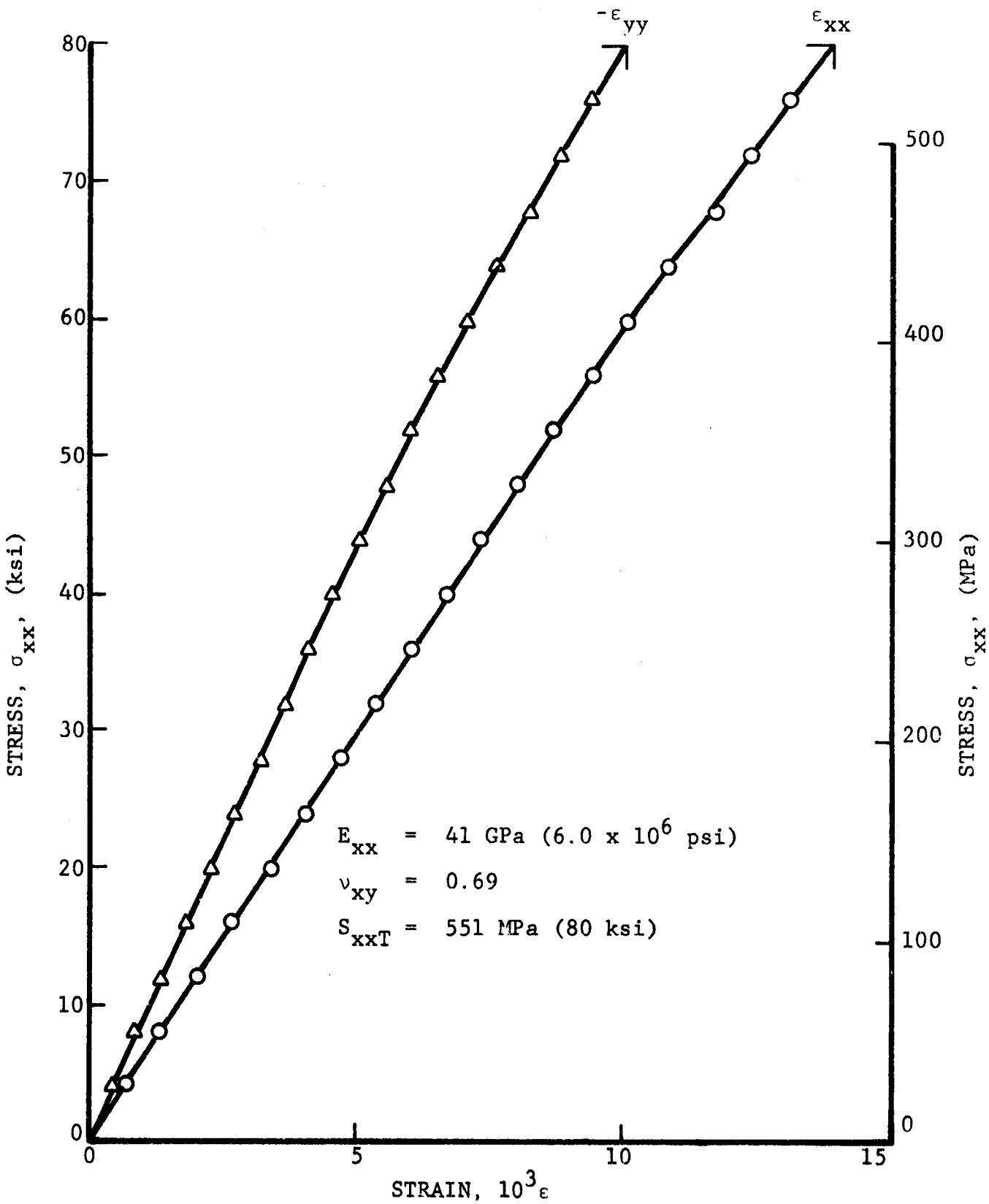

Fig. 59 STRAINS IN UNIAXIALLY LOADED FLATTENED TUBE OF $[+45^C/0^P]_S$ HT-GRAPHITE/PRD-49/EPOXY AFTER SURVIVING 10^7 CYCLES OF TENSILE CYCLING FATIGUE TO 259 MPa (37.6 ksi)

Figure 58 shows the stress-strain curve for one of the surviving specimens of $[\pm 45^{C}/0_2{}^{G}]_s$ HT graphite/S-glass/epoxy. The nonlinear behavior to failure is essentially the same as for the static specimens. The modulus is lower than the average obtained for the static specimens but is close to one of them. Hence the specimen modulus probably did not degrade due to cycling. Poisson's ratio shows no significant difference from the initial values.

Figure 59 shows the stress-strain data for the surviving specimen of $[\pm 45^{C}/0^{P}]_s$ HT graphite/PRD-49-III/epoxy. The nonlinear behavior to failure is similar to that obtained for the static specimens. The modulus and Poisson's ratio show no significant differences from the average values obtained for the static tests. The strength is, of course, higher than for the static tests because the surviving specimen failed in the test section and the static specimens did not. It can be concluded that the material properties did not degrade due to cycling.

5.0 SUMMARY, CONCLUSIONS AND RECOMMENDATIONS FOR FUTURE WORK

The objective of this program was to determine static and fatigue properties of three composite materials and hybrids thereof with edgeless cylindrical specimens. The materials investigated were graphite/epoxy, S-glass/epoxy and PRD-49 (Kevlar 49)/epoxy in various angle-ply configurations.

A new type of edgeless cylindrical specimen was developed. It is a flattened tube with two flat sides connected by curved sections and it is handled much like the standard flat coupon. A generally satisfactory fabrication technique was developed. The prepreg plies are first rolled around a cylindrical rod mandrel then the mandrel is removed and a silicone rubber tube inserted in its place. The specimen then, wrapped with separator and bleeder layers, is inserted into a specially made molding tool and pressurized internally against the mold, through the silicone rubber tube during the curing cycle. Better results were obtained by bagging the whole assembly and applying vacuum, by increasing the internal pressure to 1380 kPa (200 psi) and by introducing a precure stage of 6 hours at 399 degK (150°F) with pressure.

Tabbing consisted of bonding two exterior glass/epoxy tabs, identical to those used in flat coupons, and similar inserts bonded to the inside of the tube. It was found necessary to provide additional reinforcement in the tab area of the specimen. The most satisfactory reinforcement technique found consisted of inserting additional short plies between the continuous plies at both ends of the specimen during fabrication. However, this reinforcing technique was introduced late in the program and the number of specimens tested was not sufficient for a definite assessment.

Hybrid specimens tended to result in more tab failures than other specimens of a single material. Proper tabbing and reinforcement is thus more critical for hybrid specimens.

Axial modulus, Poisson's ratio, strength and ultimate strain were obtained under static loading from flattened tube specimens of nine laminate configurations. In a few cases these results were compared with those of corresponding flat coupon specimens. In the case of graphite/epoxy of $[\pm 45/0]_s$ and $[\pm 45/0_2]_s$ layup the tubular specimens appeared to yield somewhat higher strength and ultimate strain values than flat specimens. In the case of PRD-49-III/epoxy and S-glass/epoxy of $[\pm 45/0_2]_s$ layup the results were inconclusive when compared with corresponding flat coupons. However, indications are that with improved specimen quality and interply tab region reinforcement the tubular specimen will show higher strength. No comparisons between tubular and flat specimens were made for the hybrid laminates.

All specimens containing S-glass/epoxy or PRD-49-III/epoxy $\pm$45-degree plies failed in a characteristic "stretch-pinch" mode attributable to the deformations of the edgeless specimen.

Tensile fatigue tests were conducted with flattened tubular specimens for all nine laminate configurations. Rudimentary S-N curves were obtained from the few specimens tested. Although no direct comparison was made with flat coupons, indications are that in some cases the fatigue strength of tubular specimens is higher than might be expected from previous experience with flat coupons. Definitive conclusions will have to await further systematic testing of tubular specimens

and flat coupons of the same materials and layup.

Fatigue specimens which survived 10^7 cycles were subsequently tested statically to failure to determine residual properties. No stiffness or strength degradation was observed in these tests.

The major contribution of this program has been the development of fabrication and tab reinforcement techniques for an edgeless flattened tubular specimen. These techniques have by no means been optimized and there is considerable room for improvement. One modification which is worth considering is that of a completely flattened tubular specimen. If that specimen proves valid, then fabrication would be greatly simplified. The possible advantages of the tubular specimen would be more highlighted with an optimized and consistent specimen fabrication technique.

A systematic comparison of tubular and flat specimens of the same material and layup is needed to properly evaluate the edgeless specimen. Specimens of both $[\pm 45/0_2]_s$ and $[0_2/\pm 45]_s$ layup, resulting in edge interlaminar normal stresses of opposite signs, should be investigated in this comparative study. Two sufficiently large sets of tubular and flat specimens should be compared on the basis of stress-strain resporse to failure, static strength, cycles to failure and residual modulus and strength after cyclic loading.

REFERENCES

1. I.M. Daniel and T. Liber, "Lamination Residual Stresses in Fiber Composites," IITRI Report D6073-I for NASA-Lewis Research Center; NASA CR-134826, March 1976.

2. R.B. Pipes and N.J. Pagano, "Interlaminar Stresses in Composite Laminates Under Uniform Axial Extension," J. Composite Materials, Vol. 4, 1970, p. 538.

3. A.H. Puppo and H.A. Evensen, "Interlaminar Shear in Laminated Composites under Generalized Plane Stress," J. Composite Materials, Vol. 4, 1970, p. 204.

4. R.B. Pipes and I.M. Daniel, "Moire Analysis of the Interlaminar Shear Edge Effect in Laminated Composites," J. Composite Materials, Vol. 5, 1971, pp. 255-259.

5. I.M. Daniel, R.E. Rowlands and J.B. Whiteside, "Effects of Material and Stacking Sequence on Behavior of Composite Plates with Holes," Exp. Mechanics, Vol. 14, 1974, pp. 1-9.